**Diplomarbeit**

# Transport through quantum dot devices with superconducting leads


Sebastian Pfaller
aus
Regensburg

September 2011

durchgeführt am Institut Physik I
Theoretische Physik
Universität Regensburg
unter Anleitung von Prof. Dr. Milena Grifoni

For my parents

There is a theory which states
that if ever anyone discovers
exactly what the Universe is for
and why it is here, it will
instantly disappear and be
replaced by something even
more bizarre and inexplicable.
There is another which states
that this has already happened.

---

*(Douglas Adams)*

# Contents

# 1. Introduction

Since its discovery in 1911 by H. Kamerlingh Onnes in Leiden, superconductivity was studied extensively for decades. Then, in the 1950s people began to developed a complete theory for 'classical' superconductors and finally in 1957 Bardeen, Cooper, and Schrieffer published their remarkable paper 'Theory of Superconductivity' [2] establishing the so called BCS-theory. In 1986, when a new type superconductor, the so called high-temperature or high $T_c$ superconductor, was discovered, people realized that the microscopic mechanism of this new type of superconductors cannot be phonon mediated as it was the case for conventional ones.

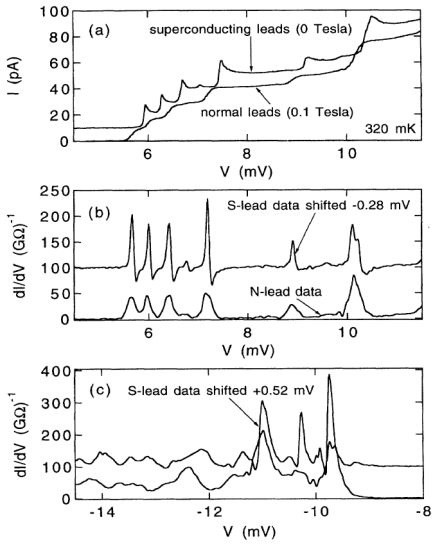


**Figure 1.1.:** I-V curves and dI/dV-V curves for normal and for superconducting leads of a *Al* nanoparticle [19]. *Copyright (1994) by The American Physical Society.*

A new theoretical description of the microscopic mechanism of high $T_c$ superconductivity was needed; still the problem is not completely solved until today. Nevertheless, the BCS-theory has not lost its validity as it is only assumed that there must be some sort of an attractive potential between the pairs of electrons which form so called Cooper pairs. In particular, the BCS ground state or Cooper pair condensate describes

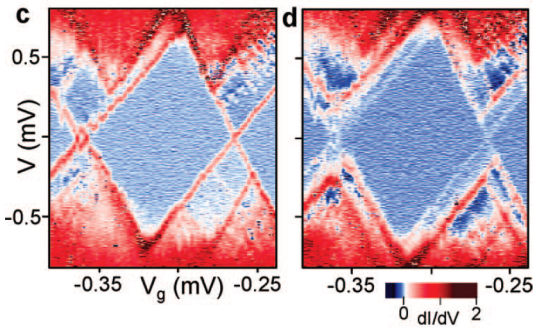


**Figure 1.2.:** Differential conductance as a function of bias and gate voltage of a $InP$ semiconductor nanowire coupled to $Ti/Al$ leads. In the left figure superconductivity is suppressed by a small magnetic field. In the right figure the magnetic field is turned off and we can see that the superconducting gap opens a gap between the two diamond tips. [9] *Copyright (2008) by The American Chemical Society.*

a macroscopic quantum state and is one of the most remarkable phenomena in physics. It is even used beyond condensed matter physics, for example to describe the state inside the heart of a neutron star. Due to the enormous density protons and neutrons may dissolve into fermionic quarks, which then are free to pair among themselves [7]. Based on the BCS-theory Josephson published his groundbreaking paper 'Possible new effects in superconductive tunneling' [15] in 1962 which opened the wide field of superconducting tunnel junctions. The most prominent example is the superconducting quantum interference device (SQUID). One possible application of the SQUID is to measure small magnetic fields with very high precision, using the Josephson effect. Modern biological magnetic field studies, especially on the detection of the fields from the heart and the brain are using magnetometers based on superconducting quantum interference devices [6]. Only lately SQUID's have been used as building blocks for quantum computation to realize so called superconducting quantum bits [8].

Recent advances in modern nanofabrication techniques made it possible to attach superconducting leads to nanostructures like quantum dots, where transport of single electrons can be controlled. Quantum dot systems have been the subject of intense research for a long time to study coherent transport of electrons. With these new hybrid devices of non-superconducting quantum dots with superconducting leads a new possibility arises, namely to study superconducting correlations in quantum dot systems. These correlations are complex many body effect that arise from the pair interaction of the electrons in the Cooper pair condensate.
The first experiments on this subject were done by Ralph et al. [19] in 1995, who

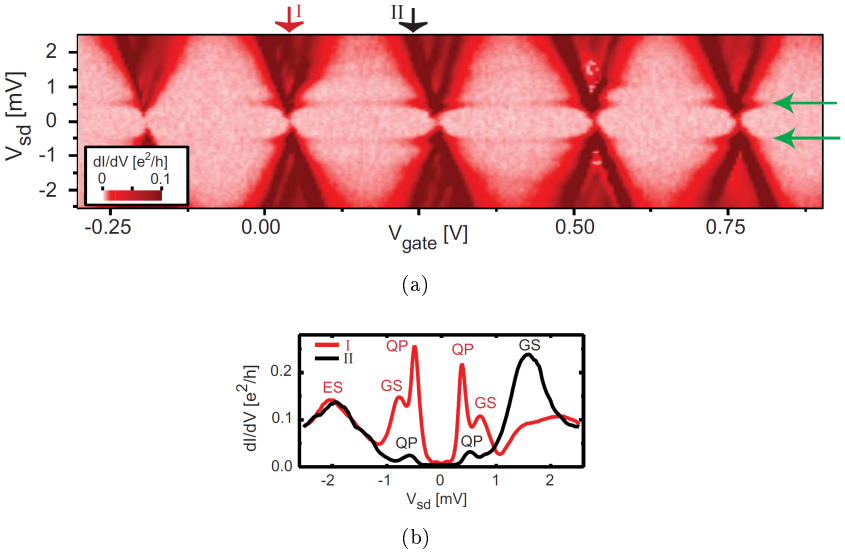


**Figure 1.3.:** **(a)** Differential conductance of a single-wall carbon nanotube (SWCNT) quantum dot coupled to niobium based superconducting leads plotted against bias and gate voltage. **(b)** Bias cuts of figure **(a)** at the two positions I and II. [12] *Copyright (2009) by The American Physical Society*

measured the current-voltage characteristic of an $Al$ nanoparticle with a diameter $< 10$ nm, coupled to two superconducting leads. Negative differential conductance features which reflect the BCS density of states in the two leads were observed, compare Fig. 4.7. Further investigations of the dependence on particle size or tunnel coupling were hindered by experimental difficulties in the device fabrication process [9]. In recent years experimentalists succeed in producing hybrid structures, for instance an $InP$ semiconductor nanowire connected to superconducting $Ti/Al$ leads [9]. In Fig. 1.2 we illustrate a differential conductance measurement of such a device, for normal conducting (left figure) and for superconducting leads (right figure), respectively. In the normal conducting case superconductivity was suppressed by applying a sufficiently strong magnetic field.

In 2009, experiments on carbon nanotube quantum dots [12] and on $C_{60}$ fullerene molecules [23] coupled to superconducting leads have been reported. In Fig. 1.3 we show the differential conductance plot of the carbon nanotube set-up. The two horizontal arrows point at the characteristic gap between the two diamond tips, which reflects the BCS density of states. The experiment on the fullerene molecule is depicted in Fig. 1.4. It shows a high resolution measurement of the differential conductance

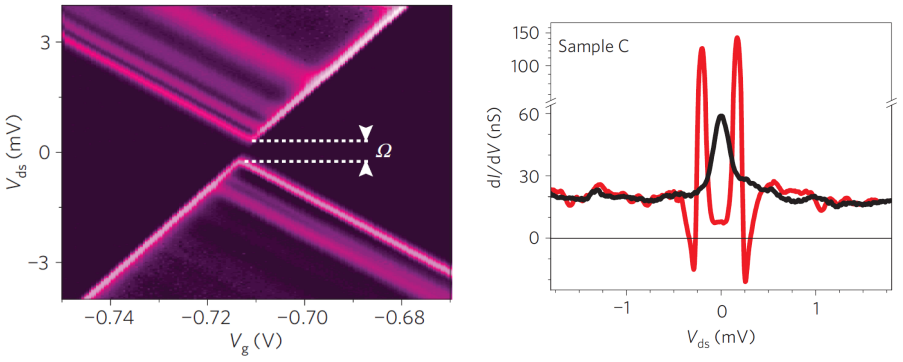


**Figure 1.4.:** **(a)** Differential conductance of a $C_{60}$ fullerene molecule in the superconducting weak link regime, we observe a separation of the diamond tips with width $\Omega = 4|\Delta|$. **(b)** Differential conductance as a function of bias voltage, red line shows the typical negative differential conductance in the Coulomb blockade regime. Figures are taken from *Winkelmann et al.* [23].

plotted against the bias and the gate voltage. Again we observe the characteristic gap in the plot.
Other experiments were done with a superconducting quantum interference device, where indium arsenide (InAs) was used as semiconductor weak link in combination with local gate electrodes in order to obtain quantum dots with a tuneable coupling to superconducting leads [21]. Supercurrents through these devices in the weak coupling regime were studied. This, however, can lead to a positive or a negative supercurrent when subsequent tunneling events are coherent [21]. In Fig. 1.5 we illustrate the SQUID set-up and the measurements of the supercurrent reversal.

## 1.1. Outline

The task of this thesis is to develop a closed microscopic theory of nanostructures coupled to superconducting leads in order to describe transport properties of structures similar to the ones introduced above. We have seen that at present superconducting hybrid structures are the subject of intense research and have promising potential for future applications. One of the most successful theories for quantum transport is the so called 'density matrix theory' which is used extensively to describe nanosturctures with normal conducting contacts. We will extend this theory to the case of superconducting leads and access the interesting research field of superconducting hybrid structures theoretically.

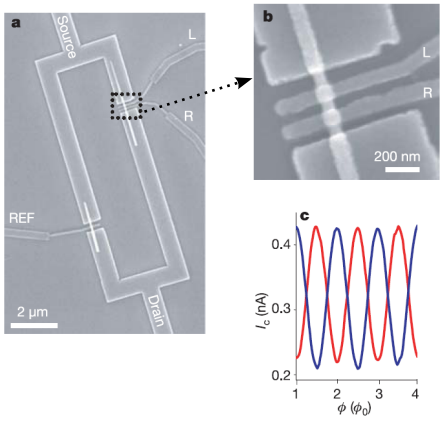


**Figure 1.5.:** **(a)** Scanning electron mircrograph of the InAs nanowire SQUID. **(b)** High-resolution image of the top nanowire, shown in the dotted box in (a), where a quantum dot with two aluminum top gates was defined. **(c)** Supercurrent as a function of the magnetic flux quantum $\phi_0 = \frac{h}{2e}$. Figures are taken from *J. A. van Dam et al.* [21].

We start from scratch and construct the Hamiltonian of the superconducting leads using mean field theory. Here it is important to describe the electrons in the superconductors as quasiparticle excitations and Cooper pairs. The quasiparticles, also called bogoliubons, are fermionic excitations of the Cooper pair condensate. We theoretically describe them by defining the Cooper pair condensate as the vacuum state of the bogoliubons. The essential step to find a consistent theoretical description of transport through such systems, is to transform the electron operators in a particle-number-conserving way to quasiparticle operators and Cooper pair operators.
We accomplish this goal by using a modified version of the Bogoliubov transformation [4] following Josephson [15]. Finally the lead Hamiltonian will contain all necessary information about the correlations in the superconductors. We are able to embed the lead Hamiltonian in the general master equation formalism and gain a transport theory for quantum dot devices with superconducting leads up to second order in the tunneling Hamiltonian. Eventually, we will demonstrate the validity of the theory investigating two simple models, the single impurity Anderson model (SIAM) which describes the simplest single dot, and the quantum double dot. We will show that we can reproduce the most characteristic features of the experiments. Specifically, the gap which appears in the stability diagrams and the characteristic form of both the current and the differential conductance as a function of the bias voltage for fixed gate voltage.

# Theory of nanojunctions coupled to superconducting leads

# 2. BCS-theory for superconductive tunneling

## 2.1. Model Hamiltonian for the tunnel-coupled leads and system

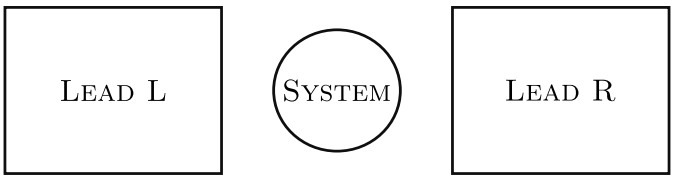


**Figure 2.1.:** Sketch of the transport setup studied in this thesis. It shows a system connected with tunnel-junctions to superconducting leads (**L**eft / **R**ight).

Throughout this work we study transport setups of quantum dot devices coupled to superconducting leads as sketched in Fig. 2.1. The setup is described by a system-bath model:

$$\hat{H} = \hat{H}_B + \hat{H}_T + \hat{H}_S. \tag{2.1}$$

$\hat{H}_S$: Hamiltonian for the system, represented by the quantum dot device.

$\hat{H}_B$: Hamiltonian for the leads, considered as thermal bath.

$\hat{H}_T$: Hamiltonian for the weak tunnel-junctions.

In the following we discuss in detail the different contributions to this model.

### 2.1.1. System Hamiltonian

In this work we are investigating two systems, the quantum single dot (SD) and the quantum double dot (DD).

| particle number | energy | state |
|---|---|---|
| 0 | 0 | $\|0\rangle$ |
| 1 | $\epsilon_d$ | $\|1\sigma\rangle$ |
| 2 | $2\epsilon_d + U$ | $\|2\rangle$ |

Table 2.1.: Eigenstates and eigenenergies of the SD, where $\sigma = \uparrow / \downarrow$ denotes the spin.

### Single Quantum Dot

We describe the SD with the Hamiltonian of the Single Impurity Anderson model (SIAM):

$$\hat{H}_{SD} = \sum_{\sigma} \epsilon_d \, \hat{\mathrm{d}}_{\sigma}^{\dagger} \, \hat{\mathrm{d}}_{\sigma} + U \; \hat{n}_{\uparrow} \hat{n}_{\downarrow} \; , \tag{2.2}$$

where

$$\hat{n}_{\sigma} = \hat{\mathrm{d}}_{\sigma}^{\dagger} \, \hat{\mathrm{d}}_{\sigma} \tag{2.3}$$

is the number operator of the electrons in the SD.
This model describes a dot with on-site single particle energies $\epsilon_d$ and Coulomb repulsion $U$, which can be occupied by at most two electrons. The highest occupied state is defined as

$$|2\rangle = \hat{\mathrm{d}}_{\uparrow}^{\dagger} \, \hat{\mathrm{d}}_{\downarrow}^{\dagger} \, |0\rangle \, . \tag{2.4}$$

The one particle states read:

$$|1\sigma\rangle \equiv \hat{\mathrm{d}}_{\sigma}^{\dagger} \, |0\rangle \, . \tag{2.5}$$

In Tab. 2.1 we present the eigenstates and the eigenenergies of the SD Hamiltonian.

### The Double Dot Hamiltonian

We describe the DD by a modified version of the Pariser-Parr-Pople Hamiltonian [16, 18] in the most general form:

$$\begin{aligned} H_{DD} = & \sum_{\substack{\alpha \in \{L,R\} \\ \sigma \in \{\uparrow,\downarrow\}}} \epsilon_{\alpha\sigma} \, \hat{\mathrm{d}}_{\alpha\sigma}^{\dagger} \, \hat{\mathrm{d}}_{\alpha\sigma} + \sum_{\sigma} \Big( b \, \hat{\mathrm{d}}_{L\sigma}^{\dagger} \, \hat{\mathrm{d}}_{R\sigma} + b^{*} \, \hat{\mathrm{d}}_{R\sigma}^{\dagger} \, \hat{\mathrm{d}}_{L\sigma} \Big) \\ & + \sum_{\alpha} U_{\alpha} \big( \hat{n}_{\alpha\uparrow} - \frac{1}{2} \big) \big( \hat{n}_{\alpha\downarrow} - \frac{1}{2} \big) + V \big( \hat{n}_{L} - 1 \big) \big( \hat{n}_{R} - 1 \big). \end{aligned} \tag{2.6}$$

Here, $\hat{\mathrm{d}}^\dagger_{\alpha\sigma}$ are the creation operators for an electron on site $\alpha \in \{L, R\}$ and with spin $\sigma$. They define the number operators $\hat{n}_{\alpha\sigma} = \hat{\mathrm{d}}^\dagger_{\alpha\sigma}\,\hat{\mathrm{d}}_{\alpha\sigma}$. The operator $\hat{n}_\alpha = \hat{n}_{\alpha\uparrow} + \hat{n}_{\alpha\downarrow}$ counts the number of electrons on site $\alpha$. In the general case we distinguish between the two on-site energies $\epsilon_{\alpha\sigma}$ and on-site Coulomb interactions $U_\alpha$, but for later purpose we will set them equal. Electrons in two different sites can interact through the inter-dot Coulomb interaction $V$; $b$ describes the hopping between the two sites. In the following we want to consider a symmetric DD by defining the on-site energies and the on-site Coulomb interaction to be site-independent; in this case the Hamiltonian can be diagonalized analytically. We present the results for the symmetric case in Tab. 2.2, where we defined the highest occupied state as follows:

$$|2,2\rangle \equiv \hat{\mathrm{d}}^\dagger_{L\uparrow}\,\hat{\mathrm{d}}^\dagger_{R\uparrow}\,\hat{\mathrm{d}}^\dagger_{L\downarrow}\,\hat{\mathrm{d}}^\dagger_{R\downarrow}\,|0\rangle\,. \tag{2.7}$$

At the same time Eq. (2.7) defines the order of the creation operators in a many body state. The double dot system can either be empty or filled with one, two, three, or four electrons. Each has the spin degree of freedom, giving a total of 16 different possible states. For the notation we adapted the one of the SD, meaning we are labeling the states as

$$\hat{\mathrm{d}}^\dagger_{L\sigma}\,|0\rangle = |1\sigma, 0\rangle\,, \tag{2.8}$$

which describes a state with one electron of spin $\sigma$ in the left dot. A state with two electrons in the left dot and one spin up electron in the right is defined as:

$$\hat{\mathrm{d}}^\dagger_{L\uparrow}\,\hat{\mathrm{d}}^\dagger_{R\uparrow}\,\hat{\mathrm{d}}^\dagger_{L\downarrow}\,|0\rangle = |2, 1\uparrow\rangle\,. \tag{2.9}$$

It is important to notice the order of the creation operators.

### 2.1.2. Lead Hamiltonian

The model Hamiltonian of the superconducting leads is based on the so called pairing Hamiltonian, see for example [20, p. 53]. Let us first consider a single lead $\eta \in \{L, R\}$:

$$\hat{H}_{B,\eta} = \sum_{k\sigma} \epsilon_k\,\hat{\mathrm{c}}^\dagger_{\eta k\sigma}\,\hat{\mathrm{c}}_{\eta k\sigma} + \sum_{kl} V_{kl}\,\hat{\mathrm{c}}^\dagger_{\eta k\uparrow}\,\hat{\mathrm{c}}^\dagger_{\eta -k\downarrow}\,\hat{\mathrm{c}}_{\eta -l\downarrow}\,\hat{\mathrm{c}}_{\eta l\uparrow}\,. \tag{2.10}$$

Here we defined $\epsilon_k = \frac{\hbar^2 k^2}{2m}$ and $V_{kl}$ is the pair interaction.
We denote the total electron number operator of lead $\eta$ by:

$$\hat{N}_\eta = \sum_{k\sigma} \hat{\mathrm{c}}^\dagger_{\eta k\sigma}\,\hat{\mathrm{c}}_{\eta k\sigma}\,. \tag{2.11}$$

In order to introduce the chemical potential in Eq. (2.10) we are subtracting and adding $\mu_\eta \hat{N}_\eta$:

| particle number | energy | degeneracy | state |
|---|---|---|---|
| 0 | $\frac{U}{2}+V$ | 1 | $\lvert 0\rangle$ |
| 1 | $\epsilon+b$ | 2 | $\frac{1}{\sqrt{2}}\big(\lvert 1\sigma,0\rangle+\lvert 0,1\sigma\rangle\big)$ |
| | $\epsilon-b$ | 2 | $\frac{1}{\sqrt{2}}\big(\lvert 1\sigma,0\rangle-\lvert 0,1\sigma\rangle\big)$ |
| 2 | $2\epsilon-\frac{V}{2}-R$ | 1 | $\frac{\beta}{\sqrt{2}}\big(\lvert 2,0\rangle+\lvert 0,2\rangle\big)+$ $+\frac{\alpha}{\sqrt{2}}\big(\lvert 1\uparrow,1\downarrow\rangle+\lvert 1\downarrow,1\uparrow\rangle\big)$ |
| | $2\epsilon-\frac{U}{2}$ | 3 | $\lvert 1\sigma,1\sigma\rangle$ |
| | | | $\frac{1}{\sqrt{2}}\big(\lvert 1\uparrow,1\downarrow\rangle-\lvert 1\downarrow,1\uparrow\rangle\big)$ |
| | $2\epsilon+\frac{U}{2}-V$ | 1 | $\frac{1}{\sqrt{2}}\big(\lvert 2,0\rangle-\lvert 0,2\rangle\big)$ |
| | $2\epsilon-\frac{V}{2}+R$ | 1 | $\frac{\alpha}{\sqrt{2}}\big(\lvert 2,0\rangle+\lvert 0,2\rangle\big)-$ $-\frac{\beta}{\sqrt{2}}\big(\lvert 1\uparrow,1\downarrow\rangle+\lvert 1\downarrow,1\uparrow\rangle\big)$ |
| 3 | $3\epsilon+b$ | 2 | $\frac{1}{\sqrt{2}}\big(\lvert 2,1\sigma\rangle+\lvert 1\sigma,2\rangle$ |
| | $3\epsilon-b$ | 2 | $\frac{1}{\sqrt{2}}\big(\lvert 2,1\sigma\rangle-\lvert 1\sigma,2\rangle$ |
| 4 | $4\epsilon+\frac{U}{2}+V$ | 1 | $\lvert 2,2\rangle$ |

Table 2.2.: Table of the eigenstates and eigenenergies of the DD-Hamiltonian with equally gated sites, ordered by energy. Above we used the short hand notation: $R=\sqrt{\frac{(U-V)^2}{4}+4t^2}$, $\alpha=\frac{4t}{\sqrt{16t^2+(U-V-2-2R)^2}}$, and $\alpha^2+\beta^2=1$.

$$\hat{H}_{B,\eta} = \sum_{k\sigma} \left(\epsilon_k - \mu_\eta\right) \hat{\mathrm{c}}^\dagger_{\eta k\sigma}\, \hat{\mathrm{c}}_{\eta k\sigma} + \sum_{kl} V_{kl}\, \hat{\mathrm{c}}^\dagger_{\eta k\uparrow}\, \hat{\mathrm{c}}^\dagger_{\eta -k\downarrow}\, \hat{\mathrm{c}}_{\eta -l\downarrow}\, \hat{\mathrm{c}}_{\eta l\uparrow} + \mu_\eta \hat{N}_\eta. \tag{2.12}$$

Finally we obtain the Hamiltonian for both leads by summing over both contributions:

$$\hat{H}_B = \sum_{\eta\in\{L,R\}} \hat{H}_{B,\eta}. \tag{2.13}$$

### 2.1.3. Tunneling Hamiltonian

The tunneling Hamiltonian $\hat{H}_T$:

$$\hat{H}_T = \sum_{\eta k\sigma j} \left( t\, \hat{\mathrm{c}}^\dagger_{\eta k\sigma}\, \hat{\mathrm{d}}_{j\sigma} + t^*\, \hat{\mathrm{d}}^\dagger_{j\sigma}\, \hat{\mathrm{c}}_{\eta k\sigma} \right), \tag{2.14}$$

describes tunneling of electrons between the leads and the system. We denote the tunneling coefficient $t$, and distinguish between electron operators of the leads, $\hat{\mathrm{c}}^\dagger_{\eta k\sigma}$ and the ones of the system $\hat{\mathrm{d}}^\dagger_{j\sigma}$. In Eq. (2.14) $j$ accounts for all quantum numbers of the system beside the spin. In the case of the double dot we should mention that the tunneling Hamiltonian of Eq. (2.14) describes tunneling to both quantum dot sites with the same probability, see Fig. 4.15.

## 2.2. Diagonalization of the lead Hamiltonian

In this section we will derive the model Hamiltonian for one of the superconducting leads mentioned in Sect. 2.1. We start with the pairing Hamiltonian of Eq. (2.12), where we insert an identity composed of so called Cooper pair operators:

$$\hat{\mathrm{S}}\,\hat{\mathrm{S}}^{\dagger} = 1, \tag{2.15}$$

which we specify in Sect. 2.3.
We find

$$\hat{H}_{B,\eta} = \sum_{k\sigma} \xi_k\, \hat{\mathrm{c}}^{\dagger}_{\eta k\sigma}\, \hat{\mathrm{c}}_{\eta k\sigma} + \sum_{kl} V_{kl}\, \hat{\mathrm{c}}^{\dagger}_{\eta k\uparrow}\, \hat{\mathrm{c}}^{\dagger}_{\eta -k\downarrow}\, \hat{\mathrm{S}}\,\hat{\mathrm{S}}^{\dagger}\, \hat{\mathrm{c}}_{\eta -l\downarrow}\, \hat{\mathrm{c}}_{\eta l\uparrow} + \mu_\eta \hat{N}_\eta, \tag{2.16}$$

where $\xi_{k\eta} = \epsilon_k - \mu_\eta$.
In the following we drop the lead index $\eta$ ($\xi_{k\eta} \to \xi_k$).

**Mean field form of the lead Hamiltonian**

We know [2] that the BCS ground state is some phase coherent superposition of many-body states with pairs of Bloch states $(\mathbf{k}\uparrow, -\mathbf{k}\downarrow)$ occupied or unoccupied as units. Because of this, we have nonzero expectation values of operators like $\hat{\mathrm{c}}_{-k\downarrow}\,\hat{\mathrm{c}}_{k\uparrow}$ or $\hat{\mathrm{c}}^{\dagger}_{k\uparrow}\,\hat{\mathrm{c}}^{\dagger}_{-k\downarrow}$. Moreover, because of the large numbers of particles involved, the fluctuation about these expectation values should be small [20]. Therefore, we can use a mean-field approach in order to simplify the many-body part of the pairing Hamiltonian of Eq. (2.10) to a single particle Hamiltonian. Specifically,

$$\hat{\mathrm{S}}^{\dagger}\,\hat{\mathrm{c}}_{-k\downarrow}\,\hat{\mathrm{c}}_{k\uparrow} = \langle \hat{\mathrm{S}}^{\dagger}\,\hat{\mathrm{c}}_{-k\downarrow}\,\hat{\mathrm{c}}_{k\uparrow}\rangle + \underbrace{\left(\hat{\mathrm{S}}^{\dagger}\,\hat{\mathrm{c}}_{-k\downarrow}\,\hat{\mathrm{c}}_{k\uparrow} - \langle \hat{\mathrm{S}}^{\dagger}\,\hat{\mathrm{c}}_{-k\downarrow}\,\hat{\mathrm{c}}_{k\uparrow}\rangle\right)}_{\substack{\text{Fluctuations about the expectation value}\\ \to\text{small quantity}}}, \tag{2.17}$$

where the expectation value $\langle \hat{\mathrm{S}}^{\dagger}\,\hat{\mathrm{c}}_{-k\downarrow}\,\hat{\mathrm{c}}_{k\uparrow}\rangle$ is meant to be the thermodynamic average in the grand canonical ensemble with the mean-field Hamiltonian

$$\langle \hat{\mathrm{S}}^{\dagger}\,\hat{\mathrm{c}}_{-k\downarrow}\,\hat{\mathrm{c}}_{k\uparrow}\rangle = \frac{1}{Z_G}\,\mathrm{Tr}\left\{ e^{-\beta\left(\hat{H}_{MF} - \mu\hat{N}\right)}\, \hat{\mathrm{S}}^{\dagger}\,\hat{\mathrm{c}}_{-k\downarrow}\,\hat{\mathrm{c}}_{k\uparrow}\right\} \tag{2.18}$$

and has to be determined self-consistently.
Now we are able to express the pair interaction term of Eq. (2.10) in mean-field theory:

$$\begin{aligned}\hat{H}_{MF} = \sum_{k} \xi_k\, \hat{\mathrm{c}}^{\dagger}_{k\sigma}\, \hat{\mathrm{c}}_{k\sigma} + \sum_{kl} V_{kl} \Big( & \langle \hat{\mathrm{S}}^{\dagger}\,\hat{\mathrm{c}}_{-l\downarrow}\,\hat{\mathrm{c}}_{l\uparrow}\rangle\, \hat{\mathrm{c}}^{\dagger}_{k\uparrow}\,\hat{\mathrm{c}}^{\dagger}_{-k\downarrow}\,\hat{\mathrm{S}} \\ & + \langle \hat{\mathrm{c}}^{\dagger}_{k\uparrow}\,\hat{\mathrm{c}}^{\dagger}_{-k\downarrow}\,\hat{\mathrm{S}}\rangle\, \hat{\mathrm{S}}^{\dagger}\,\hat{\mathrm{c}}_{-l\downarrow}\,\hat{\mathrm{c}}_{l\uparrow} - \langle \hat{\mathrm{c}}^{\dagger}_{k\uparrow}\,\hat{\mathrm{c}}^{\dagger}_{-k\downarrow}\,\hat{\mathrm{S}}\rangle\, \langle \hat{\mathrm{S}}^{\dagger}\,\hat{\mathrm{c}}_{-l\downarrow}\,\hat{\mathrm{c}}_{l\uparrow}\rangle \Big) + \mu\hat{N}.\end{aligned} \tag{2.19}$$

Introducing

$$\begin{aligned} \Delta_k &\equiv -\sum_l V_{kl} \langle \hat{\mathrm{S}}^\dagger \, \hat{\mathrm{c}}_{-l\downarrow} \, \hat{\mathrm{c}}_{l\uparrow} \rangle \\ \text{and} \quad \Delta_k^* &\equiv -\sum_l V_{lk} \langle \hat{\mathrm{c}}_{l\uparrow}^\dagger \, \hat{\mathrm{c}}_{-l\downarrow}^\dagger \, \hat{\mathrm{S}} \rangle \,, \end{aligned} \tag{2.20}$$

leads to the conventional form of the mean-field BCS Hamiltonian

$$\begin{aligned} \hat{H}_{MF} &= \sum_k \xi_k \, \hat{\mathrm{c}}_{k\sigma}^\dagger \, \hat{\mathrm{c}}_{k\sigma} \\ &- \sum_k \Big( \Delta_k \, \hat{\mathrm{c}}_{k\uparrow}^\dagger \, \hat{\mathrm{c}}_{-k\downarrow}^\dagger \, \hat{\mathrm{S}} + \Delta_k^* \, \hat{\mathrm{S}}^\dagger \, \hat{\mathrm{c}}_{-k\downarrow} \, \hat{\mathrm{c}}_{k\uparrow} - \Delta_k \langle \hat{\mathrm{c}}_{k\uparrow}^\dagger \, \hat{\mathrm{c}}_{-k\downarrow}^\dagger \, \hat{\mathrm{S}} \rangle \Big) + \mu \hat{N}. \end{aligned} \tag{2.21}$$

**Bogoliubov transformation**

The most famous way to diagonalize the mean-field Hamiltonian of Eq. (2.21) was first introduced by Bogoliubov [4] in 1958, one year after the publication of the BCS-theory. He used a canonical transformation method, that is an alternative to the BCS method. We will follow Josephson [15] and introduce a particle number conserving version of the Bogoliubov transformation on an abstract level. In Sects. 2.3 and 2.4 we investigate the constituents on a more precise level. Specifically,

$$\begin{pmatrix} \hat{\mathrm{c}}_{k\uparrow} \\ \hat{\mathrm{c}}_{-k\downarrow}^\dagger \end{pmatrix} = \begin{pmatrix} u_k^* & v_k \, \hat{\mathrm{S}} \\ -v_k^* \, \hat{\mathrm{S}}^\dagger & u_k \end{pmatrix} \begin{pmatrix} \hat{\gamma}_{k\uparrow} \\ \hat{\gamma}_{-k\downarrow}^\dagger \end{pmatrix} \tag{2.22}$$

$$\begin{pmatrix} \hat{\mathrm{c}}_{k\uparrow}^\dagger \\ \hat{\mathrm{c}}_{-k\downarrow} \end{pmatrix} = \begin{pmatrix} u_k & v_k^* \, \hat{\mathrm{S}}^\dagger \\ -v_k \, \hat{\mathrm{S}} & u_k^* \end{pmatrix} \begin{pmatrix} \hat{\gamma}_{k\uparrow}^\dagger \\ \hat{\gamma}_{-k\downarrow} \end{pmatrix} \tag{2.23}$$

Here $\hat{\gamma}_{k\sigma}$ are fermionic quasiparticle operators often called bogoliubons. The coefficients $u_k$ and $v_k$ are complex numbers and are connected by the relation:

$$|u_k|^2 + |v_k|^2 = 1. \tag{2.24}$$

We rewrite Eq. (2.21) in terms of quasiparticle and Cooper pair operators and systematically eliminate the off-diagonal contributions. This can be done by choosing the coefficients in an appropriate way:

$$u_k \equiv \sqrt{\frac{1}{2}\left(1 + \frac{\xi_k}{|E_k|}\right)}, \tag{2.25}$$

$$v_k \equiv e^{i\Phi}\sqrt{\frac{1}{2}\left(1-\frac{\xi_k}{|E_k|}\right)}, \tag{2.26}$$

where $\Phi$ turns out to be the phase of the macroscopic condensate wave function in the Ginzburg-Landau theory [20, p. 50].
The full calculation is too lengthy to be presented here and we have to refer to App. A.1. The mean-field Hamiltonian for the superconducting leads finally reads:

$$\boxed{\hat{H}_{MF} = \sum_{k\tau} E_k\, \hat{\gamma}^\dagger_{k\tau}\, \hat{\gamma}_{k\tau} + E_G + \mu\hat{N},} \tag{2.27}$$

where

$$E_k = \sqrt{\xi_k^2 + |\Delta|^2}, \qquad \Delta = \Delta_k. \tag{2.28}$$

The constant $E_G$ is sometimes referred to as the ground state energy of the superconducting condensate.
We generalize the result for two leads by introducing again the lead index $\eta$.

$$\hat{H}_B = \sum_\eta \hat{H}_{B,\eta} = \sum_{\eta k\tau} E_{\eta k}\, \hat{\gamma}^\dagger_{\eta k\tau}\, \hat{\gamma}_{\eta k\tau} + E_G + \sum_\eta \mu_\eta \hat{N}_\eta. \tag{2.29}$$

Eventually, we should mention that we did not include the term $\mu\hat{N}$ in the diagonalization. For further calculations we should remember that it is still written in terms of electron operators.

## 2.3. The BCS ground state and its connection with the Cooper pair operators

In 1957 Bardeen, Cooper and Schrieffer published their remarkable paper 'Theory of Superconductivity' [2] in which they pointed out that in the superconducting state electrons condense in a ground state of paired electrons. This so-called BCS ground state is the basis for many theories which describe superconducting phenomena in the framework of the BCS theory. For example tunneling processes involving superconductors as used in this thesis. In this section we will write down the ground state in a different but very instructive manner, in order order to find an analytical expression for the Cooper pair operator postulated in Sect. 2.2. In particular we will see that the BCS ground state can be written as a superposition of states with a certain Cooper pair number.
Let us start with the most common representation of the BCS ground state [17, p. 81]:

$$\begin{aligned} |\mathrm{GS}\rangle &\equiv \prod_k \left(u_k + v_k\ \hat{\mathrm{c}}^\dagger_{k\uparrow}\,\hat{\mathrm{c}}^\dagger_{-k\downarrow}\right)|\varnothing\rangle \\ &= \prod_k u_k\left(1 + \frac{v_k}{u_k}\ \hat{\mathrm{c}}^\dagger_{k\uparrow}\,\hat{\mathrm{c}}^\dagger_{-k\downarrow}\right)|\varnothing\rangle\,, \end{aligned} \tag{2.30}$$

where $|\varnothing\rangle$ denotes the vacuum state of the electrons defined by:

$$\hat{\mathrm{c}}_{k\sigma}\,|\varnothing\rangle = 0. \tag{2.31}$$

Eq. (2.30) can be written as an exponential by exploiting the fermionic properties of the electron operators, $\hat{\mathrm{c}}^\dagger_{k\sigma}\,\hat{\mathrm{c}}^\dagger_{k\sigma} = 0$:

$$|\mathrm{GS}\rangle = \prod_k u_k\ \exp\!\left(\frac{v_k}{u_k}\ \hat{\mathrm{c}}^\dagger_{k\uparrow}\,\hat{\mathrm{c}}^\dagger_{-k\downarrow}\right)|\varnothing\rangle\,. \tag{2.32}$$

To proceed, we split the product in two parts, one of the $u_k$'s and one of the exponentials:

$$\begin{aligned} |\mathrm{GS}\rangle &= \underbrace{\prod_k u_k}_{\equiv\mathcal{N}}\ \exp\!\left(\sum_k \frac{v_k}{u_k}\ \hat{\mathrm{c}}^\dagger_{k\uparrow}\,\hat{\mathrm{c}}^\dagger_{-k\downarrow}\right)|\varnothing\rangle \\ &= \mathcal{N}\sum_{n=0}^{\infty}\frac{1}{n!}\left(\sum_k \frac{v_k}{u_k}\,\hat{\mathrm{R}}^\dagger_k\right)^n|\varnothing\rangle\,, \end{aligned} \tag{2.33}$$

where we Taylor expanded the exponential in the last step and defined an operator

$$\hat{\mathrm{R}}_k^\dagger \equiv \hat{\mathrm{c}}_{k\uparrow}^\dagger \, \hat{\mathrm{c}}_{-k\downarrow}^\dagger \,. \tag{2.34}$$

This fulfills the commutation relations:

$$\left[\hat{\mathrm{R}}_k^\dagger, \hat{\mathrm{R}}_q\right] = \delta_{kq}\left(\hat{\mathrm{c}}_{k\uparrow}^\dagger \, \hat{\mathrm{c}}_{k\uparrow} + \hat{\mathrm{c}}_{-k\downarrow}^\dagger \, \hat{\mathrm{c}}_{-k\downarrow} - 1\right), \tag{2.35}$$

$$\left[\hat{\mathrm{R}}_k^\dagger, \hat{\mathrm{R}}_q^\dagger\right] = 0, \tag{2.36}$$

$$\left[\hat{N}, \hat{\mathrm{R}}_q^\dagger\right] = 2\,\hat{\mathrm{R}}_q^\dagger. \tag{2.37}$$

### 2.3.1. BCS ground state as superposition of Cooper pair states

We can write Eq. (2.33) as a superposition of states with a fixed number of Cooper pairs $|n\rangle$, we proof this property in the next paragraph. We define:

$$|\mathrm{GS}\rangle = \mathcal{N} \sum_{n=0}^{\infty} \frac{a_n}{n!} \, |n\rangle = \sum_{n=0}^{\infty} b_n \, |n\rangle \,, \tag{2.38}$$

where

$$|n\rangle \equiv \frac{1}{a_n} \left( \sum_k \frac{v_k}{u_k} \hat{\mathrm{R}}_k^\dagger \right)^n |\varnothing\rangle \,, \tag{2.39}$$

$$b_n = \mathcal{N} \frac{a_n}{n!}. \tag{2.40}$$

We introduced the factor $a_n$ to normalize the Cooper pair states, using Eq. (2.35):

$$\begin{aligned} \langle n|m\rangle &= \frac{1}{a_n a_m} \langle \varnothing| \left( \sum_k \frac{v_k^*}{u_k^*} \hat{\mathrm{R}}_k \right)^n \left( \sum_q \frac{v_q}{u_q} \hat{\mathrm{R}}_q^\dagger \right)^m |\varnothing\rangle \\ &= \frac{\delta_{nm}}{a_n^2} \langle \varnothing| \left( \sum_{kq} \frac{v_k^* v_q}{u_k^* u_q} \left( \delta_{kq} + \hat{\mathrm{R}}_k^\dagger \hat{\mathrm{R}}_q - \delta_{kq} \sum_\sigma \hat{n}_{k\sigma} \right) \right)^n |\varnothing\rangle \\ &= \frac{\delta_{nm}}{a_n^2} \left( \sum_k \frac{|v_k|^2}{|u_k|^2} \right)^n \stackrel{!}{=} \delta_{nm}. \end{aligned} \tag{2.41}$$

We find:

$$a_n = \left( \sum_k \frac{|v_k|^2}{|u_k|^2} \right)^{n/2} \equiv a_1^n. \tag{2.42}$$

The best way to explain this is that each state $|n\rangle$ is living in a Fock space of $2n$ electrons, thus states with different number of particles are living in different subspaces and are orthogonal.
Finally we can use this to rename the normalization of the ground state:

$$\mathcal{N} = \left(\sum_n \left(\frac{1}{n!}\right)^2 a_n^2\right)^{-1/2}. \tag{2.43}$$

### 2.3.2. Occupation of the Cooper pair state

In this section we will show that the abstract reformulation of the BCS ground state has a concrete physical meaning. It will turn out that the state $|n\rangle$ contains $2n$ electrons or $n$ Cooper pairs:

$$\hat{N}\,|n\rangle = 2n\,|n\rangle\,. \tag{2.44}$$

We define a state with zero Cooper pairs as the vacuum state:

$$|0\rangle = |\varnothing\rangle\,. \tag{2.45}$$

The statement follows by induction:
**Basis:** $n = 1$

$$\hat{N}\,|1\rangle = \hat{N}\frac{1}{a_1}\sum_k \frac{v_k}{u_k}\hat{\mathrm{R}}_k^\dagger\,|0\rangle\,, \tag{2.46}$$

exploiting the commutation relation of Eq. (2.37):

$$\hat{N}\,|1\rangle = 2\,\frac{1}{a_1}\sum_k \frac{v_k}{u_k}\hat{\mathrm{R}}_k^\dagger\,|0\rangle = 2\,|1\rangle\,. \tag{2.47}$$

**Inductive step:**

$$\begin{aligned}
\hat{N}\,|n+1\rangle &= \hat{N}\left(\frac{1}{a_1}\right)^{n+1}\left(\sum_k \frac{v_k}{u_k}\hat{\mathrm{R}}_k^\dagger\right)^{n+1}|0\rangle \\
&= \hat{N}\frac{1}{a_1}\sum_k \frac{v_k}{u_k}\hat{\mathrm{R}}_k^\dagger\,|n\rangle \\
&= \frac{1}{a_1}\sum_k \frac{v_k}{u_k}\left(2\,\hat{\mathrm{R}}_k^\dagger + \hat{\mathrm{R}}_k^\dagger\hat{N}\right)|n\rangle \\
&= 2(n+1)\,|n+1\rangle \quad \square
\end{aligned} \tag{2.48}$$

In the step from the first to the second line of Eq. (2.48) we used the definition of the state $|n\rangle$, Eq. (2.39). As it can be seen from Eq. (2.39) Cooper pairs can be created with the following operator:

$$\hat{\mathrm{S}}^\dagger \equiv \frac{1}{a_1} \sum_k \frac{v_k}{u_k} \hat{\mathrm{R}}_k^\dagger. \tag{2.49}$$

We find that we are able to express a state with $n$ Cooper pairs by simply applying the Cooper pair creation operator $n$ times on the vacuum state:

$$|n\rangle \equiv \left(\hat{\mathrm{S}}^\dagger\right)^n |0\rangle\,, \tag{2.50}$$

such that

$$\hat{\mathrm{S}}^\dagger |n\rangle = \hat{\mathrm{S}}^\dagger \left(\hat{\mathrm{S}}^\dagger\right)^n |0\rangle = |n+1\rangle\,. \tag{2.51}$$

Note that the macroscopic phase which is present in this definition of the Cooper pair operator enters through the factor

$$v_k = e^{i\Phi} \sqrt{\frac{1}{2}\left(1 - \frac{\xi_k}{|E_k|}\right)}, \tag{2.52}$$

accordingly

$$\hat{\mathrm{S}}^\dagger \equiv e^{i\Phi} \frac{1}{a_1} \sum_k \frac{|v_k|}{|u_k|} \hat{\mathrm{R}}_k^\dagger. \tag{2.53}$$

### 2.3.3. Properties of the Cooper pair creation and annihilation operator

At the end of the previous section we identified the Cooper pair creation operator $\hat{\mathrm{S}}^\dagger$ which we will investigate in the following. We start with the commutation relation

$$\begin{aligned}
[\hat{\mathrm{S}}^\dagger, \hat{\mathrm{S}}] &= \left(\frac{1}{a_1}\right)^2 \sum_{kq} \frac{v_k v_q^*}{u_k u_q^*} [\hat{\mathrm{R}}_k^\dagger, \hat{\mathrm{R}}_q] \\
&= \left(\frac{1}{a_1}\right)^2 \sum_{k\sigma} \frac{|v_k|^2}{|u_k|^2} \left(\hat{n}_{k\sigma} - \frac{1}{2}\right) \\
&= -1 + \left(\frac{1}{a_1}\right)^2 \sum_{k\sigma} \frac{|v_k|^2}{|u_k|^2}\, \hat{n}_{k\sigma},
\end{aligned} \tag{2.54}$$

where we put a factor $\frac{1}{2}$ to compensate the spin summation and $\hat{n}_{k\sigma} = \hat{\mathrm{c}}_{k\sigma}^\dagger\, \hat{\mathrm{c}}_{k\sigma}$ is the number operator. We can calculate the commutator by acting on the groundstate, Eq. (2.30):

$$\left[\hat{\mathrm{S}}^\dagger, \hat{\mathrm{S}}\right] |\mathrm{GS}\rangle = -1 + \left(\frac{1}{a_1}\right)^2 \sum_{k\sigma} \frac{|v_k|^2}{|u_k|^2}\, \hat{n}_{k\sigma} \prod_l \left(u_l + v_l\, \hat{\mathrm{c}}^\dagger_{l\uparrow}\, \hat{\mathrm{c}}^\dagger_{-l\downarrow}\right) |\varnothing\rangle\,. \tag{2.55}$$

We use that $\hat{n}_{k\sigma}$ commutes with all terms of the product, except in the case $l = k$, thus

$$\begin{aligned}
&\left[\hat{\mathrm{S}}^\dagger, \hat{\mathrm{S}}\right] |\mathrm{GS}\rangle \\
&= -1 + \left(\frac{1}{a_1}\right)^2 \sum_{k\sigma} \frac{|v_k|^2}{|u_k|^2} \prod_{l\neq k} \left(u_l + v_l\, \hat{\mathrm{c}}^\dagger_{l\uparrow}\, \hat{\mathrm{c}}^\dagger_{-l\downarrow}\right) \hat{n}_{k\sigma} \left(u_k + v_k\, \hat{\mathrm{c}}^\dagger_{k\uparrow}\, \hat{\mathrm{c}}^\dagger_{-k\downarrow}\right) |\varnothing\rangle \\
&= -1 + \left(\frac{1}{a_1}\right)^2 \sum_{k\sigma} \frac{|v_k|^2}{|u_k|^2} \prod_{l\neq k} \left(u_l + v_l\, \hat{\mathrm{c}}^\dagger_{l\uparrow}\, \hat{\mathrm{c}}^\dagger_{-l\downarrow}\right) v_k\, \hat{\mathrm{c}}^\dagger_{k\uparrow} \left(\delta_{\sigma\uparrow} + \hat{n}_{k\sigma}\right) \hat{\mathrm{c}}^\dagger_{-k\downarrow} |\varnothing\rangle\,.
\end{aligned} \tag{2.56}$$

In Eq. (2.56) we use $[\hat{n}_{k\sigma}, \hat{\mathrm{c}}^\dagger_{-k\downarrow}] = 0$

$$\left[\hat{\mathrm{S}}^\dagger, \hat{\mathrm{S}}\right] |\mathrm{GS}\rangle = -1 + \left(\frac{1}{a_1}\right)^2 \sum_k \frac{|v_k|^2}{|u_k|^2} |\varnothing\rangle\,. \tag{2.57}$$

Inserting Eq. (2.42) we find:

$$\left[\hat{\mathrm{S}}^\dagger, \hat{\mathrm{S}}\right] = 0. \tag{2.58}$$

Furthermore, we present the commutator of the Cooper pair operator with the total electron number operator $\hat{N} = \sum_{k\sigma} \hat{\mathrm{c}}^\dagger_{k\sigma}\, \hat{\mathrm{c}}_{k\sigma}$:

$$\left[\hat{N}, \hat{\mathrm{S}}^\dagger\right] = 2\,\hat{\mathrm{S}}^\dagger, \tag{2.59}$$

and

$$\left[\hat{N}, \hat{\mathrm{S}}\right] = -2\,\hat{\mathrm{S}}\,. \tag{2.60}$$

Notice that the hermitian conjugate of the Cooper pair operator indeed lowers the occupation number of a state with $n$ Cooper pairs $|n\rangle$ by one. We can show this by using Eq. (2.60):

$$\hat{N}\,\hat{\mathrm{S}}\,|n\rangle = \left(-2\,\hat{\mathrm{S}} + \hat{\mathrm{S}}\,\hat{N}\right)|n\rangle = 2(n-1)\,\hat{\mathrm{S}}\,|n\rangle \equiv \hat{N}\,|n-1\rangle\,. \tag{2.61}$$

The next step is to observe the combination $\hat{\mathrm{S}}\,\hat{\mathrm{S}}^\dagger$. Again we act on the ground state, Eq. (2.38):

$$\hat{\mathrm{S}}\,\hat{\mathrm{S}}^\dagger\,|\mathrm{GS}\rangle = \sum_n b_n\,\hat{\mathrm{S}}\,\hat{\mathrm{S}}^\dagger\,|n\rangle = \sum_n b_n\,\hat{\mathrm{S}}\,|n+1\rangle = \sum_n b_n\,|n\rangle = 1\,|\mathrm{GS}\rangle\,. \tag{2.62}$$

So we find, using Eq. (2.58):

$$\hat{\mathrm{S}}\,\hat{\mathrm{S}}^{\dagger} = 1 = \hat{\mathrm{S}}^{\dagger}\,\hat{\mathrm{S}}\,. \tag{2.63}$$

## 2.4. Construction of a particle-number-conserving Bogoliubov transformation

For the diagonalization of the lead Hamiltonian in Sect. 2.2 we used the Bogoliubov transformation, Eqs. (2.22) and (2.23), introduced by Josephson [15]. He modified the transformation of Bogoliubov [4] with additional Cooper pair operators to conserve the particle number, but did not specified them further. In this section, we investigate if the transformation still suffices the requirements of a unitary transformation, when we insert the expression for the Cooper pair operators of Eq. (2.49). In addition the transformation should conserve the anticommutation relations of the electrons, and the average particle number. We can write the Bogoliubov transformation in a compact form:

$$\hat{c}_{k\sigma} = u_k^* \, \hat{\gamma}_{k\sigma} + \operatorname{sgn}\sigma \; v_k \, \hat{S} \, \hat{\gamma}^\dagger_{-k\bar{\sigma}} \,, \tag{2.64}$$

and its hermitian conjugate

$$\hat{c}^\dagger_{k\sigma} = u_k \, \hat{\gamma}^\dagger_{k\sigma} + \operatorname{sgn}\sigma \; v_k^* \, \hat{\gamma}_{-k\bar{\sigma}} \, \hat{S}^\dagger \,, \tag{2.65}$$

where

$$\operatorname{sgn}\sigma = \begin{cases} +1 & \text{for } \sigma = \uparrow \,, \\ -1 & \text{for } \sigma = \downarrow \,, \end{cases} \tag{2.66}$$

$$\bar{\sigma} = -\sigma. \tag{2.67}$$

We should notice that the coefficients $u_k$ and $v_k$ appear in the definition of the Bogoliubov transformation as well as in the definition of the BCS ground state, Eq. (2.30). This has historical reasons. In 1958, Bogoliubov found a new method to diagonalize the BCS Hamiltonian [4] and found formulas for $u_k$ and $v_k$ that confirm those of the BCS theory. In this section it is important to remember Eq. (2.24), i.e., that

$$|u_k|^2 + |v_k|^2 = 1 \,. \tag{2.68}$$

It turns out that in particular the analytical form of the Cooper pair operators is crucial for this work. For completeness we will also present the inversion of the transformation

$$\begin{pmatrix} \hat{\gamma}_{k\uparrow} \\ \hat{\gamma}^\dagger_{-k\downarrow} \end{pmatrix} = \begin{pmatrix} u_k & -v_k \, \hat{S} \\ v_k^* \, \hat{S}^\dagger & u_k^* \end{pmatrix} \begin{pmatrix} \hat{c}_{k\uparrow} \\ \hat{c}^\dagger_{-k\downarrow} \end{pmatrix}, \tag{2.69}$$

$$\begin{pmatrix} \hat{\gamma}^\dagger_{k\uparrow} \\ \hat{\gamma}_{-k\downarrow} \end{pmatrix} = \begin{pmatrix} u_k^* & -v_k^* \, \hat{S}^\dagger \\ v_k \, \hat{S} & u_k \end{pmatrix} \begin{pmatrix} \hat{c}^\dagger_{k\uparrow} \\ \hat{c}_{-k\downarrow} \end{pmatrix}, \tag{2.70}$$

which can be generalized to

$$\hat{\gamma}_{k\sigma} = u_k\,\hat{\mathrm{c}}_{k\sigma} - \operatorname{sgn}\sigma\, v_k\,\hat{\mathrm{S}}\,\hat{\mathrm{c}}^\dagger_{-k\bar{\sigma}}, \tag{2.71}$$

and its hermitian conjugate

$$\hat{\gamma}^\dagger_{k\sigma} = u^*_k\,\hat{\mathrm{c}}^\dagger_{k\sigma} - \operatorname{sgn}\sigma\, v^*_k\,\hat{\mathrm{S}}^\dagger\,\hat{\mathrm{c}}_{-k\bar{\sigma}}\,. \tag{2.72}$$

The generalized inverse transformation can easily be verified by inserting it in Eqs. (2.64) and (2.65).

### 2.4.1. Fermionic anticommutation relation

In the electron picture the following anticommutation relation holds

$$\{\hat{\mathrm{c}}^\dagger_{k\uparrow}, \hat{\mathrm{c}}_{k'\uparrow}\} \stackrel{!}{=} \delta_{kk'}. \tag{2.73}$$

Applying the Bogoliubov transformation of Eqs. (2.64) and (2.65) it follows

$$\begin{aligned}
&\{\hat{\mathrm{c}}^\dagger_{k\sigma}, \hat{\mathrm{c}}_{k'\sigma'}\} = \{u_k\,\hat{\gamma}^\dagger_{k\sigma} + \operatorname{sgn}\sigma\; v^*_k\,\hat{\gamma}_{-k\bar{\sigma}}\,\hat{\mathrm{S}}^\dagger, u^*_{k'}\,\hat{\gamma}_{k'\sigma'} + \operatorname{sgn}\sigma'\; v_{k'}\,\hat{\mathrm{S}}\,\hat{\gamma}^\dagger_{-k'\bar{\sigma}'}\} \\
&= u_k u^*_{k'}\{\hat{\gamma}^\dagger_{k\sigma}, \hat{\gamma}_{k'\sigma'}\} + \operatorname{sgn}\sigma \operatorname{sgn}\sigma' v^*_k v_{k'}\{\hat{\gamma}_{-k\bar{\sigma}}\,\hat{\mathrm{S}}^\dagger, \hat{\mathrm{S}}\,\hat{\gamma}^\dagger_{-k'\bar{\sigma}'}\} \\
&+ \operatorname{sgn}\sigma'\; u_k v_{k'}\{\hat{\gamma}^\dagger_{k\sigma}, \hat{\mathrm{S}}\,\hat{\gamma}^\dagger_{-k'\bar{\sigma}'}\} + \operatorname{sgn}\sigma\; v^*_k u^*_{k'}\{\hat{\gamma}_{-k\bar{\sigma}}\,\hat{\mathrm{S}}^\dagger, \hat{\gamma}_{k'\sigma'}\} \stackrel{!}{=} \delta_{kk'}\delta_{\sigma\sigma'}.
\end{aligned} \tag{2.74}$$

In the last line we demand that Eq. (2.73) is still valid.

#### Separation of Cooper pairs and bogoliubons

As the Cooper pair condensate is the vacuum state of the bogoliubons, they live in different spaces and we find that

$$\left[\hat{\mathrm{S}}, \hat{\gamma}^\dagger_{k\sigma}\right] = 0. \tag{2.75}$$

Using additionally the fermionic statistics of the bogoliubon operators

$$\{\hat{\gamma}^\dagger_{k\sigma}, \hat{\gamma}_{k'\sigma'}\} = \delta_{kk'}\delta_{\sigma\sigma'}, \tag{2.76}$$

we see that Eq. (2.74) is fulfilled.

### 2.4.2. Expectation value of the number operator

Finally we have to investigate the particle number conservation. We calculate the ground state expectation value of the total number operator $\hat{N}$ before and after the transformation. This can be thought of as the average number of electrons in the Cooper pair condensate.

#### Expectation value of the number operator in the electron regime

In the electron regime the ground state expectation value reads:

$$\langle \mathrm{GS}| \hat{N} |\mathrm{GS}\rangle = \langle \mathrm{GS}| \sum_{k\sigma} \hat{c}^\dagger_{k\sigma} \hat{c}_{k\sigma} |\mathrm{GS}\rangle \,, \tag{2.77}$$

where we use the standard representation of the BCS ground state, see Eq. (2.30)

$$|\mathrm{GS}\rangle \equiv \prod_l \left(u_l + v_l \, \hat{c}^\dagger_{l\uparrow} \hat{c}^\dagger_{-l\downarrow}\right) |\varnothing\rangle \,. \tag{2.78}$$

We present the detailed calculation in App. A.2.1:

$$\langle \mathrm{GS}| \hat{N} |\mathrm{GS}\rangle =: \langle \hat{N} \rangle = \sum_k 2 \, |v_k|^2. \tag{2.79}$$

This result is plausible, as $|v_k|^2$ can be interpreted as the probability of finding a pair of two electrons with opposite momenta $k$ and $-k$. In the ground state, at zero temperature, all electrons condense to Cooper pairs; the expectation value of the total electron number operator is twice the sum of all these probabilities.

#### Number operator after Bogoliubov transformation

We transform the total electron number operator $\hat{N}$ and calculate again the ground state expectation value

$$\begin{aligned}
&\langle \mathrm{GS}| \hat{N} |\mathrm{GS}\rangle \\
&= \sum_{k\sigma} \Big\{ |v_k|^2 \, \langle \mathrm{GS}| \hat{\gamma}_{-k\bar{\sigma}} \hat{\mathrm{S}}^\dagger \hat{\mathrm{S}} \hat{\gamma}^\dagger_{-k\bar{\sigma}} |\mathrm{GS}\rangle \\
&\qquad + \operatorname{sgn}\sigma \; u_k v_k \, \langle \mathrm{GS}| \hat{\gamma}^\dagger_{k\sigma} \hat{\mathrm{S}} \hat{\gamma}^\dagger_{-k\bar{\sigma}} |\mathrm{GS}\rangle \\
&\qquad + \operatorname{sgn}\sigma \; u_k^* v_k^* \, \langle \mathrm{GS}| \hat{\gamma}_{-k\bar{\sigma}} \hat{\mathrm{S}}^\dagger \hat{\gamma}_{k\sigma} |\mathrm{GS}\rangle \Big\} \\
&= \sum_k 2 \, |v_k|^2.
\end{aligned} \tag{2.80}$$

We used the relation $\hat{\mathrm{S}}^\dagger \hat{\mathrm{S}} = 1$ and

$$\langle \mathrm{GS}| \hat{\gamma}^\dagger_{k\sigma} \hat{\mathrm{S}} \hat{\gamma}^\dagger_{-k\bar{\sigma}} |\mathrm{GS}\rangle = 0, \tag{2.81}$$

$$\langle \mathrm{GS}| \hat{\gamma}_{-k\bar{\sigma}} \hat{\mathrm{S}}^\dagger \hat{\gamma}_{k\sigma} |\mathrm{GS}\rangle = 0. \tag{2.82}$$

Summarizing the previous results we have justified the validity of the transformation and in particular the representation of the Cooper pair operator.

## 2.5. Thermodynamic properties of the superconductor

In Sect. 2.3 we derived a representation of the BCS ground state as a superposition of states with a different number of Cooper pairs. In this context, we found an explicit representation for the Cooper pair creation and annihilation operators and derived all necessary commutation relations. In this section we will use these methods to investigate the thermodynamic properties of the electrons in the leads which are now described by quasiparticle excitations and Cooper pairs. Thus, it is required to find the equilibrium density matrix of the superconductor through which one can calculate thermodynamic expectation values.
Usually, we define the thermodynamic average of any operator $\hat{A}$ as:

$$\langle \hat{A} \rangle_{th} = \mathrm{Tr}\big(\hat{\rho}_B \hat{A}\big)\,, \tag{2.83}$$

where we trace over the electronic degrees of freedom in the leads, meaning over Bloch states $\hat{c}^\dagger_{k\sigma}\,|\varnothing\rangle = |k\sigma\rangle$. In the case of superconducting leads, we have a different situation as we are describing the electrons as both, quasiparticle excitations and Cooper pairs. The question arises, if we should trace over the fermionic degrees of freedom only and keep the Cooper pairs in the equations; or we trace out the whole electronic degrees of freedom? The answer is a bit subtle, as the Cooper pair condensate is the vacuum state of the Bogoliubov quasiparticles. Hence, tracing over the excitations necessarily includes its vacuum state. This justifies the definition of the grand canonical ensemble, in the new quasiparticle-Cooper pair-description, with the chemical potential of the electrons. Following these thoughts we define the equilibrium density matrix of the leads:

$$\hat{\rho}_B = \frac{e^{-\beta \hat{H}_G}}{Z_G}, \tag{2.84}$$

where $\hat{H}_G = \hat{H}_B - \mu \hat{N}$ and

$$Z_G = \mathrm{Tr_B}\Big(e^{-\beta \hat{H}_G}\Big). \tag{2.85}$$

It might be necessary that we have to calculate thermal expectation values with Bogoliubov and additional Cooper pair operators. Thus, it is important to understand the thermodynamic average at the level of second quantization in order to examine the action of $\hat{\mathrm{S}}$, $\hat{\mathrm{S}}^\dagger$. Hence, we define the many body states of the quasi particle excitations:

$$|\{n\}\rangle = \mathcal{N} \prod_{(q\tau)\in\{n\}} \hat{\gamma}^\dagger_{q\tau}\,|\mathrm{GS}\rangle\,, \tag{2.86}$$

The state $|\{n\}\rangle$ is a short hand notation for the occupation number representation, where $\{n\}$ is a set of occupation numbers $n_{k_i\sigma_i}$:

$$|\{n\}\rangle = |n_{k_1\sigma_1}, n_{k_2\sigma_2}, \dots\rangle\,. \tag{2.87}$$

In order to calculate the trace over the many body states, we have to investigate the action of the bogoliubon number operator

$$\hat{n}_{k\sigma} = \hat{\gamma}^\dagger_{k\sigma}\,\hat{\gamma}_{k\sigma} \tag{2.88}$$

on any many body state. It fulfills the following commutation relation:

$$\left[\hat{n}_{k\sigma}, \hat{\gamma}^\dagger_{q\tau}\right] = \hat{\gamma}^\dagger_{k\sigma}\,\delta_{kq}\delta_{\sigma\tau}. \tag{2.89}$$

First of all, consider a set $\{n\}$ in which the state $(k\sigma)$ is occupied ($n_{k\sigma} = 1$):

$$\begin{aligned}
\hat{n}_{k\sigma}\,|\{n\}\rangle &= \hat{n}_{k\sigma}\left(\mathcal{N}\prod_{(q\tau)\in\{n\}}\hat{\gamma}^\dagger_{q\tau}\,|\mathrm{GS}\rangle\right)\\
&= \mathcal{N}\prod_{\substack{(q\tau)\in\\ \{n\setminus(k\sigma)\}}}\hat{\gamma}^\dagger_{q\tau}\,\hat{n}_{k\sigma}\,\hat{\gamma}^\dagger_{k\sigma}\,|\mathrm{GS}\rangle = \mathcal{N}\prod_{\substack{(q\tau)\in\\ \{n\setminus(k\sigma)\}}}\hat{\gamma}^\dagger_{q\tau}\,\hat{\gamma}^\dagger_{k\sigma}(1+\hat{n}_{k\sigma})\,|\mathrm{GS}\rangle\\
&= \mathcal{N}\prod_{(q\tau)\in\{n\}}\hat{\gamma}^\dagger_{q\tau}\,|\mathrm{GS}\rangle = |\{n\}\rangle\,,
\end{aligned} \tag{2.90}$$

on the other hand, if $n_{k\sigma} = 0$ in $\{n\}$, $\hat{n}_{k\sigma}$ commutes with all operators and gives zero. Finally we found the following relations:

$$\hat{n}_{k\sigma}\,|\{n\}\rangle = \begin{cases} |\{n\}\rangle & \text{if } n_{k\sigma} = 1 \text{ in } \{n\},\\ 0 & \text{if } n_{k\sigma} = 0 \text{ in } \{n\}. \end{cases} \tag{2.91}$$

Now we are able to calculate the following trace [10, p. 37]

$$\mathrm{Tr_B}\left(\hat{\rho}_B\hat{n}_{k\sigma}\right) = \mathrm{Tr_B}\left(\frac{e^{-\beta\hat{H}_G}}{Z_G}\hat{n}_{k\sigma}\right), \tag{2.92}$$

where we write

$$e^{-\beta\hat{H}_G} = e^{-\beta\sum_{q\tau}E_q\hat{n}_{q\tau}} = \prod_{(q\tau)} e^{-\beta E_q\hat{n}_{q\tau}}. \tag{2.93}$$

We start calculating the denominator:

$$Z_G = \mathrm{Tr_B}\left(\prod_{(q\tau)} e^{-\beta E_q\hat{n}_{q\tau}}\right) = \sum_{\{n\}}\langle\{n\}|\prod_{(q\tau)} e^{-\beta E_q\hat{n}_{q\tau}}\,|\{n\}\rangle\,. \tag{2.94}$$

In the next step, we use the fermionic properties the bogoliubons, meaning that each exponential acting on a many body state $e^{-\beta E_q \hat{n}_{q\tau}} |\{n\}\rangle$ equals $e^{-\beta E_q n_{q\tau}}$, if the state $(q\tau)$ is occupied, or 1, if not. Therefore, we can write the trace as:

$$\begin{aligned} &\sum_{n_{k_1\sigma_1}} \langle n_{k_1\sigma_1}| e^{-\beta E_{k_1} n_{k_1\sigma_1}} |n_{k_1\sigma_1}\rangle \sum_{n_{k_2\sigma_2}} \langle n_{k_2\sigma_2}| e^{-\beta E_{k_2} n_{k_2\sigma_2}} |n_{k_2\sigma_2}\rangle \times \dots \\ &\dots \times \sum_{n_{k_\infty\sigma_\infty}} \langle n_{k_\infty\sigma_\infty}| e^{-\beta E_{k_\infty} n_{k_\infty\sigma_\infty}} |n_{k_\infty\sigma_\infty}\rangle , \end{aligned} \tag{2.95}$$

where each part can be evaluated separately:

$$\sum_{n_{k_i\sigma_i}=0,1} \langle n_{k_i\sigma_i}| e^{-\beta E_{k_i} n_{k_i\sigma_i}} |n_{k_i\sigma_i}\rangle = 1 + e^{-\beta E_{k_i}} . \tag{2.96}$$

On the other hand, we have the nominator

$$\mathrm{Tr_B}\left( \prod_{(q\tau)} e^{-\beta E_q \hat{n}_{q\tau}} \hat{n}_{k\sigma} \right) = \sum_{\{n\}} \langle \{n\}| \prod_{(q\tau)} e^{-\beta E_q \hat{n}_{q\tau}} \hat{n}_{k\sigma} |\{n\}\rangle , \tag{2.97}$$

that splits exactly as before into products of the single occupation numbers only differing by one term:

$$\sum_{n_{k\sigma}=0,1} e^{-\beta E_k n_{k\sigma}} n_{k\sigma} = e^{-\beta E_k} . \tag{2.98}$$

Finally, all terms apart from

$$\frac{e^{-\beta E_k}}{1 + e^{-\beta E_k}} = \frac{1}{e^{\beta E_k} + 1} = f^+(E_k) \tag{2.99}$$

cancel. Eq. (2.99) gives the desired Fermi function.
For clarity, we will present an example of the calculation of the trace in a very small toy model with only two states $|\{n\}\rangle = |\{n_1, n_2\}\rangle$. Here we can have the following configurations

$$|\{n_1, n_2\}\rangle = \begin{cases} |0,0\rangle \\ |1,0\rangle \\ |0,1\rangle \\ |1,1\rangle \end{cases} \tag{2.100}$$

yielding:

$$\begin{aligned}
&\mathrm{Tr_B}(e^{-\beta\sum_k E_k\hat{n}_k}) = \sum_{\{n\}} \langle\{n\}|\, e^{-\beta E_k\hat{n}_k}\,|\{n\}\rangle \\
&= \langle 0,0|\, e^0\,|0,0\rangle + \langle 1,0|\, e^{-\beta E_1}\,|1,0\rangle \\
&+ \langle 0,1|\, e^{-\beta E_2}\,|0,1\rangle + \langle 1,1|\, e^{-\beta(E_1+E_2)}\,|1,1\rangle \\
&= (1+e^{-\beta E_1})(1+e^{-\beta E_1}) \\
&= \sum_{n_1=0,1} e^{-\beta E_1 n_1} \sum_{n_2=0,1} e^{-\beta E_2 n_2}.
\end{aligned} \tag{2.101}$$

**Influence of the Cooper pair operator on the trace over the leads** Consider the case where we trace over a combination of Bogoliubov and Cooper pair operators:

$$\mathrm{Tr_B}\big(\hat{\rho}_B\,\hat{\gamma}^\dagger_{k\sigma}\,\hat{\gamma}_{k\sigma}\,\hat{\mathrm{S}}^\dagger\big). \tag{2.102}$$

The operator $\hat{\mathrm{S}}^\dagger$ is commuting with the bogoliubon creation and annihilation operators. Thus we are only interested in the BCS ground state expectation value of the Cooper pair operator. Using the representation of the BCS ground state derived in Sect. 2.3, we get:

$$\begin{aligned}
\langle \mathrm{GS}|\,\hat{\mathrm{S}}^\dagger\,|\mathrm{GS}\rangle &= \sum_{n,m} b_n b_m\,\langle n|\,\hat{\mathrm{S}}^\dagger\,|m\rangle \\
&= \sum_{n,m} b_n b_m\,\delta_{n,m+1} = \sum_n b_{n+1} b_n.
\end{aligned} \tag{2.103}$$

Inserting the definition of $b_n$, we obtain:

$$\begin{aligned}
\langle \mathrm{GS}|\,\hat{\mathrm{S}}^\dagger\,|\mathrm{GS}\rangle &= \mathcal{N}^2 \sum_n \frac{a_n a_{n+1}}{n!(n+1)!} \\
&= \mathcal{N}^2 \sum_n \frac{(a_1)^{2n+1}}{(n!)(n+1)!}.
\end{aligned} \tag{2.104}$$

Using the series definition of the modified Bessel function of first kind [1, p. 375]

$$I_1(x) = \sum_{k=0}^{\infty} \frac{\left(\frac{x}{2}\right)^{2k+1}}{k!(k+1)!)} \tag{2.105}$$

permits us to express the sum of Eq. (2.104) as a Bessel function:

$$\sum_n \frac{(a_1)^{2n+1}}{(n!)^2(n+1)} = I_1(2a_1). \tag{2.106}$$

Together with the normalization, App. A.3,

$$\mathcal{N}^2 = \frac{1}{I_0(2a_1)}, \tag{2.107}$$

the ground state expectation value of the Cooper pair operator becomes:

$$\langle \mathrm{GS}| \hat{\mathrm{S}}^\dagger |\mathrm{GS}\rangle = \frac{I_1(2a_1)}{I_0(2a_1)} \xrightarrow{a_1 \xrightarrow{V\to\infty}\infty} 1. \tag{2.108}$$

The value of the limes is obvious, if one considers the asymptotic expansion of the modified Bessel functions [5, p. 529]

$$I_n(x) = \frac{e^x}{\sqrt{2\pi x}}\big[1 + \mathcal{O}(\frac{1}{x})\big], \tag{2.109}$$

which is independent of $n$.
Eventually, we can calculate the trace in exactly the same way as in the last paragraph, Eq. (2.97). The procedure becomes clear, if we look again at the example of Eq. (2.101). Specifically the Cooper pair operator appears in every term like

$$\langle 0,0| \hat{\mathrm{S}}^\dagger |0,0\rangle = 1, \tag{2.110}$$

or

$$e^{-\beta E_1} \langle 1,0| \hat{\mathrm{S}}^\dagger |1,0\rangle = e^{-\beta E_1}, \tag{2.111}$$

meaning that we end up with the same sum as before, since the ground state expectation value of $\hat{\mathrm{S}}^\dagger$ is equal to one. We find again the Fermi function:

$$\mathrm{Tr_B}\big(\hat{\rho}_B\, \hat{\gamma}^\dagger_{k\sigma}\, \hat{\gamma}_{k\sigma}\, \hat{\mathrm{S}}^\dagger\big) = \frac{1}{e^{\beta E_k}+1}. \tag{2.112}$$

# 3. Quantum transport theory and the Generalized Master Equation

In Chap. 2.1 we introduced the Hamiltonian for a general transport setup of a quantum dot device weakly coupled to superconducting leads. The aim of this chapter is to develop a transport theory which enables us to calculate measurable quantities like the current or the differential conductance. We use the so called Generalized Master Equation (GME) approach, generalized in the Bloch-Redfield form of the GME at the end of this chapter. The general master equation, derived in the following, describes the time evolution of the density matrix up to second order in the tunneling Hamiltonian, which we use as perturbation due to the weak tunneling links.

## 3.1. Derivation of the Master Equation

### 3.1.1. General introduction to the master equation

We start with the Liouville equation in the interaction picture, which can easily be derived using

$$\hat{\rho}_I(t) = \hat{\mathrm{U}}_\mathrm{I}^\dagger(t)\hat{\rho}(0)\,\hat{\mathrm{U}}_\mathrm{I}(t), \tag{3.1}$$

and

$$i\hbar\frac{\partial}{\partial t}\,\hat{\mathrm{U}}_\mathrm{I}(t) = \hat{V}_I(t)\,\hat{\mathrm{U}}_\mathrm{I}(t), \tag{3.2}$$

where $\hat{V}_I(t)$ is the interaction term of the Hamiltonian in the interaction picture. Matching both, we arrive at the **Liouville equation in the interaction picture**:

$$\boxed{i\hbar\frac{\partial}{\partial t}\hat{\rho}_I(t) = \big[\hat{V}_I(t), \hat{\rho}_I(t)\big].} \tag{3.3}$$

Eq. (3.3) can formally be integrated

$$\hat{\rho}_I(t) = \hat{\rho}_I(0) - \frac{i}{\hbar}\int_0^t dt' \big[\hat{V}_I(t'), \hat{\rho}_I(t')\big], \tag{3.4}$$

and then inserted into itself, yielding

$$\boxed{i\hbar\frac{\partial}{\partial t}\hat{\rho}_I(t) = \left[\hat{V}_I(t), \hat{\rho}_I(0)\right] - \frac{i}{\hbar}\int_0^t dt' \left[\hat{V}_I(t), \left[\hat{V}_I(t'), \hat{\rho}_I(t')\right]\right].} \tag{3.5}$$

With Eq. (3.5) we have a form of the master equation which is still **exact** at this level and allows a perturbative treatment in the perturbation $\hat{V}(t)$. In this thesis we are only interested in second order perturbation theory, so we can stop at this level of iteration.

### 3.1.2. The reduced density matrix

As already mentioned in Sect. 2.1, the total Hamiltonian consists of three parts: One for the leads, the second one containing the quantum dot, and a tunneling part, which we treat as a perturbation in the weak tunneling limit. Since we are only interested in the properties of the dot, we can trace out the lead degrees of freedom. This procedure leads to an equation for the reduced density matrix:

$$\begin{aligned}\dot{\hat{\rho}}_{red,I}(t) = &-\frac{i}{\hbar}\,\mathrm{Tr_B}\Big\{\left[\hat{V}_I(t), \hat{\rho}_I(0)\right]\Big\} \\ &-\left(\frac{1}{\hbar}\right)^2 \int_0^t dt'\,\mathrm{Tr_B}\Big\{\left[\hat{V}_I(t), \left[\hat{V}_I(t'), \hat{\rho}_I(t')\right]\right]\Big\},\end{aligned} \tag{3.6}$$

where

$$\hat{\rho}_{red,I}(t) := \mathrm{Tr_B}\big\{\hat{\rho}_I(t)\big\}. \tag{3.7}$$

In order to proceed, we have to make some assumptions on the structure of $\hat{\rho}$. Prior to $t = 0$, we assume that the leads (B) and the system (S) do not interact so that the density matrix can be written as a product of two matrices:

$$\hat{\rho}(0) = \hat{\rho}_S(0)\hat{\rho}_B(0) = \hat{\rho}_I(0). \tag{3.8}$$

Here $\hat{\rho}_B(0)$ is the equilibrium density operator in the leads, described by the usual equilibrium thermodynamics distribution introduced in Sect. 2.5:

$$\hat{\rho}_B(0) = \frac{e^{-\beta(\hat{H}_B - \mu\hat{N})}}{Z_G} \equiv \hat{\rho}_B. \tag{3.9}$$

Now we introduce another approximation in order to get a more compact expression for the time evolution of the total density operator. In our theory we consider the leads as a thermal bath, meaning that they have so many degrees of freedom that their interaction with the system dissipates away quickly. For that reason, the leads remain in thermal equilibrium up to a correction of order $\hat{V}$:

$$\hat{\rho}_I(t) = \hat{\rho}_{S,I}(t)\hat{\rho}_B(0) + \mathcal{O}(\hat{V}). \tag{3.10}$$

Finally, we can insert Eq. (3.10) in Eq. (3.6), keeping only terms up to second order in the perturbation $\hat{V}$. We obtain

$$\begin{aligned}\dot{\hat{\rho}}_{red,I}(t) = &-\frac{i}{\hbar}\,\mathrm{Tr_B}\Big\{\big[\hat{V}_I(t), \hat{\rho}_S(0)\hat{\rho}_B\big]\Big\} \\ &-\left(\frac{1}{\hbar}\right)^2 \int_0^t dt'\,\mathrm{Tr_B}\Big\{\Big[\hat{V}_I(t), \big[\hat{V}_I(t'), \hat{\rho}_{S,I}(t')\hat{\rho}_B\big]\Big]\Big\} + \mathcal{O}(\hat{V}^3).\end{aligned} \tag{3.11}$$

The first term of Eq. (3.11) vanishes, as we will show later. In order to arrive at the starting point of the transport calculations, we have to transform Eq. (3.11) back to the Schrödinger picture.
We use the relation

$$\frac{\partial}{\partial t}\hat{\rho}_{red,I}(t) = \frac{\partial}{\partial t}\big(\hat{\mathrm{U}}_0^\dagger(t)\hat{\rho}_{red}(t)\,\hat{\mathrm{U}}_0(t)\big), \tag{3.12}$$

where

$$\hat{\mathrm{U}}_0(t) = e^{-\frac{i}{\hbar}\hat{H}_S t}, \tag{3.13}$$

is the time evolution operator of the unperturbed system. Note that only the system Hamiltonian contributes to the time evolution, because the leads are already traced out. Hence,

$$\begin{aligned}&\frac{\partial}{\partial t}\hat{\rho}_{red,I}(t) = \frac{i}{\hbar}\big[\hat{H}_S, \hat{\rho}_{red,I}(t)\big] + \hat{\mathrm{U}}_0^\dagger(t)\dot{\hat{\rho}}_{red}(t)\,\hat{\mathrm{U}}_0(t) \\ \Rightarrow\quad &\dot{\hat{\rho}}_{red}(t) = \hat{\mathrm{U}}_0(t)\dot{\hat{\rho}}_{red,I}(t)\,\hat{\mathrm{U}}_0^\dagger(t) + \frac{i}{\hbar}\big[\hat{\rho}_{red}(t), \hat{H}_0\big].\end{aligned} \tag{3.14}$$

Time dependent operators with no subscript "$I$", e.g. $\hat{\rho}_{red}(t)$, are again operators in the Schrödinger picture. Now we can replace $\dot{\hat{\rho}}_{red,I}(t)$ in Eq. (3.14) by the expression of Eq. (3.11), where we neglect terms of order $\mathcal{O}(\hat{V}^3)$:

$$\begin{aligned}\dot{\hat{\rho}}_{red}(t) = &\frac{i}{\hbar}\big[\hat{\rho}_{red}(t), \hat{H}_S\big] - \\ &-\left(\frac{1}{\hbar}\right)^2 \hat{\mathrm{U}}_0(t)\int_0^t dt'\,\mathrm{Tr_B}\Big\{\Big[\hat{V}_I(t), \big[\hat{V}_I(t'), \hat{\rho}_{red,I}(t')\hat{\rho}_B\big]\Big]\Big\}\,\hat{\mathrm{U}}_0^\dagger(t).\end{aligned} \tag{3.15}$$

### Calculating the double commutators

The calculation of the double commutator in Eq. (3.15) is a lengthy, but necessary, task. At first we have to specify the perturbation $\hat{V}_I(t)$. In our case it is the tunneling Hamiltonian between the system and the leads, which is introduced in Sect. 2.1:

$$\hat{V}_I(t) \equiv \hat{H}_{T,I}(t) = \sum_{\eta k\sigma}\left( t\,\hat{c}^\dagger_{\eta k\sigma,I}(t)\,\hat{d}_{j\sigma,I}(t) + t^*\,\hat{d}^\dagger_{j\sigma,I}(t)\,\hat{c}_{\eta k\sigma,I}(t)\right). \tag{3.16}$$

The time evolution is governed by the Hamiltonians $\hat{H}_B$ and $\hat{H}_S$ respectively:

$$\hat{d}_{j\sigma,I}(t) = e^{+\frac{i}{\hbar}\hat{H}_S t}\,\hat{d}_{j\sigma}\,e^{-\frac{i}{\hbar}\hat{H}_S t}, \tag{3.17}$$

$$\hat{c}_{\eta k\sigma,I}(t) = e^{+\frac{i}{\hbar}\hat{H}_B t}\,\hat{c}_{\eta k\sigma}\,e^{-\frac{i}{\hbar}\hat{H}_B t}. \tag{3.18}$$

From the definition of the commutators it follows that

$$\begin{aligned}&\left[\hat{H}_T(t),\left[\hat{H}_T(t'),\hat{\rho}_{red}(t')\hat{\rho}_B\right]\right]\\ &= \hat{H}_T(t)\hat{H}_T(t')\hat{\rho}_{red}(t)\hat{\rho}_B + \hat{\rho}_{red}\hat{\rho}_B\hat{H}_T(t')\hat{H}_T(t)\\ &- \hat{H}_T(t)\hat{\rho}_{red}(t)\hat{\rho}_B\hat{H}_T(t') - \hat{H}_T(t')\hat{\rho}_{red}(t)\hat{\rho}_B\hat{H}_T(t).\end{aligned} \tag{3.19}$$

Inserting the tunneling Hamiltonian, Eq. (3.16 ), in Eq. (3.19) leads to 16 terms which we will not give explicitly. Nevertheless, it is useful to write down the result for $\hat{H}_T(t)\hat{H}_T(t')$, which provides the basic structure for further calculations. We have:

$$\begin{aligned}\hat{H}_T(t)\hat{H}_T(t') = \sum_{\substack{\eta\eta' kk'\\ \sigma\sigma' jj'}}\Big\{\; & |t|^2\;\{\hat{c}^\dagger_{\eta k\sigma}(t)\,\hat{d}_{j\sigma}(t)\,\hat{d}^\dagger_{j'\sigma'}(t')\,\hat{c}_{\eta' k'\sigma'}(t')\\ & + \hat{d}^\dagger_{j\sigma}(t)\,\hat{c}_{\eta k\sigma}(t)\,\hat{c}^\dagger_{\eta' k'\sigma'}(t')\,\hat{d}_{j'\sigma'}(t')\}\\ & + t^2\;\hat{c}^\dagger_{\eta k\sigma}(t)\,\hat{d}_{j\sigma}(t)\,\hat{c}^\dagger_{\eta' k'\sigma'}(t')\,\hat{d}_{j'\sigma'}(t')\\ & + (t^*)^2\;\hat{d}^\dagger_{j\sigma}(t)\,\hat{c}_{\eta k\sigma}(t)\,\hat{d}^\dagger_{j'\sigma'}(t')\,\hat{c}_{\eta' k'\sigma'}(t')\Big\}.\end{aligned} \tag{3.20}$$

#### Trace over the leads

To move on with the evaluation of the equations for the reduced density matrix, Eq. (3.15), we have to evaluate the trace over the leads by inserting the explicit form of the double commutator calculated in Eq. (3.19). As both, dot and lead operators, appear in the trace, we have to order them in such a way that all lead operators are grouped. To this end, we exploit the anticommutation relations between electrons of the lead and electrons of the system. After we have managed to group the lead operators in the trace we can put the rest outside and perform the trace. Note that the trace over some lead operators is just a number which we can move around as we like. But it is of particular importance to keep the order of the dot and the lead operators.
We will not present the whole calculation here, but rather give some interesting examples to show how it works. Afterwards we show the final result.

#### Examples of arranging the trace

1. No anticommutation necessary

$$\begin{aligned}
&\mathrm{Tr_B}\Big(\hat{\mathrm{d}}^\dagger_{j\sigma}\,\hat{\mathrm{c}}_{\eta k\sigma}\,\hat{\mathrm{c}}^\dagger_{\eta' k'\sigma'}\,\hat{\mathrm{d}}_{j'\sigma'}\,\hat{\rho}_{red}(t')\hat{\rho}_B\Big)\\
&=\hat{\mathrm{d}}^\dagger_{j\sigma}\,\mathrm{Tr_B}\Big(\hat{\mathrm{c}}_{\eta k\sigma}\,\hat{\mathrm{c}}^\dagger_{\eta' k'\sigma'}\,\hat{\rho}_B\Big)\,\hat{\mathrm{d}}_{j'\sigma'}\,\hat{\rho}_{red}(t')\\
&=\hat{\mathrm{d}}^\dagger_{j\sigma}\,\hat{\mathrm{d}}_{j'\sigma'}\,\hat{\rho}_{red}(t')\,\mathrm{Tr_B}\Big(\hat{\mathrm{c}}_{\eta k\sigma}\,\hat{\mathrm{c}}^\dagger_{\eta' k'\sigma'}\,\hat{\rho}_B\Big).
\end{aligned}\tag{3.21}$$

2. Three anticommutations ($\rightarrow$ minus sign)

$$\begin{aligned}
&\mathrm{Tr_B}\Big(\hat{\mathrm{c}}^\dagger_{\eta k\sigma}\,\hat{\mathrm{d}}_{j\sigma}\,\hat{\mathrm{c}}^\dagger_{\eta' k'\sigma'}\,\hat{\mathrm{d}}^\dagger_{j'\sigma'}\,\hat{\rho}_{red}(t')\hat{\rho}_B\Big)\\
&=\mathrm{Tr_B}\Big(\hat{\mathrm{d}}_{j\sigma}\,\hat{\mathrm{c}}^\dagger_{\eta k\sigma}\,\hat{\mathrm{d}}^\dagger_{j'\sigma'}\,\hat{\mathrm{c}}^\dagger_{\eta' k'\sigma'}\,\hat{\rho}_{red}(t')\hat{\rho}_B\Big)\\
&=-\mathrm{Tr_B}\Big(\hat{\mathrm{d}}_{j\sigma}\,\hat{\mathrm{d}}^\dagger_{j'\sigma'}\,\hat{\mathrm{c}}^\dagger_{\eta k\sigma}\,\hat{\mathrm{c}}^\dagger_{\eta' k'\sigma'}\,\hat{\rho}_{red}(t')\hat{\rho}_B\Big)\\
&=-\hat{\mathrm{d}}_{j\sigma}\,\hat{\mathrm{d}}^\dagger_{j'\sigma'}\,\hat{\rho}_{red}(t')\,\mathrm{Tr_B}\Big(\hat{\mathrm{c}}^\dagger_{\eta k\sigma}\,\hat{\mathrm{c}}^\dagger_{\eta' k'\sigma'}\,\hat{\rho}_B\Big).
\end{aligned}\tag{3.22}$$

### 3.1.3. General Master Equation for the reduced density matrix

Putting things together, we found an expression for the time evolution of the reduced density matrix in the Schrödinger picture up to second order in the perturbation, often called General Master Equation (GME). It reads:

$$
\begin{aligned}
&\dot{\hat{\rho}}_{red}(t) = \frac{i}{\hbar}\big[\hat{\rho}_{red}(t), \hat{H}_0\big] - \\
&- \left(\frac{1}{\hbar}\right)^2 \hat{\mathrm{U}}_0(t) \int_0^t dt' \sum_{\substack{\eta\eta' kk' \\ \sigma\sigma' jj'}} \Big\{ \\
&\Big[ |t|^2 \ \{ \ \hat{\mathrm{d}}_{j\sigma}(t)\, \hat{\mathrm{d}}^\dagger_{j'\sigma'}(t')\, \mathrm{Tr_B}\Big(\hat{\mathrm{c}}^\dagger_{\eta k\sigma}(t)\, \hat{\mathrm{c}}_{\eta' k'\sigma'}(t')\hat{\rho}_B\Big) + \hat{\mathrm{d}}^\dagger_{j\sigma}(t)\, \hat{\mathrm{d}}_{j'\sigma'}(t')\, \mathrm{Tr_B}\Big(\hat{\mathrm{c}}_{\eta k\sigma}(t)\, \hat{\mathrm{c}}^\dagger_{\eta' k'\sigma'}(t')\hat{\rho}_B\Big) \ \} \\
&- t^2 \ \hat{\mathrm{d}}_{j\sigma}(t)\, \hat{\mathrm{d}}_{j'\sigma'}(t')\, \mathrm{Tr_B}\Big(\hat{\mathrm{c}}^\dagger_{\eta k\sigma}(t)\, \hat{\mathrm{c}}^\dagger_{\eta' k'\sigma'}(t')\hat{\rho}_B\Big) - (t^*)^2 \ \hat{\mathrm{d}}^\dagger_{j\sigma}(t)\, \hat{\mathrm{d}}^\dagger_{j'\sigma'}(t')\, \mathrm{Tr_B}\Big(\hat{\mathrm{c}}_{\eta k\sigma}(t)\, \hat{\mathrm{c}}_{\eta' k'\sigma'}(t')\hat{\rho}_B\Big)\Big] \hat{\rho}_{red}(t') \\
&+ \hat{\rho}_{red}(t')\Big[ |t|^2 \ \{ \ \hat{\mathrm{d}}_{j'\sigma'}(t')\, \hat{\mathrm{d}}^\dagger_{j\sigma}(t)\, \mathrm{Tr_B}\Big(\hat{\mathrm{c}}^\dagger_{\eta' k'\sigma'}(t')\, \hat{\mathrm{c}}_{\eta k\sigma}(t)\hat{\rho}_B\Big) + \hat{\mathrm{d}}^\dagger_{j'\sigma'}(t')\, \hat{\mathrm{d}}_{j\sigma}(t)\, \mathrm{Tr_B}\Big(\hat{\mathrm{c}}_{\eta' k'\sigma'}(t')\, \hat{\mathrm{c}}^\dagger_{\eta k\sigma}(t)\hat{\rho}_B\Big)\} \\
&- t^2 \ \hat{\mathrm{d}}_{j'\sigma'}(t')\, \hat{\mathrm{d}}_{j\sigma}(t)\, \mathrm{Tr_B}\Big(\hat{\mathrm{c}}^\dagger_{\eta' k'\sigma'}(t')\, \hat{\mathrm{c}}^\dagger_{\eta k\sigma}(t)\hat{\rho}_B\Big) - (t^*)^2 \ \hat{\mathrm{d}}^\dagger_{j'\sigma'}(t')\, \hat{\mathrm{d}}^\dagger_{j\sigma}(t)\, \mathrm{Tr_B}\Big(\hat{\mathrm{c}}_{\eta' k'\sigma'}(t')\, \hat{\mathrm{c}}_{\eta k\sigma}(t)\hat{\rho}_B\Big)\Big] \\
&- \Big[ |t|^2 \ \{ \ \hat{\mathrm{d}}_{j\sigma}(t)\hat{\rho}_{red}(t')\, \hat{\mathrm{d}}^\dagger_{j'\sigma'}(t')\, \mathrm{Tr_B}\Big(\hat{\mathrm{c}}_{\eta' k'\sigma'}(t')\, \hat{\mathrm{c}}^\dagger_{\eta k\sigma}(t)\hat{\rho}_B\Big) + \hat{\mathrm{d}}^\dagger_{j\sigma}(t)\hat{\rho}_{red}(t')\, \hat{\mathrm{d}}_{j'\sigma'}(t')\, \mathrm{Tr_B}\Big(\hat{\mathrm{c}}^\dagger_{\eta' k'\sigma'}(t')\, \hat{\mathrm{c}}_{\eta k\sigma}(t)\hat{\rho}_B\Big) \ \} \\
&- t^2 \ \hat{\mathrm{d}}_{j\sigma}(t)\hat{\rho}_{red}(t')\, \hat{\mathrm{d}}_{j'\sigma'}(t')\, \mathrm{Tr_B}\Big(\hat{\mathrm{c}}^\dagger_{\eta' k'\sigma'}(t')\, \hat{\mathrm{c}}^\dagger_{\eta k\sigma}(t)\hat{\rho}_B\Big) - (t^*)^2 \ \hat{\mathrm{d}}^\dagger_{j\sigma}(t)\hat{\rho}_{red}(t')\, \hat{\mathrm{d}}^\dagger_{j'\sigma'}(t')\, \mathrm{Tr_B}\Big(\hat{\mathrm{c}}_{\eta' k'\sigma'}(t')\, \hat{\mathrm{c}}_{\eta k\sigma}(t)\hat{\rho}_B\Big)\Big] \\
&- \Big[ |t|^2 \ \{ \ \hat{\mathrm{d}}_{j'\sigma'}(t')\hat{\rho}_{red}(t')\, \hat{\mathrm{d}}^\dagger_{j\sigma}(t)\, \mathrm{Tr_B}\Big(\hat{\mathrm{c}}_{\eta k\sigma}(t)\, \hat{\mathrm{c}}^\dagger_{\eta' k'\sigma'}(t')\hat{\rho}_B\Big) + \hat{\mathrm{d}}^\dagger_{j'\sigma'}(t')\hat{\rho}_{red}(t')\, \hat{\mathrm{d}}_{j\sigma}(t)\, \mathrm{Tr_B}\Big(\hat{\mathrm{c}}^\dagger_{\eta k\sigma}(t)\, \hat{\mathrm{c}}_{\eta' k'\sigma'}(t')\hat{\rho}_B\Big)\} \\
&- t^2 \ \hat{\mathrm{d}}_{j'\sigma'}(t')\hat{\rho}_{red}(t')\, \hat{\mathrm{d}}_{j\sigma}(t)\, \mathrm{Tr_B}\Big(\hat{\mathrm{c}}^\dagger_{\eta k\sigma}(t)\, \hat{\mathrm{c}}^\dagger_{\eta' k'\sigma'}(t')\hat{\rho}_B\Big) - (t^*)^2 \ \hat{\mathrm{d}}^\dagger_{j'\sigma'}(t')\hat{\rho}_{red}(t')\, \hat{\mathrm{d}}^\dagger_{j\sigma}(t)\, \mathrm{Tr_B}\Big(\hat{\mathrm{c}}_{\eta k\sigma}(t)\, \hat{\mathrm{c}}_{\eta' k'\sigma'}(t')\hat{\rho}_B\Big)\Big]\Big\} \hat{\mathrm{U}}^\dagger_0(t).
\end{aligned}
\tag{3.23}
$$

In the last equation we dropped the subscript $I$ at the electron operators of the leads and system, respectively. If we look closer at Eq. (3.23) we see that there are only four different traces which have to be calculated:

$$\sum_{kk'\sigma\sigma'} \mathrm{Tr_B}\Big(\hat{c}^\dagger_{\eta k\sigma,I}(t)\,\hat{c}_{\eta' k'\sigma',I}(t')\hat{\rho}_B\Big), \tag{3.24}$$

$$\sum_{kk'\sigma\sigma'} \mathrm{Tr_B}\Big(\hat{c}_{\eta k\sigma,I}(t)\,\hat{c}^\dagger_{\eta' k'\sigma',I}(t')\hat{\rho}_B\Big), \tag{3.25}$$

$$\sum_{kk'\sigma\sigma'} \mathrm{Tr_B}\Big(\hat{c}^\dagger_{\eta k\sigma,I}(t)\,\hat{c}^\dagger_{\eta' k'\sigma',I}(t')\hat{\rho}_B\Big), \tag{3.26}$$

$$\sum_{kk'\sigma\sigma'} \mathrm{Tr_B}\Big(\hat{c}_{\eta k\sigma,I}(t)\,\hat{c}_{\eta' k'\sigma',I}(t')\hat{\rho}_B\Big). \tag{3.27}$$

At this point we still have electron operators in the equation. Since we are interested in transport properties of quantum dot devices coupled to superconducting leads, we have to rewrite the traces in terms of quasiparticle excitations of the superconductor.

### 3.1.4. Introducing superconductivity

The next step in the analysis of Eq. (3.23) is to introduce the superconducting leads explicitly. The Hamiltonian describing the leads $\hat{H}_B$ is not diagonal in electron creation and annihilation operators but has a more convenient form in terms of bogoliubons as shown in Sect. 2.2:

$$\hat{H}_B = \sum_{k\tau} E_k\,\hat{\gamma}^\dagger_{k\tau}\,\hat{\gamma}_{k\tau} + \mu\hat{N}.$$

Hence, we are able to write the time evolution of the bogoliubons[1] in a quite easy way given by the following differential equation

$$\frac{\partial}{\partial t}\,\hat{\gamma}^\dagger_{\eta k\sigma,I}(t) = \frac{i}{\hbar}\big[\hat{H}_B, \hat{\gamma}^\dagger_{\eta k\sigma,I}(t)\big] = +\frac{i}{\hbar}\big(E_k+\mu\big)\,\hat{\gamma}^\dagger_{\eta k\sigma,I}(t), \tag{3.28}$$

where the commutator is calculated in App. B.1.
Solving this equation and its hermitian conjugate counterpart yields the following time dependence:

$$\boxed{\hat{\gamma}^\dagger_{\eta k\sigma,I}(t) = e^{+\frac{i}{\hbar}\left(E_k+\mu\right)t}\,\hat{\gamma}^\dagger_{\eta k\sigma}\,,} \tag{3.29}$$

[1] Note that we are still in the interaction picture.

$$\boxed{\hat{\gamma}_{\eta k\sigma,I}(t) = e^{-\frac{i}{\hbar}\left(E_k+\mu\right)t}\,\hat{\gamma}_{\eta k\sigma}\,.} \tag{3.30}$$

In addition, we find, see App. B.1, the following time evolution of the Cooper pair operators:

$$\hat{\mathrm{S}}^{\dagger}_{I}(t) = e^{+\frac{i}{\hbar}2\mu t}\,\hat{\mathrm{S}}^{\dagger}, \tag{3.31}$$

$$\hat{\mathrm{S}}_{I}(t) = e^{-\frac{i}{\hbar}2\mu t}\,\hat{\mathrm{S}}\,. \tag{3.32}$$

The time evolution of the quasiparticle and Cooper pair operators is in perfect agreement with the paper of Josephson [15].
We will now use the Bogoliubov transformation to rewrite the four traces in Eq. (3.24). We are left with four different non-vanishing contributions, those which we call "normal":

$$\begin{aligned}&\mathrm{Tr_B}\left(\hat{\mathrm{c}}^{\dagger}_{\eta k\sigma}(t)\,\hat{\mathrm{c}}_{\eta' k'\sigma}(t')\hat{\rho}_B\right) = \delta_{kk'}\delta_{\sigma\sigma'}\delta_{\eta\eta'}\times\\ &\times\left\{|u_{\eta k}|^2 f^{+}_{\eta}(E_k)\; e^{+\frac{i}{\hbar}(E_k+\mu_\eta)(t-t')} + |v_{\eta k}|^2 f^{-}_{\eta}(E_k)\; e^{-\frac{i}{\hbar}(E_k-\mu_\eta)(t-t')}\right\},\end{aligned} \tag{3.33}$$

$$\begin{aligned}&\mathrm{Tr_B}\left(\hat{\mathrm{c}}_{\eta k\sigma}(t)\,\hat{\mathrm{c}}^{\dagger}_{\eta' k'\sigma}(t')\hat{\rho}_B\right) = \delta_{kk'}\delta_{\sigma\sigma'}\delta_{\eta\eta'}\times\\ &\times\left\{|u_{\eta k}|^2 f^{-}_{\eta}(E_k)\; e^{-\frac{i}{\hbar}(E_k+\mu_\eta)(t-t')} + |v_{\eta k}|^2 f^{+}_{\eta}(E_k)\; e^{+\frac{i}{\hbar}(E_k-\mu_\eta)(t-t')}\right\},\end{aligned} \tag{3.34}$$

and those which would be zero for normal conducting leads. We call them "anomalous":

$$\begin{aligned}&\mathrm{Tr_B}\left(\hat{\mathrm{c}}_{\eta k\sigma}(t)\,\hat{\mathrm{c}}_{\eta' k'\sigma'}(t')\hat{\rho}_B\right) = \delta_{k-k'}\delta_{\sigma\bar{\sigma}'}\delta_{\eta\eta'}\,\mathrm{sgn}\,\sigma\;\times\\ &\times\quad v_{\eta k}u^{*}_{\eta k}\; e^{-\frac{i}{\hbar}2\mu_\eta t}\left\{f^{+}_{\eta}(E_k)\; e^{+\frac{i}{\hbar}(E_k+\mu_\eta)(t-t')} - f^{-}_{\eta}(E_k)\; e^{-\frac{i}{\hbar}(E_k-\mu_\eta)(t-t')}\right\},\end{aligned} \tag{3.35}$$

$$\begin{aligned}&\mathrm{Tr_B}\left(\hat{\mathrm{c}}^{\dagger}_{\eta k\sigma}(t)\,\hat{\mathrm{c}}^{\dagger}_{\eta' k'\sigma'}(t')\hat{\rho}_B\right) = \delta_{k-k'}\delta_{\sigma\bar{\sigma}'}\delta_{\eta\eta'}\,\mathrm{sgn}\,\sigma\times\\ &\times\quad v^{*}_{\eta k}u_{\eta k}\; e^{+\frac{i}{\hbar}2\mu_\eta t}\left\{f^{-}_{\eta}(E_k)\; e^{-\frac{i}{\hbar}(E_k+\mu_\eta)(t-t')} - f^{+}_{\eta}(E_k)\; e^{+\frac{i}{\hbar}(E_k-\mu_\eta)(t-t')}\right\},\end{aligned} \tag{3.36}$$

where

$$f_\eta^\pm(E_k) = \frac{1}{e^{\pm\beta E_k}+1}\ ,$$

stands for the Fermi function of the bogoliubons as derived in Sect. 2.5. The lead index $\eta$ enters through the chemical potential in

$$E_k = \sqrt{(\xi_k - \mu_\eta)^2 + |\Delta|^2}. \tag{3.37}$$

The full calculation of the traces is presented in App. B.2.

### 3.1.5. Time evolution

By now we have almost everything in order to write down the master equation. The only missing part is the full time dependence of the GME. For this purpose we should first analyze the generic structure of the time dependence of Eq. (3.23), considering time structures with arbitrary operators in the interaction picture. Before proceeding we perform the so called Markov approximation, assuming that due to the coupling of the leads the knowledge of the past behavior of the system is destroyed by damping. In other words, the density matrix only depends on its present value. We substitute [3, p. 263]:

$$\hat{\rho}_{red}(t') = \hat{\rho}_{red}(t). \tag{3.38}$$

The next step is to perform a variable transformation in the integrals of Eq. (3.23), $t_2 = t - t'$:

$$\int_0^t dt' = -\int_t^0 dt_2 = \int_0^t dt_2 \xrightarrow{t\to\infty} \int_0^\infty dt_2. \tag{3.39}$$

In the last step we extended the integration to infinity with negligible error, because the time correlation functions $\langle \hat{c}^\dagger_{\eta k\sigma}(t)\, \hat{c}_{\eta' k'\sigma'}(t')\rangle$ will be non-zero only for some short time interval $t - t' \lesssim \tau$, which is called the correlation time. In the stationary limit, when $t \to \infty$, the Markov approximation becomes exact.
The eigenstates of the system, see Sect. 2.1, we call them $\hat{H}_S\,|\xi\rangle = E_\xi\,|\xi\rangle$, form a complete set:

$$\sum_\xi\ |\xi\rangle\langle\xi|\ = \mathbb{1}. \tag{3.40}$$

Let $\hat{a}$, $\hat{b}$, and $\hat{c}$ be some arbitrary operators whose time evolution is governed by the system Hamiltonian. We find:

$$\langle\xi|\,\hat{\mathrm{U}}_0(t)\;\hat{a}_I(t)\;b_I(t-t_2)\;c_I(t)\;\;\hat{\mathrm{U}}_0^\dagger(t)\,|\xi'\rangle =$$

$$\langle\xi|\,\overbrace{\hat{\mathrm{U}}_0(t)\,\hat{\mathrm{U}}_0^\dagger(t)}^{=\mathbb{1}}\,\hat{a}\,\underbrace{\hat{\mathrm{U}}_0(t)\,\hat{\mathrm{U}}_0^\dagger(t-t_2)}_{\exp\left(-\frac{i}{\hbar}H_S t_2\right)}\,\hat{b}\,\overbrace{\hat{\mathrm{U}}_0(t-t_2)\,\hat{\mathrm{U}}_0^\dagger(t)}^{\exp\left(\frac{i}{\hbar}H_S t_2\right)}\,\hat{c}\,\underbrace{\hat{\mathrm{U}}_0(t)\,\hat{\mathrm{U}}_0^\dagger(t)}_{=\mathbb{1}}\,|\xi'\rangle$$

$$= \sum_{\xi_1\xi_2} \langle\xi|\,\hat{a}\;\;|\xi_1\rangle\langle\xi_1|\;\;e^{-\frac{i}{\hbar}E_{\xi_1}t_2}\;\hat{b}\;e^{+\frac{i}{\hbar}E_{\xi_2}t_2}\;\;|\xi_2\rangle\langle\xi_2|\;\;\hat{c}\,|\xi'\rangle\,.$$

By this example one can see the steps explicitly. The other structures can be evaluated in exactly the same way. In summary it holds:

$$\begin{aligned}&\langle\xi|\,\hat{\mathrm{U}}_0(t)\;\hat{a}_I(t)\;\hat{b}_I(t-t_2)\;\hat{c}_I(t)\;\;\hat{\mathrm{U}}_0^\dagger(t)\,|\xi'\rangle\\ &= \sum_{\xi_1\xi_2} \langle\xi|\;\;\hat{a}\;\;|\xi_1\rangle\langle\xi_1|\;\;\hat{b}\;\;|\xi_2\rangle\langle\xi_2|\;\;\hat{c}\;\;|\xi'\rangle\,e^{\frac{i}{\hbar}(E_{\xi_2}-E_{\xi_1})t_2}\;,\end{aligned} \tag{3.41}$$

$$\begin{aligned}&\langle\xi|\,\hat{\mathrm{U}}_0(t)\;\hat{c}_I(t)\;\hat{b}_I(t-t_2)\;\hat{a}_I(t)\,\hat{\mathrm{U}}_0^\dagger(t)\,|\xi'\rangle\\ &= \sum_{\xi_1\xi_2} \langle\xi|\;\;\hat{c}\;\;|\xi_1\rangle\langle\xi_1|\;\;\hat{b}\;\;|\xi_2\rangle\langle\xi_2|\;\;\hat{a}\;\;|\xi'\rangle\,e^{\frac{i}{\hbar}(E_{\xi_2}-E_{\xi_1})t_2}\;,\end{aligned} \tag{3.42}$$

$$\begin{aligned}&\langle\xi|\,\hat{\mathrm{U}}_0(t)\;\hat{a}_I(t)\;\hat{c}_I(t)\;\hat{b}_I(t-t_2)\;\;\hat{\mathrm{U}}_0^\dagger(t)\,|\xi'\rangle\\ &= \sum_{\xi_1\xi_2} \langle\xi|\;\;\hat{a}\;\;|\xi_1\rangle\langle\xi_1|\;\;\hat{c}\;\;|\xi_2\rangle\langle\xi_2|\;\;\hat{b}\;\;|\xi'\rangle\,e^{\frac{i}{\hbar}(E_{\xi'}-E_{\xi_2})t_2}\;,\end{aligned} \tag{3.43}$$

$$\begin{aligned}&\langle\xi|\,\hat{\mathrm{U}}_0(t)\;\hat{b}_I(t-t_2)\;\hat{c}_I(t)\;\hat{a}_I(t)\,\hat{\mathrm{U}}_0^\dagger(t)\,|\xi'\rangle\\ &= \sum_{\xi_1\xi_2} \langle\xi|\;\;\hat{b}\;\;|\xi_1\rangle\langle\xi_1|\;\;\hat{c}\;\;|\xi_2\rangle\langle\xi_2|\;\;\hat{a}\;\;|\xi'\rangle\,e^{\frac{i}{\hbar}(E_{\xi_1}-E_{\xi})t_2}\;.\end{aligned} \tag{3.44}$$

## 3.2. Bloch-Redfield equations

In this section we put the analysis of Eq. (3.23), done in the last section, together and write down the GME in Bloch-Redfield form. When the Born-Markov quantum master equation for the reduced density matrix is given in the energy eigenstate basis of $\hat{H}_S$, it is usually called Redfield equation. According to [3, p. 270] and [22, p. 9] the master equation is defined in the Schrödinger picture

$$\dot{\hat{\rho}}_{nm}(t) = -i\ \omega_{nm}\ \hat{\rho}_{nm}(t) - \sum_{kl} R_{nmkl}\ \hat{\rho}_{kl}(t), \tag{3.45}$$

where the Redfield tensors are defined by

$$R_{nmkl} = \delta_{lm} \sum_r \Gamma^+_{nrrk} + \delta_{nk} \sum_r \Gamma^-_{lrrm} - \Gamma^+_{lmnk} - \Gamma^-_{lmnk} \tag{3.46}$$

and with the rates given by the Golden Rule expression:

$$\begin{aligned} \Gamma^+_{lmnk} &= \left(\frac{1}{\hbar}\right)^2 \int_0^\infty dt e^{-i\omega_{nk}t}\, \mathrm{Tr_L}\{\hat{H}_{I,lm}(t)\ \hat{H}_{I,nk}(0)\hat{\rho}_L\}, \\ \Gamma^-_{lmnk} &= \left(\frac{1}{\hbar}\right)^2 \int_0^\infty dt e^{-i\omega_{lm}t}\, \mathrm{Tr_L}\{\hat{H}_{I,lm}(0)\ \hat{H}_{I,nk}(t)\hat{\rho}_L\}. \end{aligned} \tag{3.47}$$

In the superconducting theory we adopt this formalism, defining the transition rates in pretty the same way. Meaning that they are defined by the time order of the terms written in the interaction picture in Eq. (3.48). In contrast to the normal conducting theory, we have terms describing tunneling processes, which involve two electrons simultaneously (anomalous processes), these tunneling rates we will call $\Sigma^\pm$. We use $\Gamma^\pm$ for one electron tunneling processes:

$$\begin{aligned} \Gamma^+_{lmnk} + \Sigma^+_{lmnk} &:= \left(\frac{1}{\hbar}\right)^2 \int_0^\infty dt_2\, \mathrm{Tr_L}\Big\{[\hat{\mathrm{U}}_0(t)\hat{H}_{T,I}(t)]_{lm}[\hat{H}_{T,I}(t-t_2)\,\hat{\mathrm{U}}_0^\dagger(t)]_{nk}\hat{\rho}_L\Big\}, \\ \Gamma^-_{lmnk} + \Sigma^-_{lmnk} &:= \left(\frac{1}{\hbar}\right)^2 \int_0^\infty dt'\, \mathrm{Tr_L}\Big\{[\hat{\mathrm{U}}_0(t)\hat{H}_{T,I}(t-t_2)]_{lm}[\hat{H}_{T,I}(t)\,\hat{\mathrm{U}}_0^\dagger(t)]_{nk}\hat{\rho}_L\Big\}. \end{aligned} \tag{3.48}$$

Here $[\hat{H}_{T,I}(t)]_{lm}$ denotes the matrix element of the tunneling Hamiltonian in the energy eigenbasis of the system:

$$[\hat{H}_{T,I}(t)]_{lm} \equiv \langle l|\, \hat{H}_{T,I}(t)\, |m\rangle\,.$$

### 3.2.1. Bloch-Redfield form of the GME

Now we are able to identify the transition rates in the GME and bring them in the Bloch-Redfield form. The normal rates are, following Eq. (3.23):

$$\Gamma^{+}_{\xi\xi_1\xi_2\xi'} = \left(\frac{1}{\hbar}\right)^2 |t|^2 \sum_{\eta k\sigma jj'} \int_0^\infty dt_2 \; e^{\frac{i}{\hbar}(E_{\xi'}-E_{\xi_2})t_2} \times \Big\{ \\ \langle\xi|\,\hat{\mathrm{d}}_{j\sigma}\,|\xi_1\rangle\,\langle\xi_2|\,\hat{\mathrm{d}}^\dagger_{j'\sigma}\,|\xi'\rangle \left[|u_{\eta k}|^2 f^+_\eta(E_k)\; e^{+\frac{i}{\hbar}(E_k+\mu_\eta)t_2} + |v_{\eta k}|^2 f^-_\eta(E_k)\; e^{-\frac{i}{\hbar}(E_k-\mu_\eta)t_2}\right] \\ + \langle\xi|\,\hat{\mathrm{d}}^\dagger_{j\sigma}\,|\xi_1\rangle\,\langle\xi_2|\,\hat{\mathrm{d}}_{j'\sigma}\,|\xi'\rangle \left[|u_{\eta k}|^2 f^-_\eta(E_k)\; e^{-\frac{i}{\hbar}(E_k+\mu_\eta)t_2} + |v_{\eta k}|^2 f^+_\eta(E_k)\; e^{+\frac{i}{\hbar}(E_k-\mu_\eta)t_2}\right]\Big\}, \tag{3.49}$$

$$\Gamma^{-}_{\xi\xi_1\xi_2\xi'} = \left(\frac{1}{\hbar}\right)^2 |t|^2 \sum_{\eta k\sigma jj'} \int_0^\infty dt_2 \; e^{\frac{i}{\hbar}(E_{\xi_1}-E_{\xi})t_2} \times \Big\{ \\ \langle\xi|\,\hat{\mathrm{d}}_{j'\sigma}\,|\xi_1\rangle\,\langle\xi_2|\,\hat{\mathrm{d}}^\dagger_{j\sigma}\,|\xi'\rangle \left[|u_{\eta k}|^2 f^+_\eta(E_k)\; e^{-\frac{i}{\hbar}(E_k+\mu_\eta)t_2} + |v_{\eta k}|^2 f^-_\eta(E_k)\; e^{+\frac{i}{\hbar}(E_k-\mu_\eta)t_2}\right] \\ + \langle\xi|\,\hat{\mathrm{d}}^\dagger_{j'\sigma}\,|\xi_1\rangle\,\langle\xi_2|\,\hat{\mathrm{d}}_{j\sigma}\,|\xi'\rangle \left[|u_{\eta k}|^2 f^-_\eta(E_k)\; e^{+\frac{i}{\hbar}(E_k+\mu_\eta)t_2} + |v_{\eta k}|^2 f^+_\eta(E_k)\; e^{-\frac{i}{\hbar}(E_k-\mu_\eta)t_2}\right]\Big\}. \tag{3.50}$$

Those related to "anomalous" processes in contrast read:

$$\begin{aligned} &\Sigma^{+}_{\xi\xi_1\xi_2\xi'} = \\ &= \lim_{t\to\infty}\left(\frac{1}{\hbar}\right)^2 \sum_{\eta k\sigma jj'} \int_0^\infty dt_2 \; e^{\frac{i}{\hbar}(E_{\xi'}-E_{\xi_2})t_2} \; \mathrm{sgn}(\sigma) \times \Big\{ \\ &\left(t^*\right)^2 \; v_{\eta k} u^*_{\eta k}\,\langle\xi|\,\hat{\mathrm{d}}^\dagger_{j\bar\sigma}\,|\xi_1\rangle\,\langle\xi_2|\,\hat{\mathrm{d}}^\dagger_{j'\sigma}\,|\xi'\rangle \\ &e^{-\frac{i}{\hbar}2\mu_\eta t}\left[f^+_\eta(E_k)\; e^{+\frac{i}{\hbar}(E_k+\mu_\eta)t_2} - f^-_\eta(E_k)\; e^{-\frac{i}{\hbar}(E_k-\mu_\eta)t_2}\right] \\ &+ t^2 \; v^*_{\eta k} u_{\eta k}\,\langle\xi|\,\hat{\mathrm{d}}_{j\sigma}\,|\xi_1\rangle\,\langle\xi_2|\,\hat{\mathrm{d}}_{j'\bar\sigma}\,|\xi'\rangle \\ &e^{+\frac{i}{\hbar}2\mu_\eta t}\left[f^+_\eta(E_k)\; e^{+\frac{i}{\hbar}(E_k-\mu_\eta)t_2} - f^-_\eta(E_k)\; e^{-\frac{i}{\hbar}(E_k+\mu_\eta)t_2}\right]\Big\}\,, \end{aligned} \tag{3.51}$$

and

$$
\begin{aligned}
&\Sigma^{-}_{\xi\xi_1\xi_2\xi'} = \\
&= \lim_{t\to\infty}\left(\frac{1}{\hbar}\right)^2 \sum_{\eta k\sigma jj'} \int_0^\infty dt_2\; e^{\frac{i}{\hbar}(E_{\xi_1}-E_\xi)t_2}\;\mathrm{sgn}(\sigma)\times\Big\{ \\
&\left(t^*\right)^2 v_{\eta k}u^*_{\eta k}\,\langle\xi|\,\hat{\mathrm{d}}^\dagger_{j\bar\sigma}\,|\xi_1\rangle\,\langle\xi_2|\,\hat{\mathrm{d}}^\dagger_{j'\sigma}\,|\xi'\rangle \\
&e^{-\frac{i}{\hbar}2\mu_\eta t}\Big[f^+_\eta(E_k)\;e^{-\frac{i}{\hbar}(E_k-\mu_\eta)t_2} - f^-_\eta(E_k)\;e^{+\frac{i}{\hbar}(E_k+\mu_\eta)t_2}\Big] \\
&+ t^2\; v^*_{\eta k}u_{\eta k}\,\langle\xi|\,\hat{\mathrm{d}}_{j\sigma}\,|\xi_1\rangle\,\langle\xi_2|\,\hat{\mathrm{d}}_{j'\bar\sigma}\,|\xi'\rangle \\
&e^{+\frac{i}{\hbar}2\mu_\eta t}\Big[f^+_\eta(E_k)\;e^{-\frac{i}{\hbar}(E_k+\mu_\eta)t_2} - f^-_\eta(E_k)\;e^{+\frac{i}{\hbar}(E_k-\mu_\eta)t_2}\Big]\Big\}\,.
\end{aligned}
\tag{3.52}
$$

Here $\mathrm{sgn}(\sigma)$ is either $\pm 1$ depending on the direction of the spin,

$$
\mathrm{sgn}(\sigma) = \begin{cases} +1 \text{ for } \sigma = \uparrow\,, \\ -1 \text{ for } \sigma = \downarrow\,. \end{cases}
\tag{3.53}
$$

It follows that

$$
\mathrm{sgn}\,\bar\sigma = -\,\mathrm{sgn}\,\sigma.
\tag{3.54}
$$

**Rules for energy dependence** We still have to present a rule for the order of the system energies in the transition rates. In principle we have to distinguish between terms with "+" and terms with "−" as superscript. We can relate them by the following rules, illustrated by some examples:

1.
$$
\boxed{\Gamma^+_{\xi\xi_1\xi_2\xi'} \propto e^{\frac{i}{\hbar}(E_{\xi'}-E_{\xi_2})t_2}}
\tag{3.55}
$$

   We can see that the energy $E_{\xi'}$ is related to the last subscript of $\Gamma^+$ and $E_{\xi_2}$ to the third subscript of $\Gamma^+$. This rule is also valid for $\Sigma^+$.

2. For the "−" superscript it exists a similar rule:

$$
\boxed{\Sigma^-_{\xi\xi_1\xi_2\xi'} \propto e^{\frac{i}{\hbar}(E_{\xi_1}-E_{\xi})t_2}}
\tag{3.56}
$$

   Here $E_{\xi_1}$ is related to the second subscript, $E_{\xi'}$ to the first one. This rule is also valid for $\Gamma^-$.

### Generalized Master Equation in the Bloch-Redfield form

Collecting all the previous findings, we finally find the set of coupled equations for the matrix elements of the reduced density matrix in the Schrödinger picture:

$$\begin{aligned}\dot{\hat{\rho}}_{\xi\xi'}(t) = -\frac{i}{\hbar}\big(E_\xi - E_{\xi'}\big)\ \hat{\rho}_{\xi\xi'}(t) - \sum_{\xi_1\xi_2} \times \Big\{ \\ \delta_{\xi_1\xi'} \sum_\alpha \Gamma^+_{\xi\alpha\alpha\xi_2}\ \hat{\rho}_{\xi_2\xi_1}(t) + \delta_{\xi_2\xi} \sum_\alpha \Gamma^-_{\xi_1\alpha\alpha\xi'}\ \hat{\rho}_{\xi_2\xi_1}(t) \\ - \Gamma^+_{\xi_2\xi'\xi\xi_1}\ \hat{\rho}_{\xi_1\xi_2}(t) - \Gamma^-_{\xi_2\xi'\xi\xi_1}\ \hat{\rho}_{\xi_1\xi_2}(t) \\ + \delta_{\xi_1\xi'} \sum_\alpha\ \Sigma^+_{\xi\alpha\alpha\xi_2}\ \hat{\rho}_{\xi_2\xi_1}(t) + \delta_{\xi_2\xi} \sum_\alpha\ \Sigma^-_{\xi_1\alpha\alpha\xi'}\ \hat{\rho}_{\xi_2\xi_1}(t) \\ - \Sigma^+_{\xi_2\xi'\xi\xi_1}\ \hat{\rho}_{\xi_1\xi_2}(t) - \Sigma^-_{\xi_2\xi'\xi\xi_1}\ \hat{\rho}_{\xi_1\xi_2}(t) \Big\}.\end{aligned} \tag{3.57}$$

Eventually, we can rename $\xi_1 \leftrightarrow \xi_2$ in the second and fourth line of Eq. (3.57) in order to have the same indices of the density matrix:

$$\begin{aligned}\dot{\hat{\rho}}_{\xi\xi'}(t) = -\frac{i}{\hbar}\big(E_\xi - E_{\xi'}\big)\ \hat{\rho}_{\xi\xi'}(t) - \sum_{\xi_1\xi_2} \times \Big\{ \\ \left(\delta_{\xi_2\xi'} \sum_\alpha \Gamma^+_{\xi\alpha\alpha\xi_1} + \delta_{\xi_1\xi} \sum_\alpha \Gamma^-_{\xi_2\alpha\alpha\xi'}\ - \Gamma^+_{\xi_2\xi'\xi\xi_1}\ - \Gamma^-_{\xi_2\xi'\xi\xi_1}\right)\ \hat{\rho}_{\xi_1\xi_2}(t) \\ + \left(\delta_{\xi_2\xi'} \sum_\alpha\ \Sigma^+_{\xi\alpha\alpha\xi_1} + \delta_{\xi_1\xi} \sum_\alpha\ \Sigma^-_{\xi_2\alpha\alpha\xi'}\ - \Sigma^+_{\xi_2\xi'\xi\xi_1} - \Sigma^-_{\xi_2\xi'\xi\xi_1}\right)\ \hat{\rho}_{\xi_1\xi_2}(t) \Big\}.\end{aligned} \tag{3.58}$$

Equation (3.58) can be rewritten in a closed form using the Redfield tensors:

$$\dot{\hat{\rho}}_{\xi\xi'}(t) = -\,i\ \omega_{\xi\xi'}\ \hat{\rho}_{\xi\xi'}(t) - \sum_{\xi_1\xi_2}\Big(R_{\xi\xi'\xi_1\xi_2} + P_{\xi\xi'\xi_1\xi_2}\Big)\hat{\rho}_{\xi_1\xi_2}(t), \tag{3.59}$$

where, see Eq. (3.46),

$$R_{\xi\xi'\xi_1\xi_2} = \delta_{\xi_2\xi'} \sum_\alpha \Gamma^+_{\xi\alpha\alpha\xi_1} + \delta_{\xi_1\xi} \sum_\alpha \Gamma^-_{\xi_2\alpha\alpha\xi'} - \Gamma^+_{\xi_2\xi'\xi\xi_1} - \Gamma^-_{\xi_2\xi'\xi\xi_1} \tag{3.60}$$

corresponds to the Redfield tensor of the theory with normal conducting leads if we $|\Delta| \to 0$,

and

$$P_{\xi\xi'\xi_1\xi_2} = \delta_{\xi_2\xi'} \sum_{\alpha} \Sigma^{+}_{\xi\alpha\alpha\xi_1,} + \delta_{\xi_1\xi} \sum_{\alpha} \Sigma^{-}_{\xi_2\alpha\alpha\xi'} - \Sigma^{+}_{\xi_2\xi'\xi\xi_1} - \Sigma^{-}_{\xi_2\xi'\xi\xi_1} = 0, \tag{3.61}$$

is the Redfield tensor which comes from the anomalous tunneling processes and is specific for the theory with superconducting leads. It turns out, see App. B.4.2, that the anomalous contributions are vanishing in second order.
Hence we can write the GME in a compact form, the so called Bloch-Redfield form of the reduced density matrix:

$$\boxed{\dot{\hat{\rho}}_{\xi\xi'}(t) = -i\ \omega_{\xi\xi'}\ \hat{\rho}_{\xi\xi'}(t) - \sum_{\xi_1\xi_2} R_{\xi\xi'\xi_1\xi_2}\ \hat{\rho}_{\xi_1\xi_2}(t).} \tag{3.62}$$

# Applications

# 4. Transport through quantum dot systems

Since Giaever's seminal work from 1960 [11], bias spectroscopy with superconducting leads was widely used as a tool for high resolution tunneling spectroscopy [12]. More recently in 1995, a high resolution bias spectrum was measured on a single Al nanoparticle [19]. In the last few years, modern fabrication techniques allowed for the first time to connect quantum dot devices with superconducting leads. Measurements were e.g. done on carbon nanotubes [12] and $C_{60}$ fullerene molecules [23].
So far, we have derived a microscopic theory of the dynamics of the reduced density matrix (RDM) up to second order in the tunneling Hamiltonian for a quantum dot system with superconducting leads. The last part ended with the Bloch-Redfield form of the GME, which essentially contains all information necessary to calculate observable quantities like the current and the differential conductance. In the following, we will derive explicitly an expression for the current through such systems. We illustrate this with two examples, the single quantum dot, and the double dot at the end of this part.

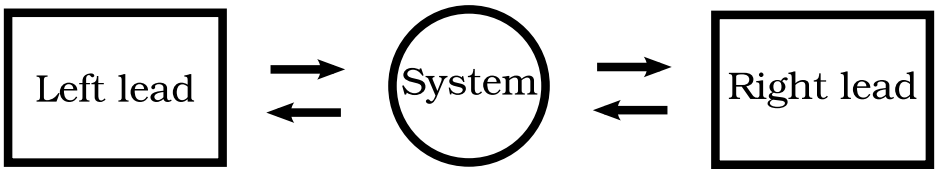


**Figure 4.1.:** Sketch of the transport setup. Electrons are tunneling in and out of the leads with a certain rate depicted by arrows.

## 4.1. Current

In this chapter we present a universal expression for the current derived from the second order GME in Bloch-Redfield form of the previous chapter. Before we start the derivation, we want to recall the GME in the Bloch Redfield form Eq. (3.58). However, now we distinguish between rates which describe processes which rise and those which

lower the occupation number of the system. This distinction is emphasized by the superscript $N \to N \pm 1$:

$$\begin{aligned}
\dot{\rho}^N_{\xi\xi'}(t) = &-\frac{i}{\hbar}\big(E_\xi - E_{\xi'}\big)\rho^N_{\xi\xi'}(t) - \sum_{\eta\xi_1\xi_2} \Bigg\{ \\
&\Bigg[\delta_{\xi_2\xi'} \sum_\alpha \Bigg( \big(\Gamma^+_{\xi\alpha\alpha\xi_1}\big)^{N\to N+1}_\eta + \big(\Gamma^+_{\xi\alpha\alpha\xi_1}\big)^{N\to N-1}_\eta \Bigg) \\
&+ \delta_{\xi_1\xi} \sum_\alpha \Bigg( \big(\Gamma^-_{\xi_2\alpha\alpha\xi'}\big)^{N\to N+1}_\eta + \big(\Gamma^-_{\xi_2\alpha\alpha\xi'}\big)^{N\to N-1}_\eta \Bigg)\Bigg] \rho^N_{\xi_1\xi_2}(t) \\
&- \Big( \big(\Gamma^+_{\xi_2\xi'\xi\xi_1}\big)^{N+1\to N}_\eta + \big(\Gamma^-_{\xi_2\xi'\xi\xi_1}\big)^{N+1\to N}_\eta \Big) \rho^{N+1}_{\xi_1\xi_2}(t) \\
&- \Big( \big(\Gamma^+_{\xi_2\xi'\xi\xi_1}\big)^{N-1\to N}_\eta + \big(\Gamma^-_{\xi_2\xi'\xi\xi_1}\big)^{N-1\to N}_\eta \Big) \rho^{N-1}_{\xi_1\xi_2}(t) \Bigg\}.
\end{aligned} \tag{4.1}$$

In the preceding equation we put the superscript $N$ to the reduced density matrix to emphasize its block diagonal form as coherences between states with different particle numbers vanish. To go on, we introduce a current operator whose thermal average gives the total current:

$$I_\eta = \mathrm{Tr}\big(\hat{I}_\eta\ \hat{\rho}_{tot}\big). \tag{4.2}$$

Generally, the current operator in the interaction picture is defined as:

$$\begin{aligned}
\hat{I}_{\eta,I}(t) = -e\ \frac{d}{dt}\hat{N}_{\eta,I}(t) &= \frac{+ie}{\hbar}\Big[\hat{N}_{\eta,I}(t), \hat{H}_{T,I}(t)\Big] \\
&= \frac{+ie}{\hbar}\Big( t\,\hat{\mathrm{c}}^\dagger_{\eta k\sigma}(t)\,\hat{\mathrm{d}}_{j\sigma}(t) - t^*\,\hat{\mathrm{d}}^\dagger_{j\sigma}(t)\,\hat{\mathrm{c}}_{\eta k\sigma}\Big).
\end{aligned} \tag{4.3}$$

Eqs. (4.2) and (4.3) define the current in lead $\eta$ as the change of the number of electrons in the lead with time. It has the advantage that we are including all electronic degrees of freedom: the number of quasiparticle excitations as well as the number of Cooper pairs. The current operator of Eq. (4.3) differs from the tunneling Hamiltonian of Eq. (3.16), besides the prefactor, only by a sign. Hence, we use the same perturbative methods to evaluate it as before.
We use Eq. (3.3), expand the integration limits to infinity

$$\hat{\rho}_{tot,I}(t) = \rho_{tot,I}(0) - \frac{i}{\hbar}\int_0^\infty dt_2 \Big[\hat{H}_{T,I}(t-t_2), \hat{\rho}_{tot,I}(t)\Big], \tag{4.4}$$

and insert Eqs. (4.4) and (4.3) in Eq. (4.2). Thus the current in the Schrödinger picture reads

$$I_\eta(t) = \frac{+ie}{\hbar} \sum_{kj\sigma} \mathrm{Tr}\Big\{ \hat{\mathrm{U}}_0(t) \Big( t\, \hat{\mathrm{c}}^\dagger_{\eta k\sigma,I}(t)\, \hat{\mathrm{d}}_{j\sigma,I}(t) - t^*\, \hat{\mathrm{d}}^\dagger_{j\sigma,I}(t)\, \hat{\mathrm{c}}_{\eta k\sigma,I}(t) \Big) \times \\ \times \left( \rho_{tot,I}(0) - \frac{i}{\hbar} \int_0^\infty dt_2 \Big[ \hat{H}_{T,I}(t-t_2), \hat{\rho}_{tot,I}(t) \Big] \right) \hat{\mathrm{U}}_0^\dagger(t) \Big\}, \tag{4.5}$$

where only terms quadratic in electron creation and annihilation operators survive:

$$I_\eta(t) = e \left(\frac{1}{\hbar}\right)^2 \sum_{kj\sigma} \int_0^\infty dt_2\, \mathrm{Tr}\Big\{ \hat{\mathrm{U}}_0(t) \Big( t\, \hat{\mathrm{c}}^\dagger_{\eta k\sigma,I}(t)\, \hat{\mathrm{d}}_{j\sigma,I}(t) - t^*\, \hat{\mathrm{d}}^\dagger_{j\sigma,I}(t)\, \hat{\mathrm{c}}_{\eta k\sigma,I}(t) \Big) \times \\ \times \Big[ \hat{H}_{T,I}(t-t_2), \hat{\rho}_{tot,I}(t) \Big] \hat{\mathrm{U}}_0^\dagger(t) \Big\}. \tag{4.6}$$

Here we transformed the operators inside the trace from the interaction picture back to the Schrödinger picture. We notice that, neglecting the prefactors, Eq. (4.6) has the same structure as the first and the second block of Eq. (3.23), but with some differences: The sign is reverted whenever we have $\hat{\mathrm{d}}^\dagger_{j\sigma,I}(t)$ as the left-most operator, and we do not sum over the lead index $\eta$. These two blocks can be identified in the Bloch-Redfield form of the GME. They correspond to the rates $\Gamma_\eta$ with the superscript "+" in the second line, and to the rates with the superscript "−" in the last two lines of Eq. (4.1). Hence, we are able to write the current in terms of rates

$$I_\eta(t) = e \sum_{\xi_1\xi_2} \mathrm{Tr}_S \Big\{ \delta_{\xi_2\xi'} \sum_\alpha \Big( \big(\Gamma^+_{\xi\alpha\alpha\xi_1}\big)^{N\to N+1}_\eta - \big(\Gamma^+_{\xi\alpha\alpha\xi_1}\big)^{N\to N-1}_\eta \Big)\, \hat{\rho}^N_{\xi_1\xi_2}(t) \\ + \big(\Gamma^-_{\xi_2\xi'\xi\xi_1}\big)^{N-1\to N}_\eta\, \hat{\rho}^{N-1}_{\xi_1\xi_2}(t) - \big(\Gamma^-_{\xi_2\xi'\xi\xi_1}\big)^{N+1\to N}_\eta\, \hat{\rho}^{N+1}_{\xi_1\xi_2}(t) \Big\}. \tag{4.7}$$

Notice, that the labeling $N \to N \pm 1$ is arbitrary and is equivalent to $N \mp 1 \to N$, since we trace over all states. After reordering Eq. (4.7) and applying the trace by summing over $\xi' = \xi$ we can exploit the fact that

$$\Gamma^-_{\xi\xi_1\xi_2\xi'} = \big(\Gamma^+_{\xi'\xi_2\xi_1\xi}\big)^*, \tag{4.8}$$

and that the density matrix is a Hermitian operator, meaning that

$$\Gamma^{N\to N\pm1}_{\xi\xi_1\xi_2\xi'} = (\Gamma^+_{\xi\xi_1\xi_2\xi'})^{N\to N\pm1} + (\Gamma^-_{\xi'\xi_2\xi_1\xi})^{N\to N\pm1} = 2Re\Big( (\Gamma^+_{\xi\xi_1\xi_2\xi'})^{N\to N\pm1} \Big). \tag{4.9}$$

We finally obtain:

$$\boxed{I_\eta(t) = e \sum_{\xi_1 \xi} \sum_{\alpha} \left( \left(\Gamma^{N\to N+1}_{\xi\alpha\alpha\xi_1}\right)_\eta - \left(\Gamma^{N\to N-1}_{\xi\alpha\alpha\xi_1}\right)_\eta \right) \hat{\rho}^N_{\xi_1\xi}(t).} \tag{4.10}$$

This is a very general result and can be applied to any transport set-up where an arbitrary system with discrete levels is weakly coupled to superconducting leads as well as to normal conducting leads if we send $\Delta \to 0$. In most cases we are interested in the stationary current, which can be obtained by finding the stationary solution of the GME, Eq. (4.1), and insert the result in the current, Eq. (4.10).
To close this section, we want to briefly sketch the general solution for the rates. A detailed calculation can be found in App. B.4.2[1]. They read:

$$\left(\Gamma^{N\to N+1}_{\xi\xi_1\xi_2\xi'}\right)_\eta = |t|^2 \, \frac{2\pi}{\hbar} \sum_{\sigma j j'} \langle \xi | \, \hat{\mathrm{d}}_{j\sigma} \, | \xi_1 \rangle \, \langle \xi_2 | \, \hat{\mathrm{d}}^\dagger_{j'\sigma} \, | \xi' \rangle \, D(E_{\xi_2\xi'} - \mu_\eta) f^+_\eta(E_{\xi_2\xi'} - \mu_\eta), \tag{4.11}$$

$$\left(\Gamma^{N\to N-1}_{\xi\xi_1\xi_2\xi'}\right)_\eta = |t|^2 \, \frac{2\pi}{\hbar} \sum_{\sigma j j'} \langle \xi | \, \hat{\mathrm{d}}^\dagger_{j\sigma} \, | \xi_1 \rangle \, \langle \xi_2 | \, \hat{\mathrm{d}}_{j'\sigma} \, | \xi' \rangle \, D(E_{\xi'\xi_2} - \mu_\eta) \; f^-_\eta(E_{\xi'\xi_2} - \mu_\eta), \tag{4.12}$$

where

$$D(E) = \frac{Vm}{2\pi\hbar^2} \frac{|E|}{\sqrt{E^2 - |\Delta|^2}} \Theta\big(|E| - |\Delta|\big) \tag{4.13}$$

is the density of states (DOS) and

$$f^\pm(E - \mu_\eta) = \frac{1}{e^{\pm\beta(E-\mu_\eta)} + 1}, \tag{4.14}$$

is the Fermi function. Moreover, we introduced a short hand notation for energy differences of the system:

$$E_{\xi_1\xi_2} \equiv E_{\xi_1} - E_{\xi_2}. \tag{4.15}$$

For later reference, we collect all constants and define the tunneling coupling:

$$\hbar g := \hbar \, |t|^2 \, \frac{Vm}{\hbar^3}, \tag{4.16}$$

[1] Notice that the rates have the correct dimension since $\left[\frac{|t|^2}{\hbar} D(E)\right] = \left[\frac{\mathrm{J}^2}{\mathrm{Js}} \frac{1}{\mathrm{J}}\right] = \frac{1}{\mathrm{s}}$. Therefore the current is given in Ampere A.

$$\big[\hbar g\big] = \big[\hbar |t|^2 D(E) \frac{1}{\hbar}\big] = \big[E\big]. \tag{4.17}$$

Thus, the current is proportional to[2]

$$I_\eta \propto \frac{e}{\hbar}\, \hbar g. \tag{4.18}$$

[2] We find $e/\hbar = 0.2434 \cdot 10^{-3} \frac{\mathrm{A}}{\mathrm{eV}}$.

| particle number | energy | state |
|---|---|---|
| 0 | 0 | $\|0\rangle$ |
| 1 | $\epsilon_d$ | $\|1\sigma\rangle$ |
| 2 | $2\epsilon_d + U$ | $\|2\rangle$ |

Table 4.1.: Eigenstates and eigenenergies of the SD, where $\sigma = \uparrow / \downarrow$ denotes the spin.

## 4.2. Single quantum dot

The simplest example of a quantum dot system is the single quantum dot (SD), which we describe by the Anderson impurity model presented in Sect. 2.1:

$$\hat{H}_{SD} = \sum_{\sigma} \epsilon_d \, \hat{\mathrm{d}}_{\sigma}^{\dagger} \, \hat{\mathrm{d}}_{\sigma} + U \; \hat{n}_{\uparrow} \hat{n}_{\downarrow} \; . \tag{4.19}$$

Because this model is so well investigated for normal as well as for superconducting leads [12] [23] [19], it works well to test the theory we developed so far. Based on this model, we can start to understand the most important mechanisms which result from the superconducting leads. Due to its simplicity we are able to perform many calculations analytically and gain a good basis of knowledge for more sophisticated systems.

We will start to calculate the stationary current of the single quantum dot with no magnetic field analytically. The task is to find the stationary solution of Eq. (4.1) by inserting the eigenstates of the SD, which are listed in Tab. 4.1. We are able to reduce the problem to the task of finding the nullspace of the following matrix, since all non-secular contributions of Eq. (4.1) are vanishing:

$$0 = \begin{pmatrix} \dot{\rho}_{0,0} \\ \dot{\rho}_{1\uparrow,1\uparrow} \\ \dot{\rho}_{1\downarrow,1\downarrow} \\ \dot{\rho}_{2,2} \end{pmatrix} = \begin{pmatrix} -2\,\Gamma_{1,0} & +\Gamma_{0,1} & +\Gamma_{0,1} & 0 \\ +\Gamma_{1,0} & -\Gamma_{2,1} - \Gamma_{0,1} & 0 & +\Gamma_{1,2} \\ +\Gamma_{1,0} & 0 & -\Gamma_{2,1} - \Gamma_{0,1} & +\Gamma_{1,2} \\ 0 & +\Gamma_{2,1} & +\Gamma_{2,1} & -2\,\Gamma_{1,2} \end{pmatrix} \begin{pmatrix} \rho_{0,0} \\ \rho_{1\uparrow,1\uparrow} \\ \rho_{1\downarrow,1\downarrow} \\ \rho_{2,2} \end{pmatrix} . \tag{4.20}$$

Here we used that due to the spin degeneracy of the SD Hamiltonian, the rates $\Gamma$ have a spin independent structure. Consequently it is enough to define the rates with only two indices, naturally leading to the notation

$$\begin{aligned} \Gamma_{1,0} &= \Gamma_{0,1\sigma,1\sigma,0}, \\ \Gamma_{2,1} &= \Gamma_{1\sigma,2,2,1\sigma}, \end{aligned} \tag{4.21}$$

used in Eq. (4.20).
Short calculations of the nullspace of Eq. (4.20) reveal the following stationary solutions:

$$\begin{aligned}
\left(\rho_{0,0}\right)_{stat} &= \frac{\Gamma_{01}\Gamma_{12}}{\Gamma_{01}\Gamma_{12}+2\Gamma_{10}\Gamma_{12}+\Gamma_{10}\Gamma_{21}},\\
\left(\rho_{1\sigma,1\sigma}\right)_{stat} &= \frac{\Gamma_{10}\Gamma_{12}}{\Gamma_{01}\Gamma_{12}+2\Gamma_{10}\Gamma_{12}+\Gamma_{10}\Gamma_{21}},\\
\left(\rho_{2,2}\right)_{stat} &= \frac{\Gamma_{10}\Gamma_{21}}{\Gamma_{01}\Gamma_{12}+2\Gamma_{10}\Gamma_{12}+\Gamma_{10}\Gamma_{21}},
\end{aligned} \tag{4.22}$$

where we already normalized the density matrix

$$\mathrm{Tr}\left(\rho_{\xi\xi}\right) = 1. \tag{4.23}$$

Finally, we are able to write down the current in lead $\eta$:

$$\begin{aligned}
I_\eta = 2\,e\Big(&\left(\Gamma^{N\to N+1}_{0,1\sigma,1\sigma,0}\right)_\eta\left(\rho_{0,0}\right)_{stat} + \left(\Gamma^{N\to N+1}_{1\sigma,2,2,1\sigma}\right)_\eta\left(\rho_{1\sigma,1\sigma}\right)_{stat}\\
&- \left(\Gamma^{N\to N-1}_{1\sigma,0,0,1\sigma}\right)_\eta\left(\rho_{1\sigma,1\sigma}\right)_{stat} - \left(\Gamma^{N\to N-1}_{2,1\sigma,1\sigma,2}\right)_\eta\left(\rho_{2,2}\right)_{stat}\Big).
\end{aligned} \tag{4.24}$$

In Eq. (4.24) we put an additional factor 2 due to spin degeneracy. This result is completely analogous to the normal conducting case, the rates only differ when $\Delta \neq 0$.

### 4.2.1. Discussion

In Fig. 4.2, we illustrate the numerical implementation of the stationary current and the differential conductance of a SD coupled to superconducting (SC) leads at very low temperatures. For comparison we show the normal conducting case in the same figure, where we keep the same parameters as in the plot for SC leads, see Tab. 4.2. The most conspicuous difference between the two cases is the gap of width of four times the superconducting gap, $4\Delta$, which appears between the tips of the diamonds. It has been observed many times in experiments [12, 19]. In the green regions no current is allowed to flow, this phenomena is called Coulomb blockade, due to the fact that no more electrons can enter the dot due to Coulomb repulsion. We are able to explain all features of the diamonds using energy conservation. The Fermi functions in the rates which describe the increase and the decrease of the occupation number in the

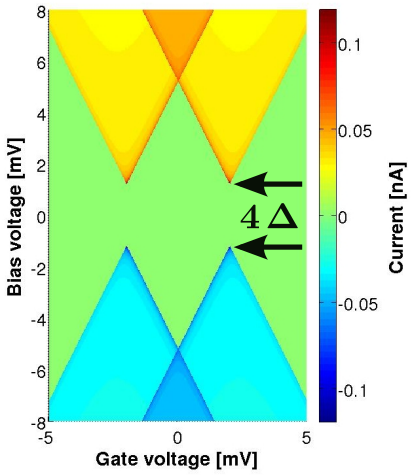


(a) Current as a function of the bias and gate voltage of a SD coupled into superconducting leads.

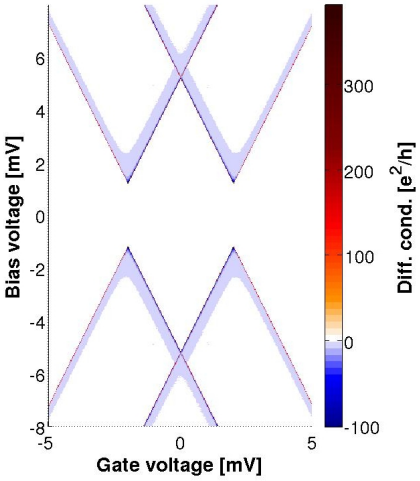


(b) Differential conductance as a function of the bias and gate voltage of SD coupled to superconducting leads.

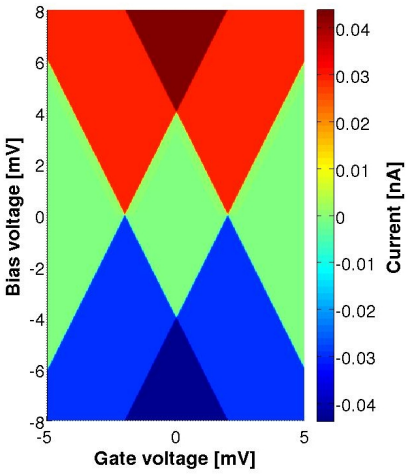


(c) Current-voltage characteristics of a SD coupled to normal conducting leads.

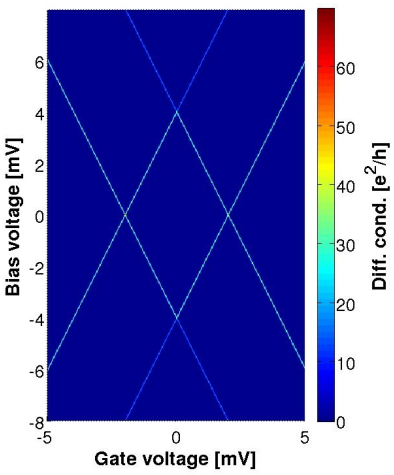


(d) Differential conductance as a function of the bias and gate voltage of a SD coupled to normal conducting leads.

**Figure 4.2.:** Current and differential conductance of the SIAM for SC and NC leads.

| | | |
|---|---|---|
| On-site Coulomb | $U$ | 4 meV |
| Level position | $\epsilon_d$ | -2 meV |
| Superconducting gap | $\Delta$ | 0.6 meV |
| Tunneling coupling | $\hbar g$ | 0.09 $\mu$eV |
| Thermal energy (low/high) | $k_B T$ | 0.01 meV (0.12K)/ 0.2 meV (2.3 K) |

Table 4.2.: Parameters used for the shown plots of the SD.

quantum dot, Eqs. (4.11), and (4.12), are giving the conditions for energy conservation and hence the configuration of the voltages for which current is allowed to flow. On top of that, we have an additional Heaviside step function which yields additional restrictions on the voltage configuration. Specifically, the rates are proportional to:

$$(\Gamma^{N\to N+1}_{\xi\xi_1\xi_1\xi'})_\eta \propto f^+(E_{\xi_1\xi'} - \mu_\eta)\Theta(|E_{\xi_1\xi'} - \mu_\eta| - |\Delta|), \tag{4.25}$$

$$(\Gamma^{N\to N-1}_{\xi\xi_1\xi_1\xi'})_\eta \propto f^-(E_{\xi_1\xi} - \mu_\eta)\Theta(|E_{\xi_1\xi} - \mu_\eta| - |\Delta|). \tag{4.26}$$

We illustrate the derivation of the voltage configuration by means of Eq. (4.25). The function $f^+_\eta$ tells us, neglecting thermal broadening, that $E_{\xi_1\xi'} - \mu_\eta \leq 0$; with the additional restriction of the step function we obtain the inequality:

$$E_{\xi_1\xi'} - \mu_\eta \leq -|\Delta|. \tag{4.27}$$

The last equations contain the energy difference $E_{\xi_1\xi'}$ which is always of the form $E_{N+1} - E_N$. We are able to manipulate the on-site energies of the quantum dot with a gate voltage that enters in the energies by the transformation $\epsilon_d \to \epsilon_d + V_g$. Thus we introduce the abbreviation $E_{\xi_1\xi'} = \Delta E + V_g$, where $\Delta E$ denotes the difference of two energy levels and has two possible values:

$$\Delta E = \begin{cases} \epsilon_d & 0 \leftrightarrow 1, \\ \epsilon_d + U & 1 \leftrightarrow 2. \end{cases} \tag{4.28}$$

Besides, we use that the electrochemical potentials of the two leads are arranged due to

$$\mu_\eta = \mu_0 \pm \frac{V_b}{2}, \tag{4.29}$$

where the left lead is defined with the plus.
Applying these considerations for the two rates and leads, we obtain eight inequalities describing the transition lines in the diamonds. These are the boundaries of the regions of constant current:

| | $N \to N \pm 1$ | Lead |
|---|---|---|
| $eV_b \geq 2eV_g + 2\|\Delta\| + 2\epsilon_d$ | $0 \to 1$ | L |
| $eV_b \leq -2eV_g - 2\|\Delta\| - 2\epsilon_d$ | $0 \to 1$ | R |
| $eV_b \leq 2eV_g - 2\|\Delta\| + 2\epsilon_d$ | $1 \to 0$ | L |
| $eV_b \geq -2eV_g + 2\|\Delta\| - 2\epsilon_d$ | $1 \to 0$ | R |
| $eV_b \geq 2eV_g + 2\|\Delta\| + 2(\epsilon_d + U)$ | $1 \to 2$ | L |
| $eV_b \leq -2eV_g - 2\|\Delta\| - 2(\epsilon_d + U)$ | $1 \to 2$ | R |
| $eV_b \leq 2eV_g - 2\|\Delta\| + 2(\epsilon_d + U)$ | $2 \to 1$ | L |
| $eV_b \geq -2eV_g + 2\|\Delta\| - 2(\epsilon_d + U)$ | $2 \to 1$ | R |

Table 4.3.: Summary of the conditions on the voltages, under which current is allowed to flow at $k_B T \ll |\Delta|$.

$$\pm V_b \geq 2V_g + 2|\Delta| + 2\Delta E, \tag{4.30}$$

and

$$\pm V_b \leq 2V_g - 2|\Delta| + 2\Delta E. \tag{4.31}$$

We summarize these conditions in Tab. 4.3. Eventually, we can plot the transition lines on top of the stability diagram of the current, see Fig. 4.3 and we find a perfect agreement. We are able to explain the size of the gap between the two diamond tips. Consider the transition lines from $0 \to 1$ and from $1 \to 0$ for the left lead in Tab. 4.3. Both equations describe lines in the bias-gate voltage, $V_b$-$V_g$, plane. They cut the $V_b$ axis, for $V_g = 0$, at $eV_b = 2(\epsilon_d - |\Delta|))$ and $eV_b = 2(\epsilon_d + |\Delta|))$. The distance between the two cuts is $4|\Delta|$. Since both lines are parallel it is the same distance as between the tips of the diamonds. For a full understanding of the lines in Fig. 4.3 we should mention that we chose the on-site energies $\epsilon_d < 0$ in the simulation, see Tab. 4.2.

For a better comparison of our simulations with experiments we plotted the current and the differential conductance versus bias voltage for fixed gate $V_g$, see Figs. 4.4 and 4.5, which is a so-called bias cut of Figs. 4.2 (a), and 4.2 (b). Our results are in good qualitative agreement with many experiments, e.g. [19] which is shown in

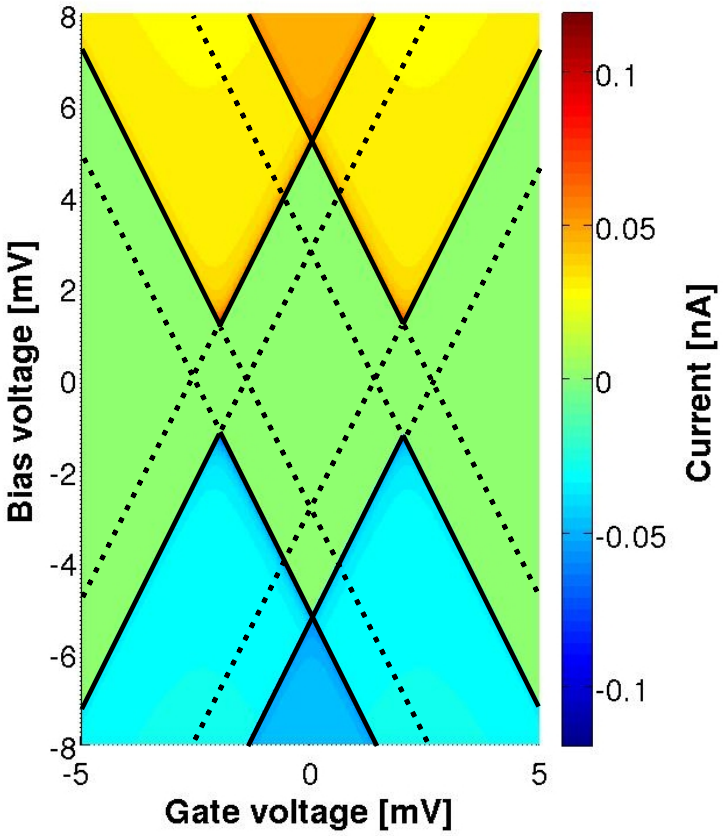


**Figure 4.3.:** Current of SD coupled to superconducting leads at low temperatures. On top we plotted the transition lines determined by the conditions on Tab. 4.3.

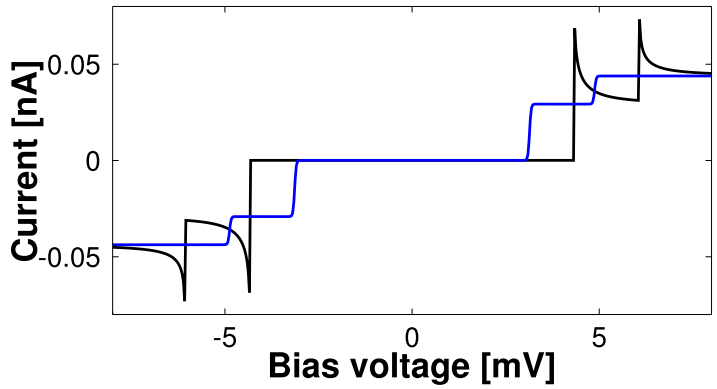


(a) Gate voltage $V_g = 0.4341$ mV.

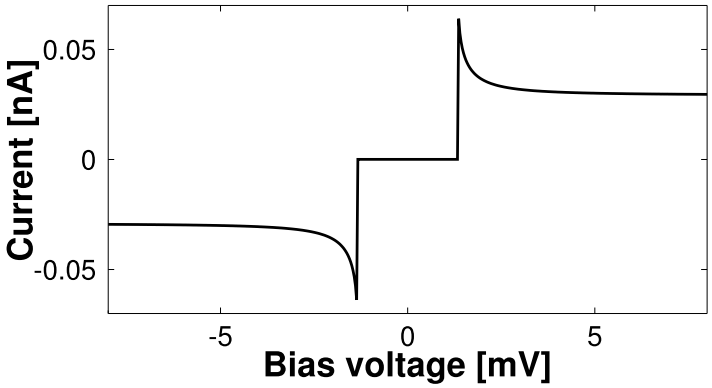


(b) Gate voltage $V_g = 2.0740$ mV.

**Figure 4.4.:** Current vs. bias voltage for fixed gate voltage of a SD coupled to SC leads. Data are taken from the current voltage characteristics of Fig. 4.2. In **(a)** we additionally plotted the current for the normal conducting case (blue line).

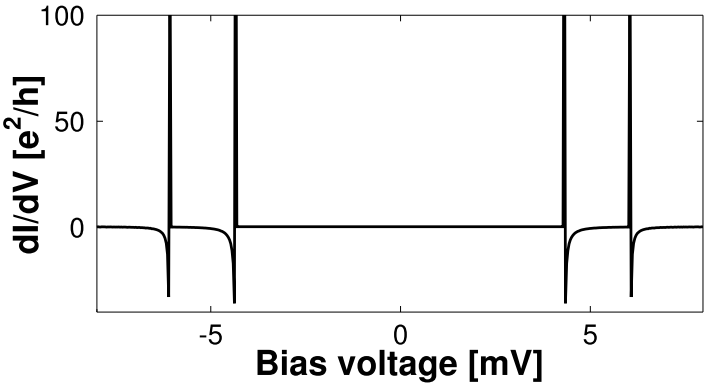


(a) Gate voltage $V_g = 0.4341$ mV.

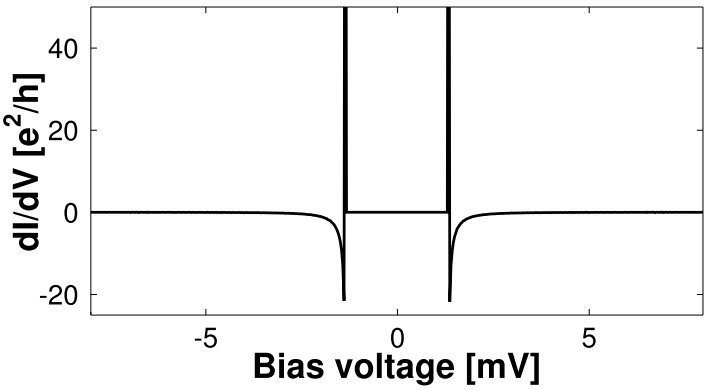


(b) Gate voltage $V_g = 2.0740$ mV.

**Figure 4.5.:** Differential conductance vs. bias voltage for fixed gate of a SD coupled to SC leads. Data are taken from the simulations of Fig. 4.2(b).

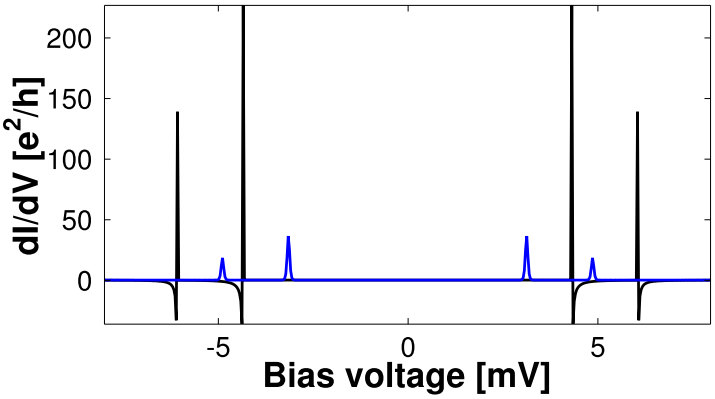


**Figure 4.6.:** Comparison of the differential conductance of a device coupled to superconducting leads (black line) with the one of a normal conducting device.

Fig. 4.7. These measurements were done for an *Al* nanoparticle which has discrete well-separated levels at 320 mK. We can clearly see the same step like behavior of the current where the gap edges of the DOS are reflected. Also the differential conductance shows the same behavior as our simulations, where the sharp peaks are characteristic. Another experiment was done by Grove-Rasmussen et al. [12], see Fig. 4.8, where low-temperature transport through carbon nanotube quantum dots in the Coulomb blockade regime coupled to niobium-based superconducting leads was studied. In Fig. 4.8 (a) we see conductance measurements which reveal a gap of magnitude $4|\Delta|$, in Fig. 4.8 (d) we see again the typical behavior of the differential conductance. Finally, we have to mention that spectroscopic features of a device coupled to SC leads are sharper compared to the normal conducting case. In Fig. 4.6 we compare the differential conductance of the SC case with the NC case and we observe higher peaks for SC.

### Thermal effects

So far, we investigated the voltage dependence of the current at low temperatures. If we increase the temperature by a factor 20, we can see additional lines in the stability diagram of the differential conductance, shown in Fig. 4.10. This additional lines are due to thermal broadening of the Fermi function, meaning that quasiparticles get thermally excited. In Fig. 4.11 we illustrate this mechanism, where we plot the product of the Fermi function with the DOS, both for low and for high temperatures, as such products appear in the transition rates, Eqs. (4.11), (4.12). In Fig. 4.11 (d) one can see an additional peak which appear due to thermal broadening of the Fermi function. This effect is relevant for temperatures which are comparable with

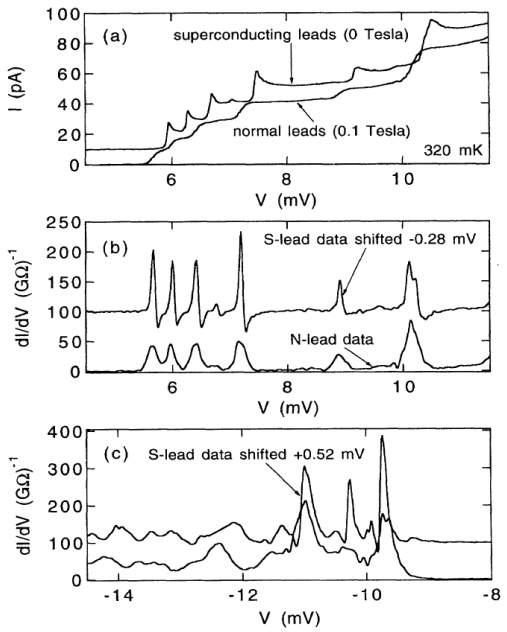


(a) Current and differential conductance due to the same device for superconducting and normal conducting leads.

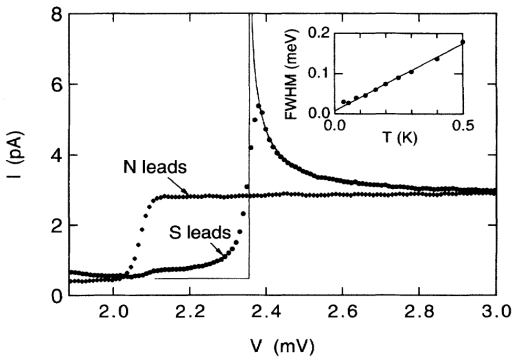


(b) Tunneling current via one electronic state at 30 mK for normal and superconducting leads.

**Figure 4.7.:** Typical measurements for the current and differential conductance of an Al nanoparticle, Figures are taken form Ralph *et al.* [19]. One can see the good qualitative agreement with our simulations. *Copyright (1994) by The American Physical Society*

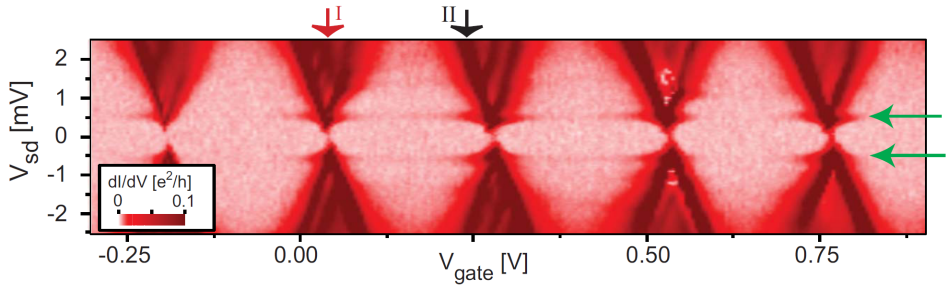


(a)

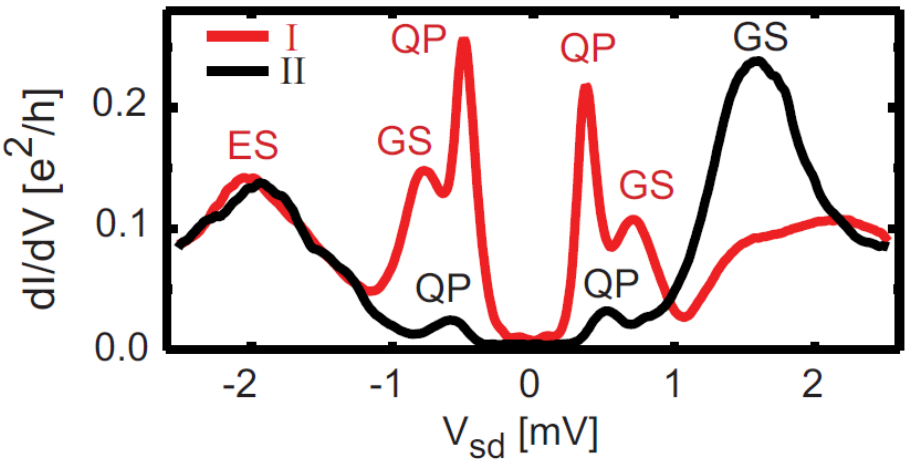


(b)

**Figure 4.8.:** **(a)** Bias spectroscopy of a SWCNT coupled to superconducting leads [12]. **(b)** Bias cut of **(a)**; conductance peaks are in good qualitative agreement with the simulations of Fig. 4.5. [12] *Copyright (2009) by The American Physical Society*

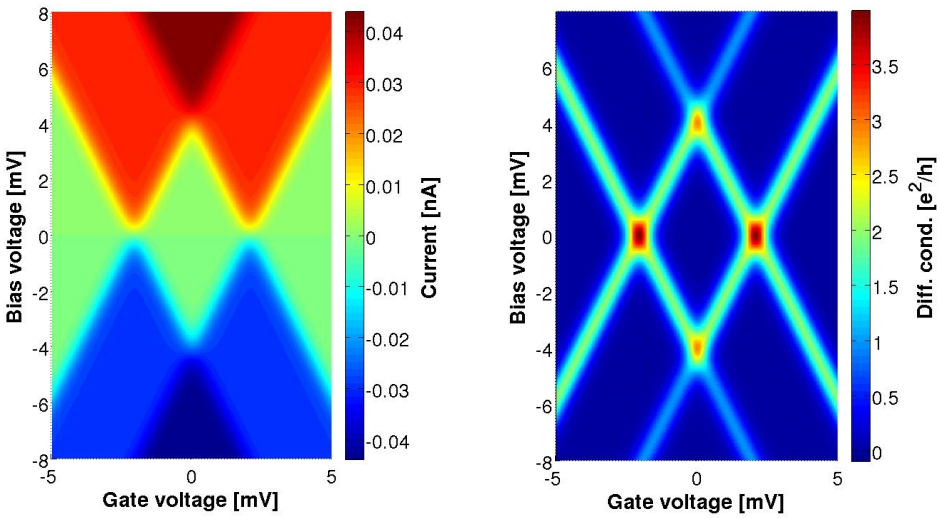


(a) Bias spectroscopy of the current at high temperatures for NC leads.

(b) Differential conductance at high temperature for NC leads.

**Figure 4.9.:** Current and Differential Conductance of a SD coupled to normal conducting leads at high temperatures.

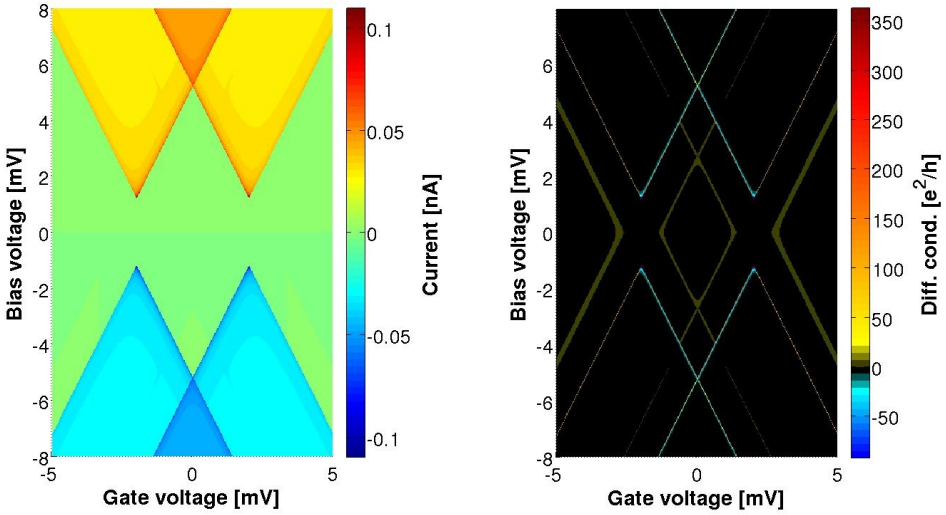


(a) Bias spectroscopy of the current at high temperatures.

(b) Differential conductance at high temperature.

**Figure 4.10.:** Current and Differential conductance of a SD coupled to superconducting leads at high temperatures. The additional lines in the differential conductance are due to thermal excited quasiparticles.

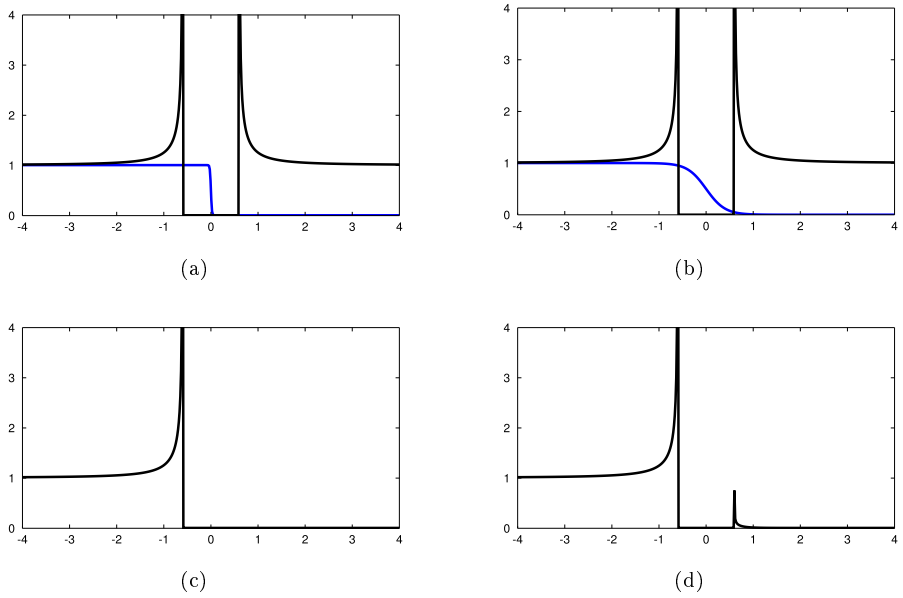


**Figure 4.11.:** In figures **(a)** and **(c)** we depicted the DOS (black line) and the Fermi function (blue line) at low and at high temperatures. Figures **(b)** and **(d)** show the product of both. In figure **(d)** one can see an additional peak due to thermal broadening.

the superconducting gap, $k_BT \lesssim \Delta$. This leads to the additional lines in the green area with almost no effect on the current. They, in fact, do not lead to additional steps but rather give a small peak, which is better visible in the differential conductance. In Fig. 4.12 we illustrate again a bias cut through the stability diagrams of the current and the differential conductance for two different gate voltages, where we can see the additional peaks mentioned before. Especially, in the bias cuts of the current we see that the thermal contributions do not lead to additional steps for increasing bias voltage. Nevertheless, we see the small peak mentioned before.
We want to close this section by mentioning the extremely high resolution of transport set-ups with superconducting leads. This is due to the peaked gap edges of the density of states. This effect leads to almost no thermal broadening of both, the current, and the differential conductance. Thus it is apparent that bias spectroscopy with superconducting leads reveals a better resolution even at higher temperatures, see Figs. 4.14 and 4.13.

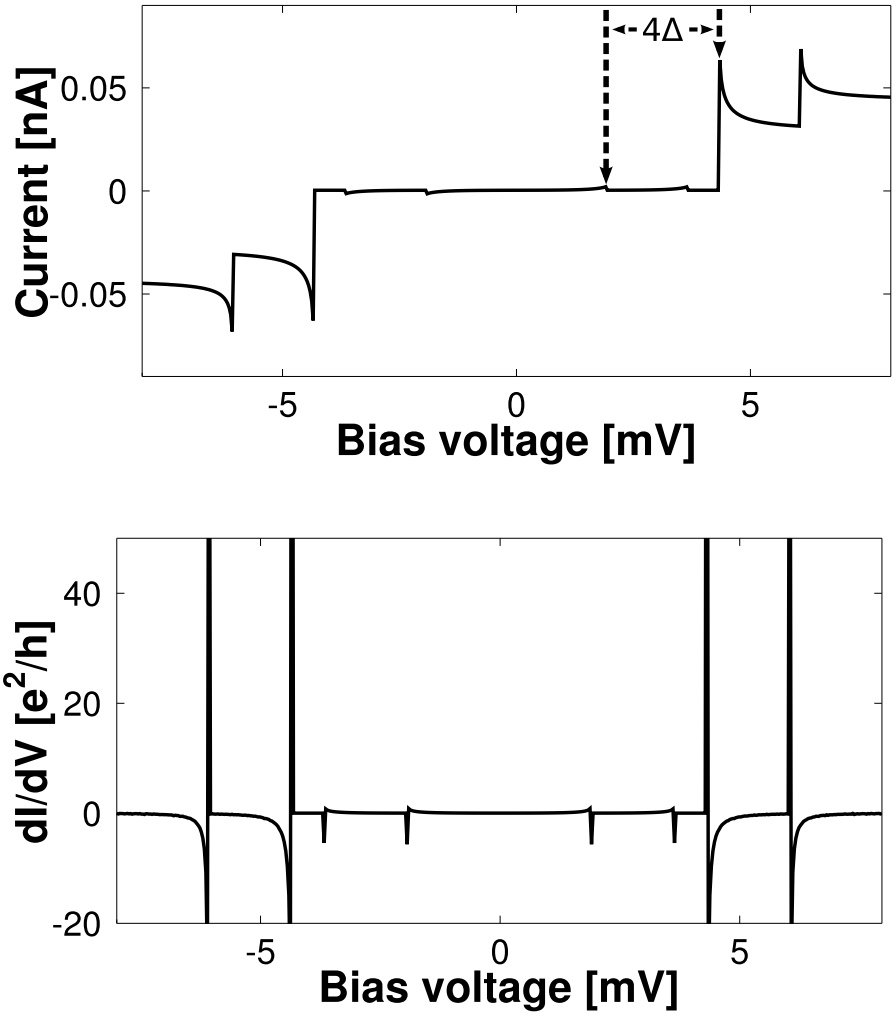


**Figure 4.12.:** Current and differential conductance vs bias voltage for fixed gate $V_g = 0.4341$ mV.

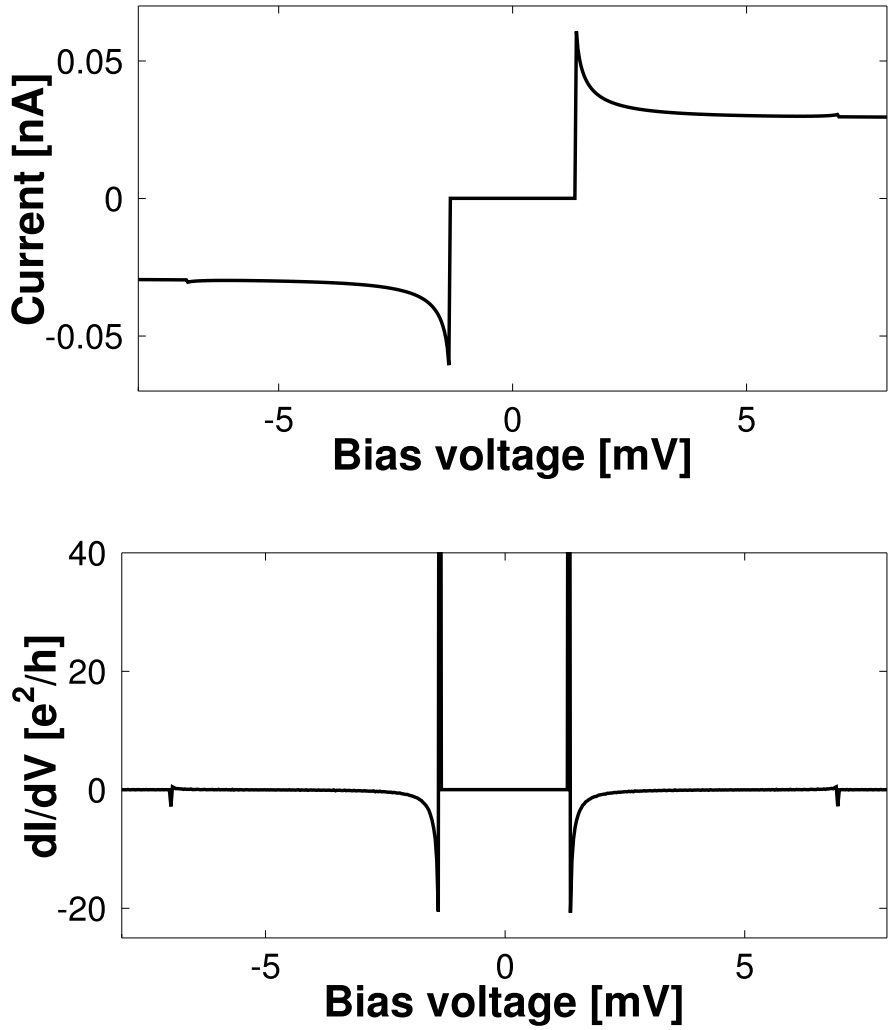


**Figure 4.13.:** Current and differential conductance vs bias voltage for fixed gate $V_g = 2.0740$ mV.

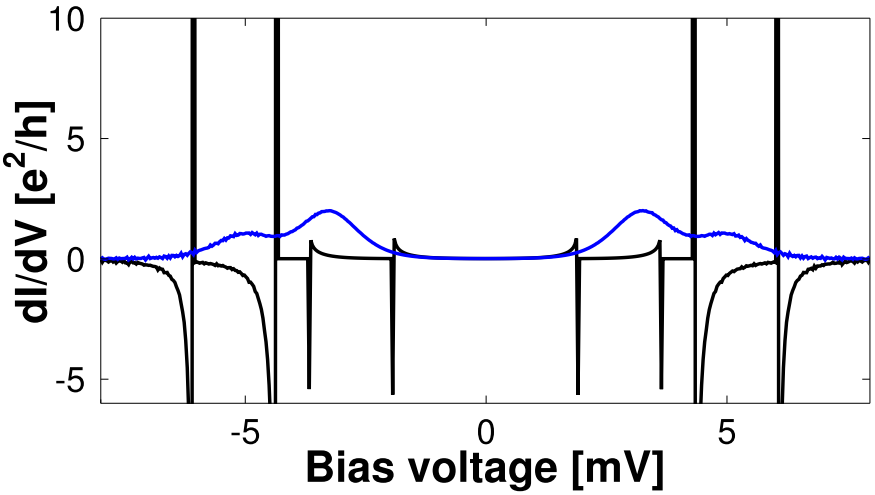


**Figure 4.14.:** Comparison of the differential conductance for normal (blue line) and superconducting leads (black line) at high temperatures for gate voltage $V_g = 0.431$ mV. One can see the extreme thermal broadening in the normal conducting case. In the superconducting case, in contrast, the differential conductance remains sharply peaked.

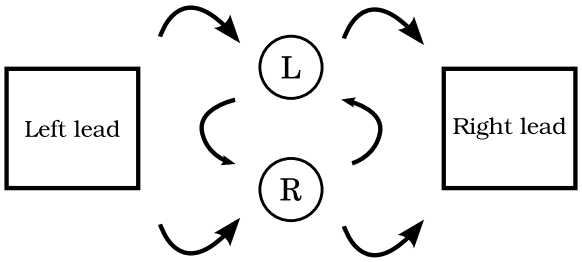


**Figure 4.15.:** Sketch of a quantum double dot (**DD**) between two leads. The arrows are indicating electron tunneling from the leads to the system and between the **L**eft and the **R**ight dot. Where we use the convention that the left lead is defined as the source.

## 4.3. Quantum Double Dot

In the last section we investigated the properties of a single quantum dot described by the single impurity Anderson model extensively and gained a good understanding about the basic physics resulting from the superconducting leads. Now we want to apply our theory to a more demanding system the quantum double dot (**DD**), sketched in Fig. 4.15. We are using a model where electrons can tunnel to both sites of the DD with the same probability and between the two sites. These transitions are illustrated as arrows in the figure.
The DD is described by a modified version of the Pariser-Parr-Pople Hamiltonian, introduced in Sect. 2.1. In this section we simplify the model Hamiltonian of Eq. (2.6), by choosing the on-site energies, and the on-site Coulomb interaction site-independent it reads:

$$\begin{aligned} H_{DD} = &\sum_{\substack{\alpha\in\{L,R\}\\ \sigma\in\{\uparrow,\downarrow\}}} \epsilon_\sigma \,\hat{\mathrm{d}}^\dagger_{\alpha\sigma}\,\hat{\mathrm{d}}_{\alpha\sigma} + \sum_\sigma \Big( b\,\hat{\mathrm{d}}^\dagger_{L\sigma}\,\hat{\mathrm{d}}_{R\sigma} + b^*\,\hat{\mathrm{d}}^\dagger_{R\sigma}\,\hat{\mathrm{d}}_{L\sigma} \Big) \\ &+ \sum_\alpha U\big(\hat{n}_{\alpha\uparrow} - \frac{1}{2}\big)\big(\hat{n}_{\alpha\downarrow} - \frac{1}{2}\big) + V\big(\hat{n}_L - 1\big)\big(\hat{n}_R - 1\big). \end{aligned} \tag{4.32}$$

We are able to implement the transport equations numerically in the same way as for the single dot. In Fig. 4.16 we showed the high temperature case of the bias voltage characteristics of the current and the differential conductance of a DD coupled to normal conducting leads. Like in the example of a single dot, we can observe Coulomb blockade in the green area. In the following, we will see what happens if we apply superconducting leads to that system. We distinguish again between the high and the low temperature cases, because we expect additional lines due to thermal effects

| | | |
|---|---|---|
| On-site Coulomb | $U$ | 4 meV |
| Inter-site Coulomb | $V$ | 3 meV |
| On-site energy | $\epsilon_\sigma$ | 0 meV |
| Inter-dot tunneling | $b$ | $-0.6$ meV |
| Tunneling coupling | $\hbar g$ | $0.04\mu$eV |
| Superconducting gap | $\lvert\Delta\rvert$ | 0.6 meV |
| Thermal energy (low/high) | $k_BT$ | 0.01 meV /0.1 meV |

Table 4.4.: Parameters used for the shown plots of the DD.

for the same reasons as in the last section. In Fig. 4.17 we depicted the current and the differential conductance of a DD coupled to superconducting leads for low temperatures, where we put the corresponding occupation number in the differential conductance plot. Analog to the last section, we are able to explain the lines appearing in the stability diagrams using Eqs. (4.30), and 4.31, where we only have to substitute the energy difference $\Delta E$.
In Fig. 4.18 and Fig. 4.19 we show the high temperature case for the DD, where we use the same temperature as in Fig. 4.16. We choose a smaller superconducting gap than before, $|\Delta| = 0.2$ meV, in order to show the thermal influence in the DD. We want to emphasize that due to the gap edges of the BCS density of states we obtain very sharp lines in the differential conductance which remain highly resolved even at high temperatures.
To close this section we like to demonstrate the high resolution spectroscopy, which is caused by the superconducting leads. As already mentioned before, we should see this effect in the vicinity of transition lines which lie close together, caused for example by a small Zeeman term. Thus we investigate a bias cut for a DD system where we apply a magnetic field $B$ of order $k_BT$ for both superconducting and normal conducting leads, compare Fig. 4.20. We can see that for normal conducting leads, thermal broadening diminishes the influence of the magnetic field. For superconducting leads, in contrast, we can clearly see the separation of the two peaks due to Zeeman splitting and which have the correct distance $4\,\mu_B|B|$.

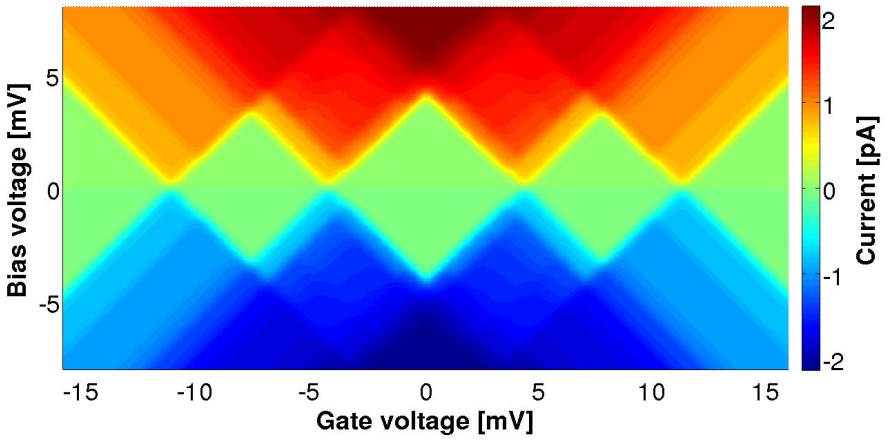


(a)

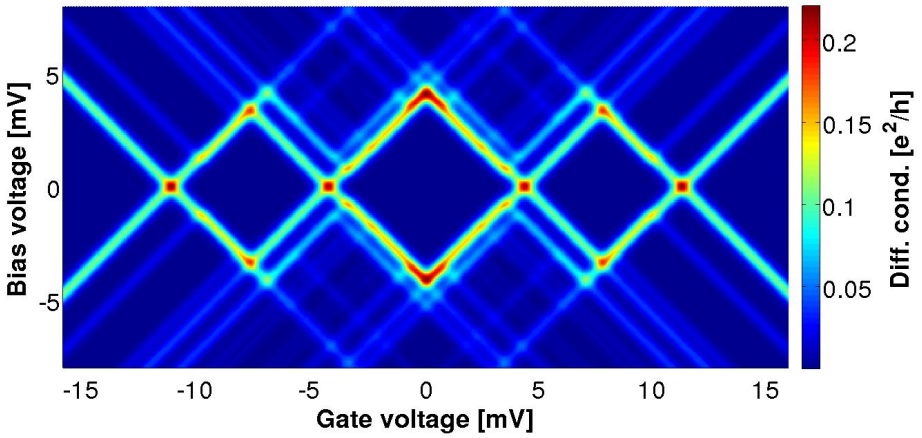


(b)

**Figure 4.16.:** Current (**a**) and differential conductance ((b)) of a quantum double dot coupled to normal conducting leads at high temperatures.

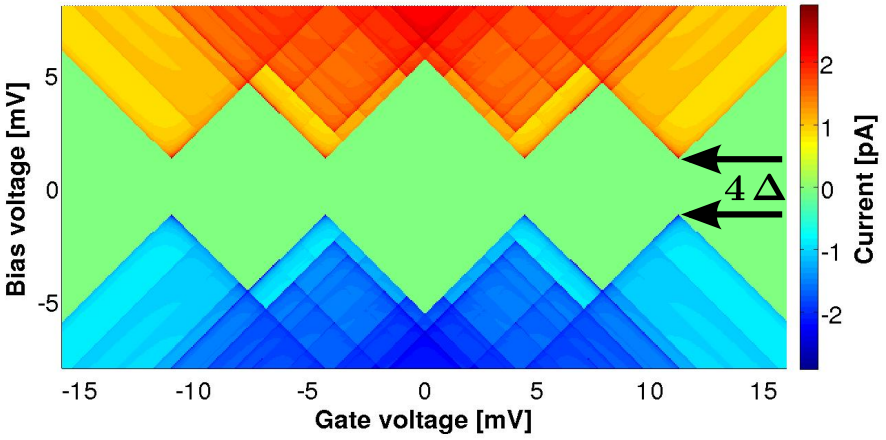


(a)

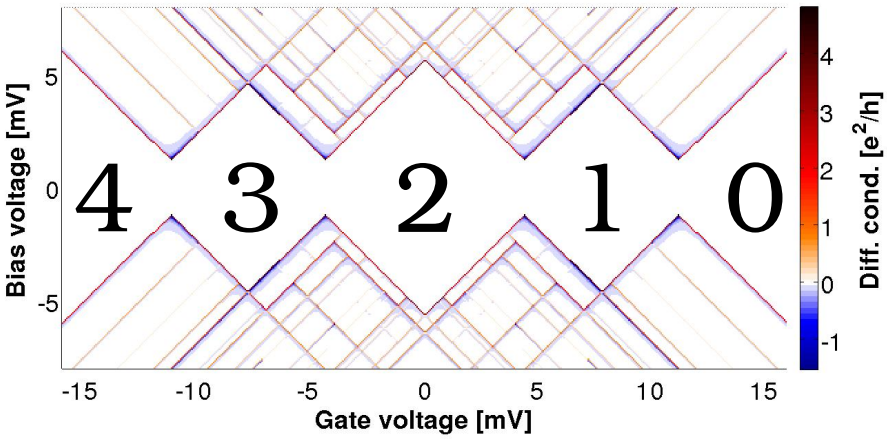


(b)

**Figure 4.17.:** Current (**a**) and differential conductance (**b**) of a DD coupled to superconducting leads at low temperatures. The numbers in the differential conductance label the occupation number of the system.

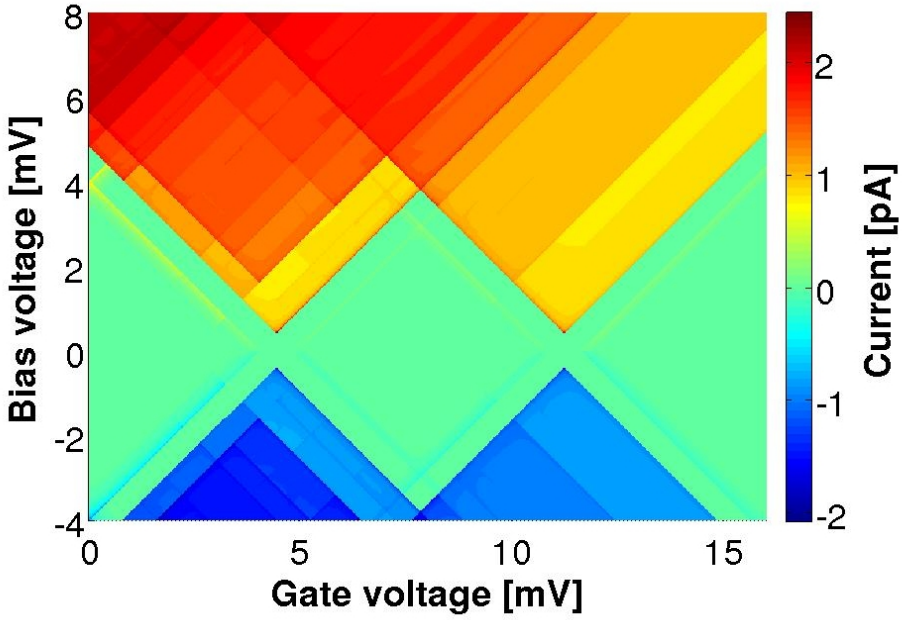


**Figure 4.18.:** Current at high temperatures in the region of two, one, and zero particle occupation. We choose a superconducting gap of $|\Delta| = 0.2$ meV and the thermal energy of $k_B T = 0.1$ meV.

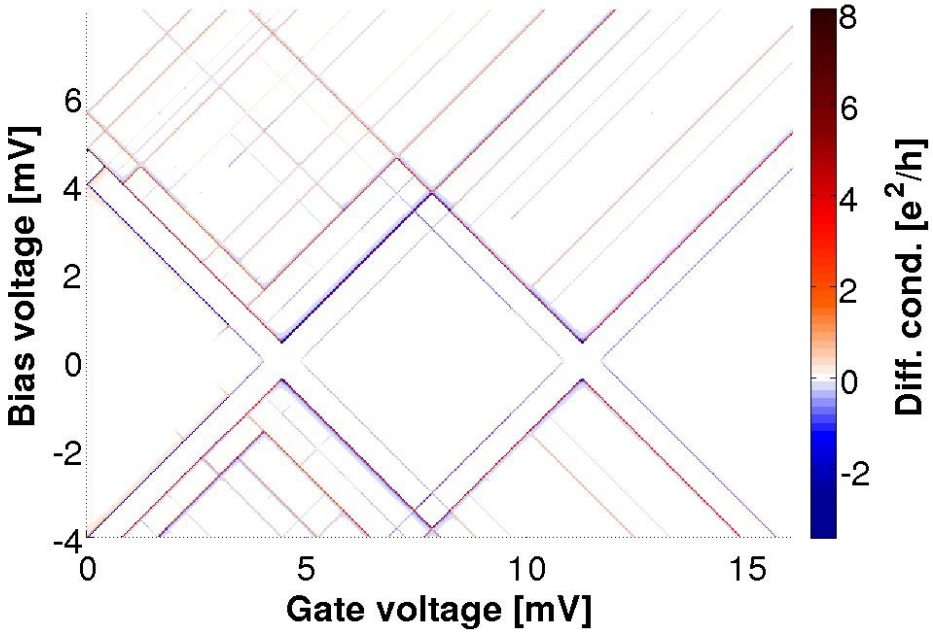


**Figure 4.19.:** Differential conductance plot in the same region as in Fig. 4.18. We choose a superconducting gap of $|\Delta| = 0.2$ meV and the thermal energy of $k_B T = 0.1$ meV. We observe additional lines which come from thermal broadening.

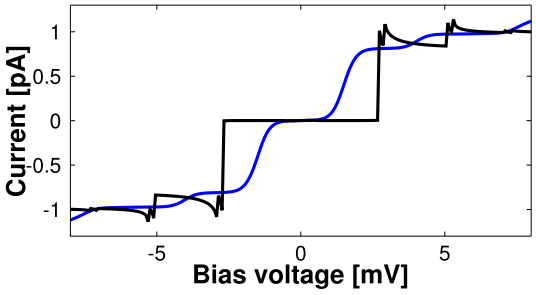


(a)

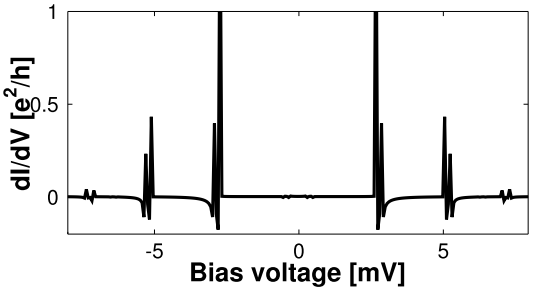


(b)

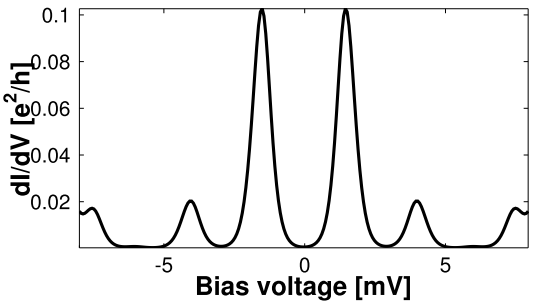


(c)

**Figure 4.20.:** Bias cuts at $V_g = 12.7936$ meV through the current and differential conductance of the quantum double dot at high temperatures and with a tiny magnetic field. **(a)** shows the comparison of the SC and the NC case, where we can see the high resolution of the superconducting leads. In **(b)** we depicted the differential conductance of SC and in **(c)** the one of NC leads.

# 5. Conclusion

In this thesis we systematically developed a transport theory for nanostructures coupled to superconducting leads and derived the General Master Equation up to second order in the tunneling Hamiltonian. In order to introduce the superconducting leads, we diagonalized the lead Hamiltonian in Sect. 2.2 with a modified version of the Bogoliubov transformation, as introduced by Josephson [15]. We transformed electrons into a combination of quasiparticle excitations of the Cooper pair condensate, and Cooper pairs. It became apparent that the analytical expression of the Cooper pair creation and annihilation operators is crucial for this work. Josephson [15], however, used a representation for the Cooper pair operators which is not adequate for our purpose. Thus we derived the Cooper pair operators explicitly in Sect. 2.3, by rewriting the BCS ground state as a coherent superposition of states with a fixed number of Cooper pairs. Having replaced the Cooper pair operators in the transformation, we showed in Sect. 2.4, that the transformation still suffices the requirements of a unitary transformation and that it conserves the total electron number. Furthermore, it turned out that when computing thermodynamic expectation values, we must not only treat fermionic quasiparticles alone, but also a combination of quasiparticles with Cooper pairs. Since the statistic of these combinations is not obvious, we investigated the thermodynamic properties of superconductors on a microscopic level in Sect. 2.5. Eventually in Chap. 3 we derived the General Master Equation, which is generalized in the Bloch-Redfield form. In contrast to theories considering normal conducting leads we found that thermodynamic averages containing two electron operators are not vanishing. Consequently, these "anomalous" contributions lead to additional transition rates, which in second order in the tunneling Hamiltonian are found to be equal to zero after evaluating them explicitly. Hence, by setting the superconducting gap equal to zero we get the same master equation as in the normal conducting case .
In Chap. 4 we calculated the current in general and applied the theory on two systems, the single, and the double quantum dot. By numerically implementing the transport equations in the stationary limit, we obtained current-voltage characteristics and stability diagrams of the differential conductance. We found the same conspicuous features as the experiments, like the spacing of the diamond tips of four times the superconducting gap, and negative differential conductance. We are able to explain the gap by using energy conservation. On top of that, we noticed an effect resulting from the thermal broadening of the Fermi function. This broadening causes additional lines in the stability diagrams, when the temperature is comparable with the superconducting gap. We interpret those lines originating from thermally excited quasiparticles.

With the experience gained from the single dot, we investigated the transport properties of the second, more advanced system, the quantum double dot. Again, we found the stability diagrams and observed high resolution images, resulting from the peaked gap edges of the BCS density of states. We demonstrated that the high resolution is even present at high temperatures by applying a small magnetic field. This leads to a Zeeman splitting of the transition lines. In the case of normal conducting leads, thermal broadening of the conductance peaks diminishes the Zeeman effect for small fields. For superconducting leads, however, the additional peaks are still visible.

## 5.1. Outlook

Summarizing the results, we developed a microscopic theory, which describes tunneling between nanostructures coupled to superconducting electrodes in general and can be extended to higher orders in perturbation theory. We expect that in fourth order perturbation theory we are able to describe higher order effects like Andreev reflection [9] or supercurrent reversal [21]. Another promising application of superconducting contacts are so called Cooper pair beam splitters, which have been demonstrated independently by L. Hofstetter et al. [14] and L. G. Herrmann et al. [13]. Both used a quantum double dot, connected to two normal conducting, and one superconducting contact. These devices are operating as Cooper pair beam splitters: Cooper pairs split into two electrons, which then tunneling to different electrodes. As Cooper pairs have been proposed as a source of natural entanglement this opens a route towards application in quantum information processing.

# Danksagung

An dieser Stelle möchte ich mich bei allen bedanken, die mich bei meiner Diplomarbeit unterstützt haben. Allen voran Milena Grifoni, die mich herzlich in ihr Team aufgenommen und sich immer Zeit für Fragen und Diskussionen genommen hat. Besonderer Dank gilt meinem guten Freund und Zimmergenossen Benjamin Siegert, für die zahlreichen Diskussionen und Anregungen und insbesondere für seine Korrekturen. Ein großes Dankeschön auch an Björn Erbe, der mir mit viele wichtigen Ratschläge zur Seite gestanden ist und die Arbeit Korrektur gelesen hat. Des weiteren möchte ich Andrea Donarini, Sascha Ratz, Manohar Awasthi und Andreas Scholz danken, die mir immer wichtige Anregungen und Ratschläge gegeben haben. Und natürlich auch ein Dankeschön an die restliche Arbeitsgruppe, die mich herzlich in die Gruppe aufgenommen haben. In diesem Sinne möchte ich auch Lizy Lazar danken, für ihre Hilfe in großen und kleinen Dingen.

Besonderer Dank geht an meine Familie, die mich in jeder Phase meines Lebens, und natürlich auch während des Studiums immer bedingungslos unterstützt haben.

Zu guter Letzt, möchte ich auch meiner Freundin Katharina danken, die mir während des ganzen Studiums immer eine große Stütze war; ohne dich wäre vieles nicht möglich gewesen.

# Appendix

# A. Basic concepts of superconductive tunneling

## A.1. Diagonalization of the lead Hamiltonian

In this section we present the diagonalization the lead Hamiltonian, Eq. (2.21), in detail. As already explained in Sect. 2.2 we rewrite the electron operators using the Bogoliubov transformation Eqs. (2.22) and (2.23).

$$\begin{aligned}\hat{H}_{MF} &= \sum_k \xi_k \, \hat{c}^\dagger_{k\sigma} \, \hat{c}_{k\sigma} \\ &- \sum_k \Big( \Delta_k \, \hat{c}^\dagger_{k\uparrow} \, \hat{c}^\dagger_{-k\downarrow} \, \hat{S} + \Delta^*_k \, \hat{S}^\dagger \, \hat{c}_{-k\downarrow} \, \hat{c}_{k\uparrow} - \Delta_k \, \langle \hat{c}^\dagger_{k\uparrow} \, \hat{c}^\dagger_{-k\downarrow} \, \hat{S} \rangle \Big) + \mu \hat{N}.\end{aligned} \tag{A.1}$$

We start with the kinetic part

$$\sum_{k\sigma} \xi_k \, \hat{c}^\dagger_{k\sigma} \, \hat{c}_{k\sigma} \ ,$$

where $\xi_k$ is quadratic in $k$, see Sect. 2.1.2, thus it is invariant under $k \leftrightarrow -k$. Hence we can write

$$\sum_{k\sigma} \xi_k \, \hat{c}^\dagger_{k\sigma} \, \hat{c}_{k\sigma} = \sum_{k\sigma} \xi_k \Big( \hat{c}^\dagger_{k\uparrow} \, \hat{c}_{k\uparrow} + \hat{c}^\dagger_{-k\downarrow} \, \hat{c}_{-k\downarrow} \Big), \tag{A.2}$$

$$
\begin{aligned}
&\sum_{k\sigma} \xi_k \, \hat{c}^\dagger_{k\sigma} \, \hat{c}_{k\sigma} = \\
&= \sum_k \xi_k \Big\{ \big(u_k \, \hat{\gamma}^\dagger_{k0} + v_k^* \, \hat{S}^\dagger \, \hat{\gamma}_{-k1}\big)\big(u_k^* \, \hat{\gamma}_{k0} + v_k \, \hat{S} \, \hat{\gamma}^\dagger_{-k1}\big) + \\
&\qquad + \big(-v_k^* \, \hat{S}^\dagger \, \hat{\gamma}_{k0} + u_k \, \hat{\gamma}^\dagger_{-k1}\big)\big(-v_k \, \hat{S} \, \hat{\gamma}^\dagger_{k0} + u_k^* \, \hat{\gamma}_{-k1}\big) \Big\} \\
&= \sum_k \xi_k \Big\{ |u_k|^2 \big(\hat{\gamma}^\dagger_{k0} \, \hat{\gamma}_{k0} + \hat{\gamma}^\dagger_{-k1} \, \hat{\gamma}_{-k1}\big) + |v_k|^2 \big(\hat{S}^\dagger \, \hat{\gamma}_{-k1} \, \hat{S} \, \hat{\gamma}^\dagger_{-k1} + \hat{S}^\dagger \, \hat{\gamma}_{k0} \, \hat{S} \, \hat{\gamma}^\dagger_{k0}\big) + \\
&\qquad + u_k v_k \big(\hat{\gamma}^\dagger_{k0} \, \hat{S} \, \hat{\gamma}^\dagger_{-k1} - \hat{\gamma}^\dagger_{-k1} \, \hat{S} \, \hat{\gamma}^\dagger_{k0}\big) + v_k^* u_k^* \big(\hat{S}^\dagger \, \hat{\gamma}_{-k1} \, \hat{\gamma}_{k0} - \hat{S}^\dagger \, \hat{\gamma}_{k0} \, \hat{\gamma}_{-k1}\big) \Big\}.
\end{aligned}
\tag{A.3}
$$

The next step is to express the pair interaction part of Eq. (2.21) in terms of bogoliubons:

$$
\begin{aligned}
&- \sum_k \Big( \Delta_k \, \hat{S} \, \hat{c}^\dagger_{k\uparrow} \, \hat{c}^\dagger_{-k\downarrow} + \Delta_k^* \, \hat{S}^\dagger \, \hat{c}_{-l\downarrow} \, \hat{c}_{l\uparrow} \Big) \\
&= - \sum_k \Big[ \Delta_k \, \hat{S} \big(u_k \, \hat{\gamma}^\dagger_{k0} + v_k^* \, \hat{S}^\dagger \, \hat{\gamma}_{-k1}\big)\big(-v_k^* \, \hat{S}^\dagger \, \hat{\gamma}_{k0} + u_k \, \hat{\gamma}^\dagger_{-k1}\big) \\
&\qquad + \Delta_k^* \, \hat{S}^\dagger \big(-v_k \, \hat{S} \, \hat{\gamma}^\dagger_{k0} + u_k^* \, \hat{\gamma}_{-k1}\big)\big(u_k^* \, \hat{\gamma}_{k0} + v_k \, \hat{S} \, \hat{\gamma}^\dagger_{-k1}\big) \\
&= - \sum_k \Big[ \Big( -\Delta_k \, \hat{S} \, u_k v_k^* \, \hat{S}^\dagger - \Delta_k^* \, \hat{S}^\dagger \, v_k u_k^* \, \hat{S} \Big) \, \hat{\gamma}^\dagger_{k0} \, \hat{\gamma}_{k0} \\
&\qquad + \Big( \Delta_k \, \hat{S} \, v_k^* u_k \, \hat{S}^\dagger + \Delta_k^* \, \hat{S}^\dagger \, v_k u_k^* \, \hat{S} \Big) \, \hat{\gamma}_{-k1} \, \hat{\gamma}^\dagger_{-k1} \\
&\qquad + \Big( \Delta_k \, \hat{S} \, u_k^2 - \Delta_k^* \, \hat{S}^\dagger \, v_k^2 \, \hat{S} \, \hat{S} \Big) \, \hat{\gamma}^\dagger_{k0} \, \hat{\gamma}^\dagger_{-k1} \\
&\qquad + \Big( -\Delta_k \, \hat{S} (v_k^*)^2 \, \hat{S}^\dagger \, \hat{S}^\dagger + \Delta_k^* \, \hat{S}^\dagger (u_k^*)^2 \Big) \, \hat{\gamma}_{-k1} \, \hat{\gamma}_{k0} \Big].
\end{aligned}
\tag{A.4}
$$

Note that we still have to rewrite $\Delta_k$ and $\Delta_k^*$ in terms of bogoliubons and Cooper pair operators, as they contain the self-consistent mean-field average:

$$
\Delta_k = - \sum_l V_{lk} \, \langle \hat{S}^\dagger \, \hat{c}_{-l\downarrow} \, \hat{c}_{l\uparrow} \rangle \, ,
\tag{A.5}
$$

$$\Delta_k^* = -\sum_l V_{kl} \langle \hat{c}_{l\uparrow}^\dagger \hat{c}_{-l\downarrow}^\dagger \hat{S} \rangle \,. \tag{A.6}$$

To keep things short, we calculate the average separately. Basically the transformation is done in Eq. (A.4):

$$\begin{aligned}
&\langle \hat{S}^\dagger \hat{c}_{-k\downarrow} \hat{c}_{k\uparrow} \rangle = \langle \hat{S}^\dagger \big(-v_k \hat{S} \hat{\gamma}_{k0}^\dagger + u_k^* \hat{\gamma}_{-k1}\big)\big(u_k^* \hat{\gamma}_{k0} + v_k \hat{S} \hat{\gamma}_{-k1}^\dagger\big)\rangle \\
&= -u_k^* v_k \langle \hat{S}^\dagger \hat{S} \hat{\gamma}_{k0}^\dagger \hat{\gamma}_{k0} \rangle + u_k^* v_k \langle \hat{S}^\dagger \hat{S} \hat{\gamma}_{-k1} \hat{\gamma}_{-k1}^\dagger \rangle \\
&- v_k^2 \underbrace{\langle \hat{S}^\dagger \hat{S} \hat{S} \hat{\gamma}_{k0}^\dagger \hat{\gamma}_{-k1}^\dagger \rangle}_{=0} + \big(u_k^*\big)^2 \underbrace{\langle \hat{S}^\dagger \hat{\gamma}_{-k1} \hat{\gamma}_{k0} \rangle}_{=0} \,,
\end{aligned}$$

$$\rightarrow \langle \hat{S}^\dagger \hat{c}_{-k\downarrow} \hat{c}_{k\uparrow} \rangle = u_k^* v_k \Big( - \langle \hat{\gamma}_{k0}^\dagger \hat{\gamma}_{k0} \rangle + \langle \hat{\gamma}_{-k1} \hat{\gamma}_{-k1}^\dagger \rangle \Big) \,, \tag{A.7}$$

and

$$\langle \hat{c}_{k\uparrow}^\dagger \hat{c}_{-k\downarrow}^\dagger \hat{S} \rangle = u_k v_k^* \Big( - \langle \hat{\gamma}_{k0}^\dagger \hat{\gamma}_{k0} \rangle + \langle \hat{\gamma}_{-k1} \hat{\gamma}_{-k1}^\dagger \rangle \Big) \,. \tag{A.8}$$

As we will see later, all contributions off-diagonal in bogoliubons are vanishing in the average so that the $\Delta$'s are becoming complex numbers:

$$\Delta_k = -\sum_l V_{lk} u_l^* v_l \Big( - \langle \hat{\gamma}_{l0}^\dagger \hat{\gamma}_{l0} \rangle + \langle \hat{\gamma}_{-l1} \hat{\gamma}_{-l1}^\dagger \rangle \Big) \,, \tag{A.9}$$

$$\Delta_k^* = -\sum_l V_{kl} u_l v_l^* \Big( - \langle \hat{\gamma}_{l0}^\dagger \hat{\gamma}_{l0} \rangle + \langle \hat{\gamma}_{-l1} \hat{\gamma}_{-l1}^\dagger \rangle \Big) \,. \tag{A.10}$$

Collecting all the previous results, we can write down the mean-field Hamiltonian expressed in bogoliubon and Cooper pair operators:

$$
\begin{aligned}
&\hat{H}_{MF} = \\
&= \sum_k \left\{ \xi_k \left( |u_k|^2 - |v_k|^2 \right) + \Delta_k v_k^* u_k + \Delta_k^* v_k u_k^* \right\} \left( \hat{\gamma}_{k0}^\dagger \, \hat{\gamma}_{k0} + \hat{\gamma}_{-k1}^\dagger \, \hat{\gamma}_{-k1} \right) \\
&+ \sum_k \left\{ 2\xi_k u_k v_k - \Delta_k \; u_k^2 + \Delta_k^* v_k^2 \; \right\} \hat{\mathrm{S}} \, \hat{\gamma}_{k0}^\dagger \, \hat{\gamma}_{-k1}^\dagger \\
&+ \sum_k \left\{ 2\xi_k v_k^* u_k^* - \Delta_k^* (u_k^*)^2 + \Delta_k (v_k^*)^2 \; \right\} \hat{\mathrm{S}}^\dagger \, \hat{\gamma}_{-k1} \, \hat{\gamma}_{k0} \\
&+ \sum_k \left\{ 2\xi_k |v_k|^2 + \Delta_k \, \langle \hat{\mathrm{c}}_{k\uparrow}^\dagger \, \hat{\mathrm{c}}_{-k\downarrow}^\dagger \, \hat{\mathrm{S}} \rangle - \left( \Delta_k v_k^* u_k + \Delta_k^* v_k u_k^* \right) \right\} + \mu \hat{N} \; .
\end{aligned}
\tag{A.11}
$$

The purpose of the transformation was to diagonalize the Hamiltonian. Thus we define the eigenenergies of the Hamiltonian as the prefactor of the diagonal contributions, that is first line of Eq. (A.11)

$$
\mathfrak{E}_k = \xi_k \left( |u_k|^2 - |v_k|^2 \right) + \Delta_k v_k^* u_k + \Delta_k^* v_k u_k^* \, ,
\tag{A.12}
$$

and demand that the off-diagonal contributions must vanish:

$$
\Delta_k^* v_k^2 \; + 2\xi_k u_k v_k - \Delta_k \; u_k^2 \stackrel{!}{=} 0 \, ,
\tag{A.13}
$$

$$
\Delta_k (v_k^*)^2 + 2\xi_k v_k^* u_k^* - \Delta_k^* (u_k^*)^2 \stackrel{!}{=} 0 \, .
\tag{A.14}
$$

Multiplying Eq. (A.13) with $\Delta_k^*/u_k^2$ and Eq. (A.14) with $\Delta_k/(u_k^*)^2$, we obtain two quadratic equations:

$$
\left( \frac{\Delta_k^* v_k}{u_k} \right)^2 + 2\xi_k \left( \frac{\Delta_k^* v_k}{u_k} \right) - |\Delta_k|^2 \stackrel{!}{=} 0 \, ,
\tag{A.15}
$$

$$
\left( \frac{\Delta_k v_k^*}{u_k^*} \right)^2 + 2\xi_k \frac{\Delta_k v_k^*}{u_k^*} - |\Delta_k|^2 \stackrel{!}{=} 0 \, .
\tag{A.16}
$$

According to Eqs. (A.9) and (A.10), $\Delta_k$ and $\Delta_k^*$ are just complex numbers a so that it is simple to solve:

$$
\frac{\Delta_k^* v_k}{u_k} = -\xi_k \pm \sqrt{\xi_k^2 + |\Delta_k|^2} \, ,
\tag{A.17}
$$

$$
\frac{\Delta_k v_k^*}{u_k^*} = -\xi_k \pm \sqrt{\xi_k^2 + |\Delta_k|^2} \, .
\tag{A.18}
$$

Since the right hand sides of Eqs. (A.17) and (A.18) are real, it follows that the left hand sides are real quantities and we can choose complex phases of $\Delta_k$, $v_k$, etc.

arbitrarily, provided in a way they are canceling. Our convention is that $v_k$ and $\Delta_k$ have the same phase $\Phi$ and we choose $u_k$ to be real. Furthermore, we choose the plus sign on the right hand side because the moduli of quantities on the left are positive, meaning that the right hand side has to be positive.
The reason for that is that the phase factors are canceling and only moduli are remaining on the left, therefore the right hand side has to be positive too.
Summarizing we obtain:

$$\frac{\Delta_k v_k^*}{u_k^*} = \frac{\Delta_k^* v_k}{u_k} = E_k - \xi_k \ , \tag{A.19}$$

where we defined

$$E_k \equiv \sqrt{\xi_k^2 + |\Delta_k|^2} \geq 0 \, . \tag{A.20}$$

Using Eq. (A.19), we can rewrite the eigenenergies, Eq. (A.12), of the Hamiltonian

$$\begin{aligned} \mathfrak{E}_k &= \xi_k \big(|u_k|^2 - |v_k|^2\big) + \frac{\Delta_k v_k^*}{u_k^*}|u_k|^2 + \frac{\Delta_k^* v_k}{u_k}|u_k|^2 \\ &= \xi_k \big(|u_k|^2 - |v_k|^2\big) + 2\,\big(-\xi_k + E_k\big)|u_k|^2 \\ &= -\xi_k \underbrace{\big(|u_k|^2 + |v_k|^2\big)}_{=1} + 2E_k\ |u_k|^2 . \end{aligned} \tag{A.21}$$

As mentioned above, we are free to choose the coefficients $u_k$ and $v_k$ as long as they fulfill Eq. (2.24). Thus we set

$$u_k \equiv \sqrt{\frac{1}{2}\left(1 + \frac{\xi_k}{|E_k|}\right)}, \tag{A.22}$$

and

$$v_k \equiv e^{i\Phi}\sqrt{\frac{1}{2}\left(1 - \frac{\xi_k}{|E_k|}\right)}\,, \tag{A.23}$$

$$\Rightarrow \quad \boxed{\mathfrak{E}_k = E_k = \sqrt{\xi_k^2 + |\Delta_k|^2}.} \tag{A.24}$$

By now we have worked out all terms of Eq. (A.11) beside the second last one. It is operator independent and we can use the results of Eqs. (A.19), (A.22), and (A.23) to write:

$$
\begin{aligned}
E_G &= \sum_k \Big\{ 2\xi_k |v_k|^2 - \big(\Delta_k v_k^* u_k + \Delta_k^* v_k u_k^*\big) + \Delta_k \langle \hat{c}_{k\uparrow}^\dagger \hat{c}_{-k\downarrow}^\dagger \hat{S}\rangle \Big\} \\
&= \sum_k \Big\{ 2\xi_k |v_k|^2 - \frac{\Delta_k v_k^*}{u_k^*}|u_k|^2 - \frac{\Delta_k^* v_k}{u_k}|u_k|^2 + \Delta_k \langle \hat{c}_{k\uparrow}^\dagger \hat{c}_{-k\downarrow}^\dagger \hat{S}\rangle \Big\} \\
&= \sum_k \Big\{ 2\xi_k |v_k|^2 - 2|u_k|^2 \big(E_k - \xi_k\big) + \Delta_k \langle \hat{c}_{k\uparrow}^\dagger \hat{c}_{-k\downarrow}^\dagger \hat{S}\rangle \Big\} \\
&= \sum_k \Big\{ 2\xi_k - E_k \big(1 - \frac{\xi_k}{E_k}\big) + \Delta_k \langle \hat{c}_{k\uparrow}^\dagger \hat{c}_{-k\downarrow}^\dagger \hat{S}\rangle \Big\} \\
&= \sum_k \Big\{ \xi_k - E_k + \Delta_k \langle \hat{c}_{k\uparrow}^\dagger \hat{c}_{-k\downarrow}^\dagger \hat{S}\rangle \Big\}.
\end{aligned}
$$

Here

$$
\begin{aligned}
\Delta_k \langle \hat{c}_{k\uparrow}^\dagger \hat{c}_{-k\downarrow}^\dagger \hat{S}\rangle = -\sum_l V_{lk} u_l^* v_l \Big( - \langle \hat{\gamma}_{l0}^\dagger \hat{\gamma}_{l0}\rangle + \langle \hat{\gamma}_{-l1} \hat{\gamma}_{-l1}^\dagger \rangle \Big) \times \\
\times \; u_k v_k^* \Big( - \langle \hat{\gamma}_{k0}^\dagger \hat{\gamma}_{k0}\rangle + \langle \hat{\gamma}_{-k1} \hat{\gamma}_{-k1}^\dagger \rangle \Big)
\end{aligned}
\tag{A.25}
$$

is a real number because all phases are canceling out and the averages are Fermi functions. So, we figured out that

$$
E_G = \sum_k \Big\{ \xi_k - E_k + \Delta_k \langle \hat{c}_{k\uparrow}^\dagger \hat{c}_{-k\downarrow}^\dagger \hat{S}\rangle \Big\} \tag{A.26}
$$

is just a real constant and gives an offset in energy, sometimes referred to as the ground state energy of the Cooper pair condensate.
Finally, we diagonalized the mean field Hamiltonian

$$
\boxed{\hat{H}_{MF} = \sum_{k\tau} E_k \hat{\gamma}_{k\tau}^\dagger \hat{\gamma}_{k\tau} + E_G + \mu \hat{N}.} \tag{A.27}
$$

## A.2. Expectation value of the number operator

In this section we investigate the expectation value of the number operator with respect to the BCS ground state, which should be independent of the chosen basis.

### A.2.1. The electron representation

First of all we use for the BCS ground state the representation of Eq. (2.30)

$$|\mathrm{GS}\rangle \equiv \prod_l \left(u_l + v_l\, \hat{\mathrm{c}}^\dagger_{l\uparrow}\, \hat{\mathrm{c}}^\dagger_{-l\downarrow}\right) |\varnothing\rangle\,. \tag{A.28}$$

Hence we have

$$\begin{aligned}
&\langle \mathrm{GS}|\, \hat{N}\, |\mathrm{GS}\rangle = \langle \mathrm{GS}| \sum_{k\sigma} \hat{\mathrm{c}}^\dagger_{k\sigma}\, \hat{\mathrm{c}}_{k\sigma}\, |\mathrm{GS}\rangle \\
&= \langle\varnothing| \prod_l \left(u_l^* + v_l^*\, \hat{\mathrm{c}}_{-l\downarrow}\, \hat{\mathrm{c}}_{l\uparrow}\right) \sum_k \left(\hat{\mathrm{c}}^\dagger_{k\uparrow}\, \hat{\mathrm{c}}_{k\uparrow} + \hat{\mathrm{c}}^\dagger_{k\downarrow}\, \hat{\mathrm{c}}_{k\downarrow}\right) \prod_{l'} \left(u_{l'} + v_{l'}\, \hat{\mathrm{c}}^\dagger_{l'\uparrow}\, \hat{\mathrm{c}}^\dagger_{-l'\downarrow}\right) |\varnothing\rangle \\
&= \sum_k \prod_{l\neq k} \prod_{l'\neq k} \langle\varnothing| \left(u_k^* + v_k^*\, \hat{\mathrm{c}}_{-k\downarrow}\, \hat{\mathrm{c}}_{k\uparrow}\right) \hat{\mathrm{c}}^\dagger_{k\uparrow}\, \hat{\mathrm{c}}_{k\uparrow} \left(u_k + v_k\, \hat{\mathrm{c}}^\dagger_{k\uparrow}\, \hat{\mathrm{c}}^\dagger_{-k\downarrow}\right) \times \\
&\qquad \times \left(u_l^* + v_l^*\, \hat{\mathrm{c}}_{-l\downarrow}\, \hat{\mathrm{c}}_{l\uparrow}\right) \left(u_{l'} + v_{l'}\, \hat{\mathrm{c}}^\dagger_{l'\uparrow}\, \hat{\mathrm{c}}^\dagger_{-l'\downarrow}\right) |\varnothing\rangle \\
&+ \sum_k \prod_{l\neq -k} \prod_{l'\neq -k} \langle\varnothing| \left(u_{-k}^* + v_{-k}^*\, \hat{\mathrm{c}}_{k\downarrow}\, \hat{\mathrm{c}}_{-k\uparrow}\right) \hat{\mathrm{c}}^\dagger_{k\downarrow}\, \hat{\mathrm{c}}_{k\downarrow} \left(u_{-k} + v_{-k}\, \hat{\mathrm{c}}^\dagger_{-k\uparrow}\, \hat{\mathrm{c}}^\dagger_{k\downarrow}\right) \times \\
&\qquad \times \left(u_l^* + v_l^*\, \hat{\mathrm{c}}_{-l\downarrow}\, \hat{\mathrm{c}}_{l\uparrow}\right) \left(u_{l'} + v_{l'}\, \hat{\mathrm{c}}^\dagger_{l'\uparrow}\, \hat{\mathrm{c}}^\dagger_{-l'\downarrow}\right) |\varnothing\rangle\,.
\end{aligned} \tag{A.29}$$

It is important to notice that we can separate terms with $l, l' \neq \pm k$ from terms with $l, l' = \pm k$. The products with $l \neq k$ have always an even number of electron operators and therefore commute with operators with quantum number $k$. So it is enough to show the action of terms with momentum $\pm k$ on $|\varnothing\rangle$ and we end up calculating

$$\begin{aligned}
&\langle\varnothing| \left(u_k^* + v_k^*\, \hat{\mathrm{c}}_{-k\downarrow}\, \hat{\mathrm{c}}_{k\uparrow}\right) \hat{\mathrm{c}}^\dagger_{k\uparrow}\, \hat{\mathrm{c}}_{k\uparrow} \left(u_k + v_k\, \hat{\mathrm{c}}^\dagger_{k\uparrow}\, \hat{\mathrm{c}}^\dagger_{-k\downarrow}\right) |\varnothing\rangle \\
&= \langle\varnothing| \Big\{ |u_k|^2\, \hat{\mathrm{c}}^\dagger_{k\uparrow}\, \hat{\mathrm{c}}_{k\uparrow} + |v_k|^2\, \hat{\mathrm{c}}_{-k\downarrow}\, \hat{\mathrm{c}}_{k\uparrow}\, \hat{\mathrm{c}}^\dagger_{k\uparrow}\, \hat{\mathrm{c}}_{k\uparrow}\, \hat{\mathrm{c}}^\dagger_{k\uparrow}\, \hat{\mathrm{c}}^\dagger_{-k\downarrow} + \\
&\quad + v_k^* u_k\, \hat{\mathrm{c}}_{-k\downarrow}\, \hat{\mathrm{c}}_{k\uparrow}\, \hat{\mathrm{c}}^\dagger_{k\uparrow}\, \hat{\mathrm{c}}_{k\uparrow} + u_k^* v_k\, \hat{\mathrm{c}}^\dagger_{k\uparrow}\, \hat{\mathrm{c}}_{k\uparrow}\, \hat{\mathrm{c}}^\dagger_{k\uparrow}\, \hat{\mathrm{c}}^\dagger_{-k\downarrow} \Big\} |\varnothing\rangle\,,
\end{aligned} \tag{A.30}$$

and

$$\begin{aligned}
&\langle\varnothing|\left(u_{-k}^{*}+v_{-k}^{*}\,\hat{c}_{k\downarrow}\,\hat{c}_{-k\uparrow}\right)\hat{c}_{k\downarrow}^{\dagger}\,\hat{c}_{k\downarrow}\left(u_{-k}+v_{-k}\,\hat{c}_{-k\uparrow}^{\dagger}\,\hat{c}_{k\downarrow}^{\dagger}\right)|\varnothing\rangle\\
&=\langle\varnothing|\Big\{|u_{-k}|^{2}\,\hat{c}_{k\downarrow}^{\dagger}\,\hat{c}_{k\downarrow}+|v_{-k}|^{2}\,\hat{c}_{k\downarrow}\,\hat{c}_{-k\uparrow}\,\hat{c}_{k\downarrow}^{\dagger}\,\hat{c}_{k\downarrow}\,\hat{c}_{-k\uparrow}^{\dagger}\,\hat{c}_{k\downarrow}^{\dagger}+\\
&\quad+u_{-k}^{*}v_{-k}\,\hat{c}_{k\downarrow}^{\dagger}\,\hat{c}_{k\downarrow}\,\hat{c}_{-k\uparrow}^{\dagger}\,\hat{c}_{k\downarrow}^{\dagger}+v_{-k}^{*}u_{-k}\,\hat{c}_{k\downarrow}\,\hat{c}_{-k\uparrow}\,\hat{c}_{k\downarrow}^{\dagger}\,\hat{c}_{k\downarrow}\Big\}|\varnothing\rangle\ .
\end{aligned}\tag{A.31}$$

It is obvious that all terms with an annihilation operator at the end or with a creator at the first place give zero. Consequently, the only non-zero terms read:

$$\begin{aligned}
&|v_{k}|^{2}\,\langle\varnothing|\,\hat{c}_{-k\downarrow}\,\hat{c}_{k\uparrow}\,\hat{c}_{k\uparrow}^{\dagger}\,\hat{c}_{k\uparrow}\,\hat{c}_{k\uparrow}^{\dagger}\,\hat{c}_{-k\downarrow}^{\dagger}\,|\varnothing\rangle\\
&=|v_{k}|^{2}\,\langle\varnothing|\,\hat{c}_{-k\downarrow}\big(1-\hat{c}_{k\uparrow}^{\dagger}\,\hat{c}_{k\uparrow}\big)\big(1-\hat{c}_{k\uparrow}^{\dagger}\,\hat{c}_{k\uparrow}\big)\,\hat{c}_{-k\downarrow}^{\dagger}\,|\varnothing\rangle\\
&=|v_{k}|^{2},
\end{aligned}\tag{A.32}$$

and

$$\begin{aligned}
&|v_{-k}|^{2}\,\langle\varnothing|\,\hat{c}_{k\downarrow}\,\hat{c}_{-k\uparrow}\,\hat{c}_{k\downarrow}^{\dagger}\,\hat{c}_{k\downarrow}\,\hat{c}_{-k\uparrow}^{\dagger}\,\hat{c}_{k\downarrow}^{\dagger}\,|\varnothing\rangle\\
&=|v_{-k}|^{2}\,\langle\varnothing|\,\hat{c}_{-k\uparrow}\big(1-\hat{c}_{k\downarrow}^{\dagger}\,\hat{c}_{k\downarrow}\big)\big(1-\hat{c}_{k\downarrow}^{\dagger}\,\hat{c}_{k\downarrow}\big)\,\hat{c}_{-k\uparrow}^{\dagger}\,|\varnothing\rangle\\
&=|v_{-k}|^{2}.
\end{aligned}\tag{A.33}$$

Inserting them in Eq. (A.29) and changing $(k\leftrightarrow -k)$, we obtain the expectation values of the total electron number operator with respect to the BCS-ground state

$$\langle\hat{N}\rangle=\sum_{k}2\,|v_{k}|^{2}.\tag{A.34}$$

### A.2.2. The quasiparticle representation

After applying the Bogoliubov transformation the ground state expectation value read:

$$\begin{aligned}
&\langle\mathrm{GS}|\,\hat{N}\,|\mathrm{GS}\rangle\\
&=\sum_{k\sigma}\langle\mathrm{GS}|\left(u_{k}\,\hat{\gamma}_{k\sigma}^{\dagger}+\operatorname{sgn}\sigma\ v_{k}^{*}\,\hat{\gamma}_{-k\bar{\sigma}}\,\hat{\mathrm{S}}^{\dagger}\right)\times\\
&\qquad\times\left(u_{k}^{*}\,\hat{\gamma}_{k\sigma}+\operatorname{sgn}\sigma\ v_{k}\,\hat{\mathrm{S}}\,\hat{\gamma}_{-k\bar{\sigma}}^{\dagger}\right)|\mathrm{GS}\rangle\\
&=\sum_{k\sigma}\langle\mathrm{GS}|\Big\{|u_{k}|^{2}\,\hat{\gamma}_{k\sigma}^{\dagger}\,\hat{\gamma}_{k\sigma}+|v_{k}|^{2}\,\hat{\gamma}_{-k\bar{\sigma}}\,\hat{\mathrm{S}}^{\dagger}\,\hat{\mathrm{S}}\,\hat{\gamma}_{-k\bar{\sigma}}^{\dagger}\\
&\qquad+\operatorname{sgn}\sigma\ u_{k}v_{k}\,\hat{\gamma}_{k\sigma}^{\dagger}\,\hat{\mathrm{S}}\,\hat{\gamma}_{-k\bar{\sigma}}^{\dagger}+\operatorname{sgn}\sigma\ u_{k}^{*}v_{k}^{*}\,\hat{\gamma}_{-k\bar{\sigma}}\,\hat{\mathrm{S}}^{\dagger}\,\hat{\gamma}_{k\sigma}\Big\}|\mathrm{GS}\rangle\,.
\end{aligned}\tag{A.35}$$

As an annihilator acts on its ground state, the first term is zero and we are left with

$$\begin{aligned}
&\langle \mathrm{GS}| \hat{N} |\mathrm{GS}\rangle \\
&= \sum_{k\sigma} \Big\{ |v_k|^2 \langle \mathrm{GS}| \hat{\gamma}_{-k\bar{\sigma}} \hat{\mathrm{S}}^\dagger \hat{\mathrm{S}} \hat{\gamma}^\dagger_{-k\bar{\sigma}} |\mathrm{GS}\rangle \\
&\qquad + \operatorname{sgn}\sigma \; u_k v_k \langle \mathrm{GS}| \hat{\gamma}^\dagger_{k\sigma} \hat{\mathrm{S}} \hat{\gamma}^\dagger_{-k\bar{\sigma}} |\mathrm{GS}\rangle \\
&\qquad + \operatorname{sgn}\sigma \; u_k^* v_k^* \langle \mathrm{GS}| \hat{\gamma}_{-k\bar{\sigma}} \hat{\mathrm{S}}^\dagger \hat{\gamma}_{k\sigma} |\mathrm{GS}\rangle \Big\} \\
&= \sum_k 2|v_k|^2.
\end{aligned} \tag{A.36}$$

where we used the relation

$$\hat{\mathrm{S}}^\dagger \hat{\mathrm{S}} = 1, \tag{A.37}$$

and find that the last two terms must be zero for every $k$:

$$\langle \mathrm{GS}| \hat{\gamma}^\dagger_{k\sigma} \hat{\mathrm{S}} \hat{\gamma}^\dagger_{-k\bar{\sigma}} |\mathrm{GS}\rangle \stackrel{!}{=} 0, \tag{A.38}$$

$$\langle \mathrm{GS}| \hat{\gamma}_{-k\bar{\sigma}} \hat{\mathrm{S}}^\dagger \hat{\gamma}_{k\sigma} |\mathrm{GS}\rangle \stackrel{!}{=} 0. \tag{A.39}$$

## A.3. Normalization of the Cooper pair state

In this section, we rewrite the normalization $\mathcal{N}$ of Sect. 2.3, by using the relation [1, p. 375]:

$$I_0(2x) = \sum_n \frac{x^{2n}}{(n!)^2}, \tag{A.40}$$

which is the modified Bessel function of first kind. It turns out that

$$\mathcal{N}^{-2} = \sum_n \frac{a_1^{2n}}{(n!)^2} = I_0(2a_1). \tag{A.41}$$

Furthermore, we calculate of $a_1$ using the density of states from App. (B.3) [1]:

$$\begin{aligned}
a_1^2 &= \sum_k \frac{|v_k|^2}{|u_k|^2} \\
\rightarrow\ & \frac{Vm}{2\pi\hbar^2}\int_{-\infty}^{\infty} dE\ \Theta\big(|E|-|\Delta|\big)\frac{|E|}{\sqrt{E^2-|\Delta|^2}}\frac{|v_k|^2}{|u_k|^2} \\
&= \frac{Vm}{2\pi\hbar^2}\ 2\int_{|\Delta|}^{\infty} dE\Big(\frac{E-\sqrt{E^2-|\Delta|^2}}{E+\sqrt{E^2-|\Delta|^2}}\Big) \\
&= \frac{Vm}{\pi\hbar^2}\int_{|\Delta|}^{\infty} dE\frac{|E|}{\sqrt{E^2-|\Delta|^2}}\Big(\frac{(E-\sqrt{E^2-|\Delta|^2})^2}{|\Delta|^2}\Big) \\
&= \frac{Vm}{\pi\hbar^2}|\Delta|\int_1^{\infty} dx\frac{x}{\sqrt{x^2-1}}\Big(x-\sqrt{x^2-1}\Big)^2 \\
&= \frac{Vm}{\pi\hbar^2}|\Delta|\int_1^{\infty} dx\Big(\frac{2x^3}{\sqrt{x^2-1}}-2x^2-\frac{x}{\sqrt{x^2-1}}\Big) \\
&= \frac{Vm}{\pi\hbar^2}|\Delta|\Big[2\big(\frac{x^2}{3}+\frac{2}{3}\big)\sqrt{x^2-1}-\frac{2x^3}{3}-\sqrt{x^2-1}\Big]_1^{\infty},
\end{aligned} \tag{A.42}$$

where $V$ is the volume of the superconductor and $m$ is the electron mass.
We have to examine the limes of $x \to \infty$ of the previous result, thus we reorder the terms and Taylor expand the square roots:

[1] Note: see e.g. Gradshteyn *Table of Integrals 6th edition* p. 92: $\int dx\frac{x^3}{\sqrt{x^2-a^2}} = \big(\frac{x^2}{3}+\frac{2}{3}\big)\sqrt{x^2-1}$ and $\int dx\frac{x}{\sqrt{x^2-1}} = \sqrt{x^2-1}$ .

$$\begin{aligned}
&\lim_{M\to\infty}\left[\frac{2}{3}x^2\sqrt{x^2-1}-\frac{2}{3}x^3+\frac{1}{3}\sqrt{x^2-1}\right]_{x=M}\\
&\approx \lim_{M\to\infty}\left[\frac{2}{3}x^3(1-\frac{1}{2x^2})-\frac{2}{3}x^3+\frac{1}{3}x(1-\frac{1}{2x^2})\right]_{x=M}\\
&= \lim_{M\to\infty}\frac{1}{6M}=0.
\end{aligned} \tag{A.43}$$

Inserting the lower integration limit in Eq. (A.42) yields

$$a_1=\frac{4}{3}\frac{Vm}{\pi\hbar^2}|\Delta|. \tag{A.44}$$

With this result we found a different expression for the normalization factor:

$$\mathcal{N}^{-2}=\sum_n\frac{a_1^{2n}}{(n!)^2}=I_0(2a_1)=I_0\left(\frac{8}{3}\frac{Vm}{\pi\hbar^2}|\Delta|\right). \tag{A.45}$$

Notice that for macroscopic systems $V\to\infty$; as $I_0(x)$ grows fast with increasing $x$, $\mathcal{N}^2$ decreases with increasing $x$.

# B. Quantum transport theory

## B.1. Time evolution of the lead operators

The purpose of this section is to calculate the time evolution of the Bogoliubov quasiparticles and of the Cooper pairs, which is governed by the lead Hamiltonian. We start with the Cooper pair operators. Here we get the expression

$$\frac{\partial}{\partial t}\,\hat{\mathrm{S}}_I^\dagger(t) = \frac{i}{\hbar}\big[\hat{H}_L, \hat{\mathrm{S}}_I^\dagger(t)\big] = \frac{i}{\hbar}\big[\hat{N}, \hat{\mathrm{S}}_I^\dagger(t)\big] = \frac{i}{\hbar} 2\mu\, \hat{\mathrm{S}}_I^\dagger(t), \tag{B.1}$$

which leads to

$$\hat{\mathrm{S}}_I^\dagger(t) = e^{+\frac{i}{\hbar}2\mu t}\ \hat{\mathrm{S}}^\dagger \tag{B.2}$$

and

$$\hat{\mathrm{S}}_I(t) = e^{-\frac{i}{\hbar}2\mu t}\ \hat{\mathrm{S}}, \tag{B.3}$$

where we used the commutation relations of Sect. 2.3.3. The next step is to calculate the time evolution of the bogoliubons, whereby we can again use the relation:

$$\frac{\partial}{\partial t}\,\hat{\gamma}_{\eta k\sigma,I}^\dagger(t) = \frac{i}{\hbar}\big[H_L, \hat{\gamma}_{\eta k\sigma,I}^\dagger(t)\big]. \tag{B.4}$$

To simplify the calculation we split the lead Hamiltonian into

$$\sum_{q\tau} E_q\big[\hat{\gamma}_{\eta q\tau}^\dagger\,\hat{\gamma}_{\eta q\tau}, \hat{\gamma}_{\eta k\sigma,I}^\dagger(t)\big] = E_k\ \hat{\gamma}_{\eta k\sigma,I}^\dagger(t) \tag{B.5}$$

and

$$\big[\hat{N}, \hat{\gamma}_{\eta k\sigma,I}^\dagger(t)\big]. \tag{B.6}$$

The last commutator must be calculated carefully, because we did not include $\hat{N}$ in the diagonalization procedure of the lead Hamiltonian and kept it as $\hat{N} = \sum_{k\sigma} \hat{\mathrm{c}}_{k\sigma}^\dagger\,\hat{\mathrm{c}}_{k\sigma}$. In this way we keep the number operator composed of electron operators and rather transform the bogoliubon operators back using the inverse Bogoliubov transformation of Eqs. (2.71) and (2.72):

$$
\begin{aligned}
&\big[\hat{N}, \hat{\gamma}^\dagger_{k\sigma}\big] = \big[\hat{N}, u^*_k\, \hat{\mathrm{c}}^\dagger_{k\sigma} - \operatorname{sgn}\sigma\, v^*_k\, \hat{\mathrm{S}}^\dagger\, \hat{\mathrm{c}}_{-k\bar{\sigma}}\big] \\
&= u^*_k \big[\hat{N}, \hat{\mathrm{c}}^\dagger_{k\sigma}\big] - \operatorname{sgn}\sigma\, v^*_k\, \hat{\mathrm{S}}^\dagger \big[\hat{N}, \hat{\mathrm{c}}_{-k\bar{\sigma}}\big] - \operatorname{sgn}\sigma\, v^*_k \big[\hat{N}, \hat{\mathrm{S}}^\dagger\big]\, \hat{\mathrm{c}}_{-k\bar{\sigma}} \\
&= u^*_k\, \hat{\mathrm{c}}^\dagger_{k\sigma} + \operatorname{sgn}\sigma\, v^*_k\, \hat{\mathrm{S}}^\dagger\, \hat{\mathrm{c}}_{-k\bar{\sigma}} - \operatorname{sgn}\sigma\, v^*_k\, 2\, \hat{\mathrm{S}}^\dagger\, \hat{\mathrm{c}}_{-k\bar{\sigma}} \\
&= \hat{\gamma}^\dagger_{\eta k\sigma}\,.
\end{aligned}
\tag{B.7}
$$

We find:

$$
\big[\hat{N}, \hat{\gamma}^\dagger_{k\sigma}\big] = \hat{\gamma}^\dagger_{\eta k\sigma} \tag{B.8}
$$

and

$$
\big[\hat{N}, \hat{\gamma}_{k\sigma}\big] = -\,\hat{\gamma}_{k\sigma}\,. \tag{B.9}
$$

Finally, we obtain for the time evolution of the bogoliubons:

$$
\hat{\gamma}^\dagger_{\eta k\sigma,I}(t) = e^{\frac{i}{\hbar}(E_k+\mu)t}\; \hat{\gamma}^\dagger_{\eta k\sigma}, \tag{B.10}
$$

$$
\hat{\gamma}_{\eta k\sigma,I}(t) = e^{-\frac{i}{\hbar}(E_k+\mu)t}\; \hat{\gamma}_{\eta k\sigma}, \tag{B.11}
$$

which is in perfect agreement with Josephson [15].

## B.2. Trace over lead degrees of freedom

In Chapter 3 we perform the trace over the electronic degrees of freedom of the leads, where we have to express the electron operators with the Bogoliubov transformation in terms of bogoliubons and Cooper pairs. In the following we present the calculation of these traces. We start with the normal contributions:

$$\begin{aligned}
&\mathrm{Tr_L}\Big(\hat{\mathrm{c}}^\dagger_{\eta k\sigma}(t)\,\hat{\mathrm{c}}_{\eta' k'\sigma'}(t')\hat{\rho}_L\Big)\\
&= \mathrm{Tr_L}\Big(\big(u_{\eta k}\,\hat{\gamma}^\dagger_{\eta k\sigma}(t) + \operatorname{sgn}\sigma\, v^*_{\eta k}\,\hat{\gamma}_{\eta -k\bar{\sigma}}(t)\,\hat{\mathrm{S}}^\dagger_\eta(t)\big)\times\\
&\qquad\times\big(u^*_{\eta' k'}\,\hat{\gamma}_{\eta' k'\sigma'}(t') + \operatorname{sgn}\sigma'\, v_{\eta' k'}\,\hat{\mathrm{S}}_{\eta'}(t')\,\hat{\gamma}^\dagger_{\eta' -k'\bar{\sigma}'}(t')\big)\hat{\rho}_L\Big)\\
&= \delta_{\eta\eta'}\delta_{kk'}\delta_{\sigma\sigma'}\Big\{|u_{\eta k}|^2\,\mathrm{Tr_L}\big(\hat{\gamma}^\dagger_{\eta k\sigma}\,\hat{\gamma}_{\eta k\sigma}\,\hat{\rho}_L\big)e^{+\frac{i}{\hbar}(E_k+\mu)(t-t')}\\
&+ |v_{\eta k}|^2\,\mathrm{Tr_L}\big(\hat{\gamma}_{\eta -k\bar{\sigma}}\,\hat{\gamma}^\dagger_{\eta -k\bar{\sigma}}\,\hat{\rho}_L\big)e^{-\frac{i}{\hbar}(E_k+\mu)(t-t')}e^{+\frac{i}{\hbar}2\mu(t-t')}\Big\}\\
&= \delta_{\eta\eta'}\delta_{kk'}\delta_{\sigma\sigma'}\times\\
&\times\Big\{|u_{\eta k}|^2 f^+_\eta(E_k)e^{+\frac{i}{\hbar}(E_k+\mu)(t-t')} + |v_{\eta k}|^2 f^-_\eta(E_k)e^{-\frac{i}{\hbar}(E_k-\mu)(t-t')}\Big\},
\end{aligned} \tag{B.12}$$

where we used the time evolution of the operators, derived in App. B.1 and that $\hat{\mathrm{S}}^\dagger\,\hat{\mathrm{S}} = 1$.
Analogously we find

$$\begin{aligned}
&\mathrm{Tr_L}\Big(\hat{\mathrm{c}}_{\eta k\sigma}(t)\,\hat{\mathrm{c}}^\dagger_{\eta' k'\sigma'}(t')\hat{\rho}_L\Big) = \delta_{\eta\eta'}\delta_{kk'}\delta_{\sigma\sigma'}\times\\
&\times\Big\{|u_{\eta k}|^2 f^-(E_k)e^{-\frac{i}{\hbar}(E_k+\mu)(t-t')} + |v_{\eta k}|^2 f^+(E_k)e^{+\frac{i}{\hbar}(E_k-\mu)(t-t')}\Big\}.
\end{aligned} \tag{B.13}$$

If we exchange $t \leftrightarrow t'$ in the two traces, we see that only the sign in the exponentials changes:

$$e^{-\frac{i}{\hbar}(E_k+\mu)(t-t')} \xrightarrow{t\leftrightarrow t'} e^{+\frac{i}{\hbar}(E_k+\mu)(t-t')}. \tag{B.14}$$

Next we calculate the traces where two electron creation or annihilation operators appear. For normal conducting leads these traces are vanishing, but in the superconducting case we get a finite contribution. The "anomalous" traces read:

$$
\begin{aligned}
&\mathrm{Tr_L}\Big(\hat{\mathrm{c}}^\dagger_{\eta k\sigma}(t)\,\hat{\mathrm{c}}^\dagger_{\eta' k'\sigma'}(t')\hat{\rho}_L\Big)\\
&=\mathrm{Tr_L}\Big(\big(u_{\eta k}\,\hat{\gamma}^\dagger_{\eta k\sigma}(t)+\operatorname{sgn}\sigma\, v^*_{\eta k}\,\hat{\gamma}_{\eta -k\bar{\sigma}}(t)\,\hat{\mathrm{S}}^\dagger_\eta(t)\big)\times\\
&\times\big(u_{\eta' k'}\,\hat{\gamma}^\dagger_{\eta' k'\sigma'}(t')+\operatorname{sgn}\sigma'\, v^*_{\eta' k'}\,\hat{\gamma}_{\eta' -k'\bar{\sigma}'}(t')\,\hat{\mathrm{S}}^\dagger_{\eta'}(t')\big)\hat{\rho}_L\Big)\\
&=\operatorname{sgn}\sigma'\,u_{\eta k}v^*_{\eta' k'}\,\mathrm{Tr_L}\big(\hat{\gamma}^\dagger_{\eta k\sigma}\,\hat{\gamma}_{\eta' -k'\bar{\sigma}'}\,\hat{\rho}_L\big)e^{+\frac{i}{\hbar}(E_k+\mu)(t-t')}e^{+\frac{i}{\hbar}2\mu t'}\\
&+\operatorname{sgn}\sigma\, v^*_{\eta k}u_{\eta' k'}\,\mathrm{Tr_L}\big(\hat{\gamma}_{\eta -k\bar{\sigma}}\,\hat{\gamma}^\dagger_{\eta' k'\sigma'}\,\hat{\rho}_L\big)e^{-\frac{i}{\hbar}(E_k+\mu)(t-t')}e^{+\frac{i}{\hbar}2\mu t}\\
&=\delta_{\eta\eta'}\delta_{k-k'}\delta_{\sigma\bar{\sigma}'}\,v^*_{\eta k}u_{\eta k}e^{+\frac{i}{\hbar}2\mu t}\Big\{\operatorname{sgn}\bar{\sigma}\,f^+_\eta(E_k)\,e^{+\frac{i}{\hbar}(E_k+\mu)(t-t')}e^{-\frac{i}{\hbar}2\mu(t-t')}\\
&+\operatorname{sgn}\sigma\,f^-_\eta(E_k)\,e^{-\frac{i}{\hbar}(E_k+\mu)(t-t')}\Big\}.
\end{aligned}
\tag{B.15}
$$

Using that $\operatorname{sgn}\bar{\sigma}=-\operatorname{sgn}\sigma$ we obtain:

$$
\begin{aligned}
&\mathrm{Tr_L}\Big(\hat{\mathrm{c}}^\dagger_{\eta k\sigma}(t)\,\hat{\mathrm{c}}^\dagger_{\eta' k'\sigma'}(t')\hat{\rho}_L\Big)=\delta_{\eta\eta'}\delta_{k-k'}\delta_{\sigma\bar{\sigma}'}\,v^*_{\eta k}u_{\eta k}e^{+\frac{i}{\hbar}2\mu t}\operatorname{sgn}\sigma\times\\
&\times\Big\{f^-_\eta(E_k)\,e^{-\frac{i}{\hbar}(E_k+\mu)(t-t')}-f^+_\eta(E_k)\,e^{+\frac{i}{\hbar}(E_k-\mu)(t-t')}\Big\}.
\end{aligned}
\tag{B.16}
$$

Eventually, we are left with one trace, namely:

$$
\begin{aligned}
&\mathrm{Tr_L}\Big(\hat{\mathrm{c}}_{\eta k\sigma}(t)\,\hat{\mathrm{c}}_{\eta' k'\sigma'}(t')\hat{\rho}_L\Big)\\
&=\mathrm{Tr_L}\Big(\big(u^*_{\eta k}\,\hat{\gamma}_{\eta k\sigma}(t)+\operatorname{sgn}\sigma\, v_{\eta k}\,\hat{\mathrm{S}}_\eta(t)\,\hat{\gamma}^\dagger_{\eta -k\bar{\sigma}}(t)\big)\times\\
&\times\big(u^*_{\eta' k'}\,\hat{\gamma}_{\eta' k'\sigma'}(t')+\operatorname{sgn}\sigma'\, v_{\eta' k'}\,\hat{\mathrm{S}}_{\eta'}(t')\,\hat{\gamma}^\dagger_{\eta' -k'\bar{\sigma}'}(t')\big)\hat{\rho}_L\Big).
\end{aligned}
\tag{B.17}
$$

Performing essentially the same steps as in the last calculation we get:

$$
\begin{aligned}
&\mathrm{Tr_L}\Big(\hat{\mathrm{c}}_{\eta k\sigma}(t)\,\hat{\mathrm{c}}_{\eta' k'\sigma'}(t')\hat{\rho}_L\Big)=\delta_{\eta\eta'}\delta_{k-k'}\delta_{\sigma\bar{\sigma}'}\,u^*_{\eta k}v_{\eta k}\operatorname{sgn}\sigma\,e^{-\frac{i}{\hbar}2\mu t}\times\\
&\times\Big\{f^+_\eta(E_k)e^{+\frac{i}{\hbar}(E_k+\mu)(t-t')}-f^-(E_k)e^{-\frac{i}{\hbar}(E_k-\mu)(t-t')}\Big\}.
\end{aligned}
\tag{B.18}
$$

The exchange of $t \leftrightarrow t'$ in the last two traces is more difficult than in the first two ones; this is due to the time dependence of the Cooper pair operators. For the "anomalous" traces we have to change the sign of the exponential and of the chemical potential simultaneously, for instance:

$$e^{+\frac{i}{\hbar}(E_k+\mu)(t-t')} \xrightarrow{t\leftrightarrow t'} e^{-\frac{i}{\hbar}(E_k-\mu)(t-t')}, \tag{B.19}$$

such that

$$\begin{aligned} &\mathrm{Tr_L}\left(\hat{c}_{\eta k\sigma}(t')\,\hat{c}_{\eta' k'\sigma'}(t)\hat{\rho}_L\right) = \delta_{\eta\eta'}\delta_{k-k'}\delta_{\sigma\bar{\sigma}'}\, u^*_{\eta k} v_{\eta k}\,\mathrm{sgn}\,\sigma\, e^{-\frac{i}{\hbar}2\mu t}\times \\ &\times\left\{f^+_\eta(E_k)e^{-\frac{i}{\hbar}(E_k-\mu)(t-t')} - f^-(E_k)e^{+\frac{i}{\hbar}(E_k+\mu)(t-t')}\right\}. \end{aligned} \tag{B.20}$$

## B.3. Density of states

In this section we derive the density of states of the superconducting leads, which is important to evaluate the sum over the wave vectors of the lead electrons. We want to consider the following transformation

$$\sum_k \to \int_{-\infty}^{\infty} dE\ D(E), \tag{B.21}$$

where $D(E)$ is formally defined as:

$$D(E) = D_d(E) = \sum_k \delta(E - E(k)). \tag{B.22}$$

In this definition of the density of states, $d$ denotes the dimension of the wave vectors $k$, so that $L^d = V$ is the volume of the contact.
Now we take the continuum limit of the wave vectors $k$, transform

$$\sum_k \to \frac{V}{(2\pi)^d} \int d^d k, \tag{B.23}$$

and rewrite the integral over wave vectors into an integral over energies, by using the dispersion relation

$$E(k) = E_k = \sqrt{\left(\frac{\hbar^2|k|^2}{2m} - \mu\right)^2 + |\Delta|^2} \equiv \sqrt{\xi_k^2 + |\Delta|^2}. \tag{B.24}$$

The exact form of $D(E)$ crucially depends on the dimension $d$ of the leads. Nevertheless, in all cases we have to get rid of the integral over $|k|$ in the density of states by using

$$\delta\big(E - E(k)\big) = \frac{\delta\big(k - k(E)\big)}{\left|\frac{\partial E(k)}{\partial k}\right|}, \tag{B.25}$$

where

$$\left|\frac{\partial E(k)}{\partial k}\right| = \left|\frac{\partial E_k}{\partial \xi_k}\frac{\partial \xi_k}{\partial k}\right| = \frac{m}{\hbar^2}\left|\frac{1}{k}\frac{E}{\sqrt{E^2 - |\Delta|^2}}\right|. \tag{B.26}$$

In the following we list the density of states for dimension 1D, 2D and 3D. Note that the integration of the delta distributions leads to the Heaviside step functions, that means the integral collects only real and positive $k$'s.
**The one dimensional density of states** reads:

$$D_1(E) = \frac{Vm}{\hbar^2}\int \frac{dk}{2\pi}\left|\frac{E}{\sqrt{E^2-|\Delta|^2}}\frac{1}{k}\right| \delta\big(k-k(E)\big).$$

So

$$\boxed{D_1(E) = \frac{Vm}{\hbar^2}\left|\frac{E}{\sqrt{E^2-|\Delta|^2}}\frac{1}{k(E)}\right|\Theta(|E|-|\Delta|),} \tag{B.27}$$

where

$$k(E) = \left|\sqrt{\frac{2m}{\hbar^2}}\left(\sqrt{E^2-|\Delta|^2}+\mu\right)^{\frac{1}{2}}\right|. \tag{B.28}$$

**The two dimensional density of states** reads:

$$\begin{aligned} D_2(E) &= \frac{Vm}{\hbar^2}\int \frac{d^2k}{(2\pi)^2}\left|\frac{E}{\sqrt{E^2-|\Delta|^2}}\frac{1}{k}\right| \delta\Big(k-k(E)\Big) \\ &= \frac{m}{\hbar^2}\int_0^\infty \frac{dk}{2\pi}\left|\frac{E}{\sqrt{E^2-|\Delta|^2}}\,k\frac{1}{k}\right| \delta\Big(k-k(E)\Big), \end{aligned}$$

$$\boxed{D_2(E) = \frac{Vm}{2\pi\hbar^2}\left|\frac{E}{\sqrt{E^2-|\Delta|^2}}\right|\Theta(|E|-|\Delta|).} \tag{B.29}$$

Finally, we find for **the three dimensional density of states**:

$$\begin{aligned} D_3(E) &= \frac{Vm}{\hbar^2}\int \frac{d^3k}{(2\pi)^3}\left|\frac{E}{\sqrt{E^2-|\Delta|^2}}\frac{1}{k}\right| \delta\Big(k-k(E)\Big) \\ &= \frac{Vm}{\hbar^2}\frac{4\pi}{(2\pi)^3}\int_0^\infty dk\left|\frac{E}{\sqrt{E^2-|\Delta|^2}}\frac{k^2}{k}\right| \delta\Big(k-k(E)\Big)\ , \end{aligned}$$

$$\boxed{D_3 = \frac{1}{2\pi^2}\frac{Vm}{\hbar^2}\left|k(E)\frac{E}{\sqrt{E^2-|\Delta|^2}}\right|\Theta(|E|-|\Delta|).} \tag{B.30}$$

The density of states in all dimensions have the correct units as can be checked easily[1].

[1] The dimension of the prefactor are:

$$\left[\frac{m}{\hbar^2}\right] = \frac{\mathrm{kg}}{\mathrm{J}^2\mathrm{s}^2}. \tag{B.31}$$

In the one dimensional case the dimensional analysis leads to:

$$\left[\frac{Vm}{\hbar^2}\frac{1}{k(E)}\right] = \frac{\mathrm{kg\ m^2}}{\mathrm{J^2 s^2}} = \frac{1}{\mathrm{J}}, \tag{B.32}$$

in two dimensions it reads:

$$\left[\frac{Vm}{\hbar^2}\right] = \frac{\mathrm{kg\ m^2}}{\mathrm{J^2 s^2}} = \frac{1}{\mathrm{J}}, \tag{B.33}$$

and in three dimensions it is:

$$\left[\frac{Vm}{\hbar^2}k(E)\right] = \frac{\mathrm{kg\ m^3}}{\mathrm{J^2 s^2 m}} = \frac{1}{\mathrm{J}}. \tag{B.34}$$

## B.4. Transition rates

In the following, we list the transition rates defined in Chap. 4.1. The idea was to split the rates $\Gamma^{\pm}$ and $\Sigma^{\pm}$ of Eqs. (3.49), (3.50), (3.51) and (3.52), into two parts, depending on the position of the system creation and annihilation operators. For instance:

$$\Gamma^{+}_{\xi\xi_1\xi_2\xi'} = \left(\Gamma^{+}_{\xi\xi_1\xi_2\xi'}\right)^{N\to N+1} + \left(\Gamma^{+}_{\xi\xi_1\xi_2\xi'}\right)^{N\to N-1}. \tag{B.35}$$

The rates for the normal processes are:

$$\left(\Gamma^{+}_{\xi\xi_1\xi_2\xi'}\right)^{N\to N+1}_{\eta} = \left(\frac{1}{\hbar}\right)^2 |t|^2 \sum_{\eta k\sigma jj'} \langle\xi|\,\hat{\mathrm{d}}_{j\sigma}\,|\xi_1\rangle\,\langle\xi_2|\,\hat{\mathrm{d}}^{\dagger}_{j'\sigma}\,|\xi'\rangle \times$$
$$\int_0^{\infty} dt_2\; e^{\frac{i}{\hbar}E_{\xi'\xi_2}t_2}\left[|u_{\eta k}|^2 f^{+}_{\eta}(E_k)\; e^{+\frac{i}{\hbar}(E_k+\mu_\eta)t_2} + |v_{\eta k}|^2 f^{-}_{\eta}(E_k)\; e^{-\frac{i}{\hbar}(E_k-\mu_\eta)t_2}\right], \tag{B.36}$$

$$\left(\Gamma^{+}_{\xi\xi_1\xi_2\xi'}\right)^{N\to N-1}_{\eta} = \left(\frac{1}{\hbar}\right)^2 |t|^2 \sum_{\eta k\sigma jj'} \langle\xi|\,\hat{\mathrm{d}}^{\dagger}_{j\sigma}\,|\xi_1\rangle\,\langle\xi_2|\,\hat{\mathrm{d}}_{j'\sigma}\,|\xi'\rangle \times$$
$$\int_0^{\infty} dt_2\; e^{\frac{i}{\hbar}E_{\xi'\xi_2}t_2}\left[|u_{\eta k}|^2 f^{-}_{\eta}(E_k)\; e^{-\frac{i}{\hbar}(E_k+\mu_\eta)t_2} + |v_{\eta k}|^2 f^{+}_{\eta}(E_k)\; e^{+\frac{i}{\hbar}(E_k-\mu_\eta)t_2}\right], \tag{B.37}$$

$$\left(\Gamma^{-}_{\xi\xi_1\xi_2\xi'}\right)^{N\to N+1}_{\eta} = \left(\frac{1}{\hbar}\right)^2 |t|^2 \sum_{\eta k\sigma jj'} \langle\xi|\,\hat{\mathrm{d}}_{j'\sigma}\,|\xi_1\rangle\,\langle\xi_2|\,\hat{\mathrm{d}}^{\dagger}_{j\sigma}\,|\xi'\rangle \times$$
$$\int_0^{\infty} dt_2\; e^{\frac{i}{\hbar}E_{\xi_1\xi}t_2}\left[|u_{\eta k}|^2 f^{+}_{\eta}(E_k)\; e^{-\frac{i}{\hbar}(E_k+\mu_\eta)t_2} + |v_{\eta k}|^2 f^{-}_{\eta}(E_k)\; e^{+\frac{i}{\hbar}(E_k-\mu_\eta)t_2}\right], \tag{B.38}$$

$$\left(\Gamma^{-}_{\xi\xi_1\xi_2\xi'}\right)^{N\to N-1}_{\eta} = \left(\frac{1}{\hbar}\right)^2 |t|^2 \sum_{\eta k\sigma jj'} \langle\xi|\,\hat{\mathrm{d}}^{\dagger}_{j'\sigma}\,|\xi_1\rangle\,\langle\xi_2|\,\hat{\mathrm{d}}_{j\sigma}\,|\xi'\rangle \times$$
$$\int_0^{\infty} dt_2\; e^{\frac{i}{\hbar}E_{\xi_1\xi}t_2}\left[|u_{\eta k}|^2 f^{-}_{\eta}(E_k)\; e^{+\frac{i}{\hbar}(E_k+\mu_\eta)t_2} + |v_{\eta k}|^2 f^{+}_{\eta}(E_k)\; e^{-\frac{i}{\hbar}(E_k-\mu_\eta)t_2}\right]. \tag{B.39}$$

The rates for the anomalous processes read:

$$\left(\Sigma^{+}_{\xi\xi_1\xi_2\xi'}\right)^{N\to N+1}_{\eta} = \lim_{t\to\infty}\frac{\left(t^*\right)^2}{\hbar^2}\sum_{\eta k\sigma jj'}\langle\xi|\,\hat{\mathrm{d}}^{\dagger}_{j\bar{\sigma}}\,|\xi_1\rangle\,\langle\xi_2|\,\hat{\mathrm{d}}^{\dagger}_{j'\sigma}\,|\xi'\rangle\;\;\mathrm{sgn}(\sigma)\;v_{\eta k}u^*_{\eta k}\times$$
$$\int_0^{\infty}dt_2\;e^{\frac{i}{\hbar}E_{\xi'\xi_2}t_2}\;\;e^{-\frac{i}{\hbar}2\mu_\eta t}\left[f^{+}_{\eta}(E_k)\;e^{+\frac{i}{\hbar}(E_k+\mu_\eta)t_2}-f^{-}_{\eta}(E_k)\;e^{-\frac{i}{\hbar}(E_k-\mu_\eta)t_2}\right], \tag{B.40}$$

$$\left(\Sigma^{+}_{\xi\xi_1\xi_2\xi'}\right)^{N\to N-1}_{\eta} = \lim_{t\to\infty}\frac{t^2}{\hbar^2}\sum_{\eta k\sigma jj'}\langle\xi|\,\hat{\mathrm{d}}_{j\sigma}\,|\xi_1\rangle\,\langle\xi_2|\,\hat{\mathrm{d}}_{j'\bar{\sigma}}\,|\xi'\rangle\;\;\mathrm{sgn}(\sigma)\;v^*_{\eta k}u_{\eta k}\times$$
$$\int_0^{\infty}dt_2\;e^{\frac{i}{\hbar}E_{\xi'\xi_2}t_2}\;\;e^{+\frac{i}{\hbar}2\mu_\eta t}\left[f^{+}_{\eta}(E_k)\;e^{+\frac{i}{\hbar}(E_k-\mu_\eta)t_2}-f^{-}_{\eta}(E_k)\;e^{-\frac{i}{\hbar}(E_k+\mu_\eta)t_2}\right], \tag{B.41}$$

$$\left(\Sigma^{-}_{\xi\xi_1\xi_2\xi'}\right)^{N\to N+1}_{\eta} = \lim_{t\to\infty}\frac{\left(t^*\right)^2}{\hbar^2}\sum_{\eta k\sigma jj'}\langle\xi|\,\hat{\mathrm{d}}^{\dagger}_{j\bar{\sigma}}\,|\xi_1\rangle\,\langle\xi_2|\,\hat{\mathrm{d}}^{\dagger}_{j'\sigma}\,|\xi'\rangle\;\;\mathrm{sgn}(\sigma)\;v_{\eta k}u^*_{\eta k}$$
$$\int_0^{\infty}dt_2\;e^{\frac{i}{\hbar}E_{\xi_1\xi}t_2}\;e^{-\frac{i}{\hbar}2\mu_\eta t}\left[f^{+}_{\eta}(E_k)\;e^{-\frac{i}{\hbar}(E_k-\mu_\eta)t_2}-f^{-}_{\eta}(E_k)\;e^{+\frac{i}{\hbar}(E_k+\mu_\eta)t_2}\right], \tag{B.42}$$

$$\left(\Sigma^{-}_{\xi\xi_1\xi_2\xi'}\right)^{N\to N-1}_{\eta} = \lim_{t\to\infty}\frac{t^2}{\hbar^2}\sum_{\eta k\sigma jj'}\langle\xi|\,\hat{\mathrm{d}}_{j\sigma}\,|\xi_1\rangle\,\langle\xi_2|\,\hat{\mathrm{d}}_{j'\bar{\sigma}}\,|\xi'\rangle\;\;\mathrm{sgn}(\sigma)v^*_{\eta k}u_{\eta k}$$
$$\int_0^{\infty}dt_2\;e^{\frac{i}{\hbar}E_{\xi_1\xi}t_2}\;e^{+\frac{i}{\hbar}2\mu_\eta t}\left[f^{+}_{\eta}(E_k)\;e^{-\frac{i}{\hbar}(E_k+\mu_\eta)t_2}-f^{-}_{\eta}(E_k)\;e^{+\frac{i}{\hbar}(E_k-\mu_\eta)t_2}\right]. \tag{B.43}$$

### B.4.1. Basic integrals

In this section we are solving the integrals which appear in the definition of the transition rates. Therefore, we analyze the most generic structure by introducing $\omega$ for the difference in the energies of the dot and a function $F(E)$ which is an abbreviation for all real functions which depend on the energy, for instance

$$F(E) = D(E)\ |u_{\eta k}(E)|^2\ f^p(E), \tag{B.44}$$

$$F(E) = D(E)\ |v_{\eta k}(E)|^2\ f^p(E), \tag{B.45}$$

$$F(E) = D(E)\ u_{\eta k}(E) v_{\eta k}(E)\ f^p(E), \tag{B.46}$$

where $p = \pm$ and $D(E)$ is the density of states, see App. B.3. The integral reads:

$$I = \lim_{\eta \to 0} \int_{-\infty}^{\infty} dE\ F(E) \int_0^{\infty} dt\ e^{\frac{i}{\hbar}(\omega + q\tilde{E}(E) + i\eta)t}. \tag{B.47}$$

Integration over time leads to

$$I = \lim_{\eta \to 0} \int_{-\infty}^{\infty} dE\ F(E) \frac{i\hbar}{\omega + q\tilde{E}(E) + i\eta}, \tag{B.48}$$

which can be separated into real and imaginary part:

$$I = \lim_{\eta \to 0} \int_{-\infty}^{\infty} dE\ F(E) \hbar \Big( \frac{\eta}{(\omega + q\tilde{E}(E))^2 + \eta^2} + iIm\big(\frac{i\hbar}{\omega + q\tilde{E}(E) + i\eta}\big) \Big). \tag{B.49}$$

Now we can use that

$$\lim_{\eta \to 0}\ \frac{\eta}{x^2 + \eta^2} = \pi\ \delta(x) \tag{B.50}$$

and obtain:

$$I = \lim_{\eta \to 0} \int_{-\infty}^{\infty} dE\ F(E) \Big( \hbar\pi\ \delta(\omega + q\tilde{E}(E)) + iIm\big(\frac{i\hbar}{\omega + q\tilde{E}(E) + i\eta}\big) \Big), \tag{B.51}$$

where $\tilde{E}(E) = E \pm \mu$.
It is common to abbreviate the second part of the integral using:

$$\int_0^{\infty} dt\ e^{\frac{i}{\hbar}Xt} = \pi\hbar\ \delta(X) + i\hbar\ \text{p.v.}\ \frac{1}{X}, \tag{B.52}$$

where p.v. denotes that we have to use the principal part if we integrate over the second term. Therefore, we can write the integral as:

$$I = \lim_{\eta \to 0} \int_{-\infty}^{\infty} dE \; F(E) \left( \hbar\pi \; \delta(\omega + q\tilde{E}(E)) + i\hbar \text{ p.v. } \frac{1}{\omega + q\tilde{E}(E)} \right). \tag{B.53}$$

### B.4.2. Calculation of the rates

In this section we will calculate the rates which appear in the expression of the current. It is helping that at least the rates of the "normal" contributions always appear in complex conjugated pairs, such that they add up to two times the real part:

$$\begin{aligned}
&\Gamma^{N\to N+1}_{\xi\xi_1\xi_2\xi'} = (\Gamma^{+}_{\xi\xi_1\xi_2\xi'})^{N\to N+1} + (\Gamma^{-}_{\xi\xi_1\xi_2\xi'})^{N\to N+1} = 2Re\Big( (\Gamma^{+}_{\xi\xi_1\xi_2\xi'})^{N\to N+1} \Big) = \\
&= 2Re\Big\{ \Big(\frac{1}{\hbar}\Big)^2 |t|^2 \sum_{\eta\sigma jj'} \langle\xi|\, \hat{\mathrm{d}}_{j\sigma}\, |\xi_1\rangle \langle\xi_2|\, \hat{\mathrm{d}}^{\dagger}_{j'\sigma}\, |\xi'\rangle \int_{-\infty}^{\infty} dE\; D(E) \int_0^{\infty} dt_2 \;\times \\
&\times e^{\frac{i}{\hbar}E_{\xi'\xi_2}t_2} \Big[ |u_{\eta k}|^2 f^{+}_{\eta}(E)\; e^{+\frac{i}{\hbar}(E+\mu_\eta)t_2} + |v_{\eta k}|^2 f^{-}_{\eta}(E)\; e^{-\frac{i}{\hbar}(E-\mu_\eta)t_2} \Big] \Big\}.
\end{aligned} \tag{B.54}$$

First of all, we can solve the time integration using the formula of App. B.4.1:

$$\begin{aligned}
&\Gamma^{N\to N+1}_{\xi\xi_1\xi_2\xi'} = (\Gamma^{+}_{\xi\xi_1\xi_2\xi'})^{N\to N+1} + (\Gamma^{-}_{\xi\xi_1\xi_2\xi'})^{N\to N+1} = 2Re\Big( (\Gamma^{+}_{\xi\xi_1\xi_2\xi'})^{N\to N+1} \Big) = \\
&= \sum_{\sigma jj'} \langle\xi|\, \hat{\mathrm{d}}_{j\sigma}\, |\xi_1\rangle \langle\xi_2|\, \hat{\mathrm{d}}^{\dagger}_{j'\sigma}\, |\xi'\rangle \;\; 2Re\Big\{ \Big(\frac{1}{\hbar}\Big)^2 |t|^2 \lim_{\eta\to 0} \int_{-\infty}^{\infty} dE\; D(E) \times \\
&\times \Big[ |u_{\eta k}|^2 f^{+}_{\eta}(E) \Big( \hbar\pi\; \delta(E_{\xi'\xi_2} + \mu_\eta + E) + iIm\big(\frac{i\hbar}{E_{\xi'\xi_2} + \mu_\eta + E + i\eta}\big) \Big) \\
&+ |v_{\eta k}|^2 f^{-}_{\eta}(E) \Big( \hbar\pi\; \delta(E_{\xi'\xi_2} + \mu_\eta - E) + iIm\big(\frac{i\hbar}{(E_{\xi'} - E_{\xi_2}) - \tilde{E}(E) + i\eta}\big) \Big) \Big] \Big\}.
\end{aligned} \tag{B.55}$$

Taking the real part and evaluate the remaining integral, we obtain:

$$\begin{aligned}
&\Gamma^{N\to N+1}_{\xi\xi_1\xi_2\xi'} = \\
&\sum_{\sigma jj'} \langle\xi|\, \hat{\mathrm{d}}_{j\sigma}\, |\xi_1\rangle \langle\xi_2|\, \hat{\mathrm{d}}^{\dagger}_{j'\sigma}\, |\xi'\rangle \times \\
&\times \frac{1}{\hbar}|t|^2\; 2\pi \Big\{ \Big[ |u_{\eta k}|^2 f^{+}_{\eta}(E)\, D(E) \Big]_{E=-(E_{\xi'\xi_2}+\mu_\eta)} \\
&+ \Big[ |v_{\eta k}|^2 f^{-}_{\eta}(E)\, D(E) \Big]_{E=E_{\xi'\xi_2}+\mu_\eta} \Big\}.
\end{aligned} \tag{B.56}$$

Now we have to remember that $|v_{\eta k}|^2$, $|u_{\eta k}|^2$, and the density of states $D(E)$ only depend on the modulus of $|E|$. Furthermore, we see that

$$f_\eta^-(E_{\xi'\xi_2}+\mu_\eta) = f_\eta^+(-(E_{\xi'\xi_2}+\mu_\eta)) = \frac{1}{e^{\beta(E_{\xi_2\xi'}-\mu_\eta)}+1}. \tag{B.57}$$

This means that we can put the Fermi function as well as the density of states out of the bracket:

$$\begin{aligned}
&\Gamma^{N\to N+1}_{\xi\xi_1\xi_2\xi'} = \\
&\sum_{\sigma jj'} \langle\xi|\,\hat{\mathrm{d}}_{j\sigma}\,|\xi_1\rangle\,\langle\xi_2|\,\hat{\mathrm{d}}^\dagger_{j'\sigma}\,|\xi'\rangle \times \\
&\times \frac{1}{\hbar}\,|t|^2\,2\pi\,\underbrace{\left(|u_{\eta k}|^2+|v_{\eta k}|^2\right)}_{=1} D(E_{\xi_2\xi'}-\mu_\eta) f_\eta^+(E_{\xi_2\xi'}-\mu_\eta),
\end{aligned} \tag{B.58}$$

Finally, we obtain:

$$\Gamma^{N\to N+1}_{\xi\xi_1\xi_2\xi'} = |t|^2\,\frac{2\pi}{\hbar}\sum_{\sigma jj'}\langle\xi|\,\hat{\mathrm{d}}_{j\sigma}\,|\xi_1\rangle\,\langle\xi_2|\,\hat{\mathrm{d}}^\dagger_{j'\sigma}\,|\xi'\rangle\,D(E_{\xi_2\xi'}-\mu_\eta) f_\eta^+(E_{\xi_2\xi'}-\mu_\eta). \tag{B.59}$$

For the rates which lower the occupation of the system the calculation is quite similar:

$$\begin{aligned}
&\Gamma^{N\to N-1}_{\xi\xi_1\xi_2\xi'} = (\Gamma^+_{\xi\xi_1\xi_2\xi'})^{N\to N-1} + (\Gamma^-_{\xi\xi_1\xi_2\xi'})^{N\to N-1} = 2Re\left((\Gamma^+_{\xi\xi_1\xi_2\xi'})^{N\to N-1}\right) = \\
&= 2Re\left\{\left(\frac{1}{\hbar}\right)^2 |t|^2 \sum_{\eta\sigma jj'}\langle\xi|\,\hat{\mathrm{d}}^\dagger_{j\sigma}\,|\xi_1\rangle\,\langle\xi_2|\,\hat{\mathrm{d}}_{j'\sigma}\,|\xi'\rangle \int_{-\infty}^{\infty} dE\; D(E) \int_0^\infty dt_2 \times \right. \\
&\left. \times \left[|u_{\eta k}|^2 f_\eta^-(E)\; e^{-\frac{i}{\hbar}(E+\mu_\eta-E_{\xi'\xi_2})t_2} + |v_{\eta k}|^2 f_\eta^+(E)\; e^{+\frac{i}{\hbar}(E-\mu_\eta+E_{\xi'\xi_2})t_2}\right]\right\}.
\end{aligned} \tag{B.60}$$

As before, we can evaluate the time integral and keep only the real part. Then we repeat the same steps as before, we get:

$$\Gamma^{N\to N-1}_{\xi\xi_1\xi_2\xi'} = \frac{2\pi}{\hbar}\,|t|^2 \sum_{\eta\sigma jj'}\langle\xi|\,\hat{\mathrm{d}}^\dagger_{j\sigma}\,|\xi_1\rangle\,\langle\xi_2|\,\hat{\mathrm{d}}_{j'\sigma}\,|\xi'\rangle\,f_\eta^-(E_{\xi'\xi_2}-\mu_\eta)\;D(E_{\xi'\xi_2}-\mu_\eta). \tag{B.61}$$

We are left with the "anomalous" rates, which are not complex conjugated. this means we are not able to combine them in the same way as before; and we must take care

of the principal part as well. Thus we calculate them separately. But we have to take care of the time integration, which we expanded to infinity in the stationary limit:

$$\begin{aligned}\left(\Sigma^{+}_{\xi\xi_1\xi_2\xi'}\right)^{N\to N+1}_{\eta} = \lim_{t\to\infty} \frac{\left(t^*\right)^2}{\hbar^2} \sum_{\sigma jj'} \langle\xi|\,\hat{\mathrm{d}}^{\dagger}_{j\bar{\sigma}}\,|\xi_1\rangle\,\langle\xi_2|\,\hat{\mathrm{d}}^{\dagger}_{j'\sigma}\,|\xi'\rangle\ \ \mathrm{sgn}(\sigma)\ e^{-\frac{i}{\hbar}2\mu_\eta t}\times \\ \int_{-\infty}^{\infty} dE\ D(E)\,v_{\eta k}u^*_{\eta k}\int_0^t dt_2\times \\ \left[f^{+}_{\eta}(E)\ e^{+\frac{i}{\hbar}(E+\mu_\eta+E_{\xi'\xi_2})t_2} - f^{-}_{\eta}(E)\ e^{-\frac{i}{\hbar}(E-\mu_\eta-E_{\xi'\xi_2})t_2}\right].\end{aligned} \tag{B.62}$$

Hence, we are considering the energy integration separately:

$$\int_{-\infty}^{\infty} dE\ D(E)\,v_{\eta k}u^*_{\eta k}\left[f^{+}_{\eta}(E)\ e^{+\frac{i}{\hbar}(E+\mu_\eta+E_{\xi'\xi_2})t_2} - f^{-}_{\eta}(E)\ e^{-\frac{i}{\hbar}(E-\mu_\eta-E_{\xi'\xi_2})t_2}\right]. \tag{B.63}$$

We exploit again the fact that $D(E)$, $v_{\eta k}$, and $u^*_{\eta k}$ only depend on $|E|$. After changing the integration variable $E \leftrightarrow -E$ in the second term we find:

$$\int_{-\infty}^{\infty} dE\ D(E)\,v_{\eta k}u^*_{\eta k}\left[f^{+}_{\eta}(E)\ e^{+\frac{i}{\hbar}(E+\mu_\eta+E_{\xi'\xi_2})t_2} - f^{-}_{\eta}(-E)\ e^{-\frac{i}{\hbar}(-E-\mu_\eta-E_{\xi'\xi_2})t_2}\right]. \tag{B.64}$$

Using that $f^{-}_{\eta}(-E) = f^{+}_{\eta}(E)$ we obtain

$$\int_{-\infty}^{\infty} dE\ D(E)\,v_{\eta k}u^*_{\eta k}\left[f^{+}_{\eta}(E)\ e^{+\frac{i}{\hbar}(E+\mu_\eta+E_{\xi'\xi_2})t_2} - f^{+}_{\eta}(E)\ e^{+\frac{i}{\hbar}(E+\mu_\eta+E_{\xi'\xi_2})t_2}\right] = 0. \tag{B.65}$$

Inserting the result of Eq. (B.65) back to Eq. (B.62) we find the anomalous rate to be equal to zero. Hence, the stationary limit $t \to \infty$ causes no further complications. We notice that the other anomalous rates are vanishing for the same reasons, as their energy integration has always the same structure. With the same arguments as before we find in general:

$$\int_{-\infty}^{\infty} F(E)\left[f^{(p)}_{\eta}(E)\,e^{\frac{i}{\hbar}(qE+\omega)t_2} - f^{(-p)}_{\eta}(E)\,e^{\frac{i}{\hbar}(-qE+\omega)t_2}\right] = 0, \tag{B.66}$$

where $F(-E) = F(E)$ and $p = \pm 1$. By comparing Eq. (B.66) with the definition of the rates in App. B.4, one can convince oneself that this special structure can be found in all anomalous terms.

We found that the anomalous rates are equal zero as they should be; to conserve the hermitian properties of the density matrix. The only non-zero contributions entering Eq. (3.2.1) are the normal rates.

# Bibliography


[1] M. Abramowitz and I. A. Stegun. *Handbook of Mathematical Functions.* Dover Publications, Inc., New York, 1972.

[2] J. Bardeen, L. N. Cooper, and J. R. Schrieffer. Theory of superconductivity. *Physical Review*, 108(5):271–281, December 1957.

[3] K. Blum. *Density Matrix Theory and Applications: Second Edition.* Plenum Press, New York, 1996.

[4] N. N. Bogoliubov. A new method in the theory of superconductivity. *Soviet Physics JETP*, 34(7):41–46, July 1958.

[5] I. N. Bronstein and K. A. Semendjajew. *Taschenbuch der Mathematik.* Harri Deutsch, 2001.

[6] D. Budker and M. Romalis. Optical magnetometry. *Nat Phys*, 3, 2007.

[7] A. Cho. Superconductivity's smorgasbord of insights: A movable feast. *Science*, 332(8):190–192, April 2011.

[8] J. Clarke and F. K. Wilhelm. Superconducting quantum bits. *Nature*, 453:1031 –1042, 2008.

[9] Yong-Joo Doh, S. De Franceschi, E. P. A. M. Bakkers, and L. P. Kouwenhoven. Andreev reflection versus coulomb blockade in hybrid semiconductor nanowire devices. *Nano Letters*, 8(12):4098–4102, 2008.

[10] A. L. Fetter and J. D. Walecka. *Quantum Theory of Many-Particle Systems.* McGraw-Hill, Inc., 1971.

[11] I. Giaever. Energy gap in superconductors measured by electron tunneling. *Phys. Rev. Lett.*, 5(4):147, 1960.

[12] K. Grove-Rasmussen, H. I. Jørgensen, B. M. Andersen, J. Paaske, T. S. Jespersen, J. Nygård, K. Flensberg, and P. E. Lindelof. Superconductivity-enhanced bias spectroscopy in carbon nanotube quantum dots. *Phys. Rev. B*, 79(13):134518, Apr 2009.

[13] L. G. Herrmann, F. Portier, P. Roche, A. Levy Yeyati, T. Kontos, and C. Strunk. Carbon nanotubes as cooper-pair beam splitters. *Phys. Rev. Lett.*, 104:026801, Jan 2010.

[14] L. Hofstetter, S. Csonka, J. Nygard, and C. Schonenberger. Cooper pair splitter realized in a two-quantum-dot y-junction. *Nature*, 461:960– 963, October 2009.

[15] B.D. Josephson. Possible new effects in superconductive tunnelling. *Physics Letters*, 1(7):251–253, July 1962.

[16] R. Pariser and R. G. Parr. A semi-empirical theory of electronic spectra and electronic structure of complex unsaturated molecules. *The Journal of Chemical Physics*, 21(3), March 1953.

[17] R. D. Parks. *Superconductivity Vol. 1.* Marcel Dekker, Inc. New York, 1969.

[18] J. A. Pople. Electron interaction in unsaturated hydrocarbons. *Trans. Faraday Soc.*, 49:1375–1385, 1953.

[19] D.C. Ralph, C. T. Black, and M. Tinkham. Spectroscopic measurements of discrete electronic states in single metal particles. *Phys. Rev. Lett.*, 74(16):3241, 1995.

[20] M. Tinkham. *Introduction to Superconductivity: Second Edition (Dover Books on Physics).* Dover Publications, 2004.

[21] J. A. van Dam, Y. V. Nazarov, E. P. A. Bakkers, S. De Franceschi, and L. P. Kouwenhoven. Supercurrent reversal in quantum dots. *Nature*, 442:667–670, 2006.

[22] U. Weiss. *Quantum Dissipative Systems: Second Edition.* World Scientific Publishing Co. Pte. Ltd., 1999.

[23] C. B. Winkelmann, N. Roch, W. Wernsdorfer, and V. Bouchiat. Superconductivity in a single-$C_{60}$ transistor. *Nature Phys.*, 5:876–879, 2009.

# Erklärung

Hiermit erkläre ich, dass ich die Diplomarbeit selbständig angefertigt und keine Hilfsmittel außer den in der Arbeit angegebenen benutzt habe.

Regensburg, den 23.09.2011

Sebastian Pfaller